Hydrologic Impact of Constructed Oyster Reefs on Flow Attenuation and Sediment Transport at an Eroding Marsh

Griffin Budzinski Yates

Charlottesville, VA

B.S. Mechanical Engineering, University of Notre Dame 2021

B.S. Environmental Sciences, University of Notre Dame 2022

A Thesis presented to the Graduate Faculty at the University of Virginia in Candidacy for the Degree of Master of Science

Department of Environmental Sciences

University of Virginia

December, 2024

Table of Contents

I. Acknowledgements

This ambitious two year research project was only possible through the abundant help and assistance from a number of people, both within and external to the University of Virginia. First and foremost, many thanks to Matthew Reidenbach for being a present and attentive advisor, as well as for providing ample guidance throughout the entire research project. Thank you to my committee, Pat Wiberg and Mike Pace, for providing much needed feedback and help refining my unpolished research interests into a concrete and achievable research plan. Thank you to the entire staff who keeps the ABCRC field station running: Tom Burkett and Sophia Hoffman for helping me deploy and retrieve field instruments even when it was an inconvenience, Donna Fauber and Cora Baird for helping schedule my research trips and navigate the world of science in the field, and Buck Compton for helping to make sure all my field instruments and associated hardware were in working order when things didn't go according to plan. Thank you to Marcus Killmon and Meriwether Pane for boating me out to my Wachapreague field sites. A huge thank you to Kelsey O'Donnell for welcoming me into the world of graduate research and the Reidenbach lab, as well as helping decipher the world of ANSYS modeling and proprietary instrument software. Thank you to Tyler Barnes for helping make sense of AMBUR, and for being hugely helpful in running the geomorphology analysis. Thank you to Savannah Atchley and Autumn Summers for driving down to the Eastern Shore and helping with field work, especially in the wake of me losing my cell phone and ability to document my study sites. And finally, thank you to my friends and family for being available to bounce ideas off of, listen to my frustrations, and for their abundant support through every part of this journey.

II. Abstract

Wachapreague, VA is a coastal town located on the East coast of the Delmarva peninsula, and historically has faced severe coastal flooding. The main marsh that mitigates Wachapreague's flooding has been eroding over the past decades, and there have been recent efforts to reduce these erosion rates through the use of oyster reef based living shorelines. Since 2020, the southern shoreline of Wachapreague marsh has been lined with constructed oyster reefs, creating a protective barrier against wave attack. However, other living shoreline projects have had varying degrees of success in reducing erosion. This project quantified the success of Wachapreague's constructed oyster reefs at reducing erosion, attenuating waves, and inducing fluid drag.

Constructed oyster reefs are currently 3-4 years old at Wachapreague marsh, on average, and display signs of healthy oyster population and shell growth rates. These reefs heavily attenuated waves during low and mid tides, but during high tide increased wave height by approximately 5%. Significant wave height was directly correlated with turbidity, which is indicative of suspended sediment concentrations and sediment transport. Despite a lack of desired sensor precision, Wachapreague's shoreline was recorded losing nearly 1 cm of sediment between June and July, 2024, with slight offshore deposition occurring between July and September, 2024. Additionally, marsh platform loss rates varied spatially across the marsh, with oyster reef installation most significantly slowing erosion rates along the shoreline's western edge.

Model results reveal that oyster reefs heavily attenuate flow below reef height, but flow velocity is likely increased near the fluid surface. Additionally, oyster castles have a region of high shear stress within the model's front chambers along the bed surface. These shear stresses are sufficient to erode sediments found within these intertidal lagoon systems, indicating that constructed oyster reefs may undergo spatially differential erosion, as opposed to natural reefs the face more evenly spaced erosional pressures. Based on these findings, constructed oyster reefs are capable of lowering incoming wave energy during low and mid tide, reducing rates of shoreline loss, lowering SSC, and fostering healthy oyster growth. Additionally, these constructed reefs attenuate both flow and shear stress below reef height; however, oyster castles may face long term issues with differential erosion and reef subsidence. Therefore, while constructed oyster reefs can reduce rates of marsh platform loss, a different oyster substrate geometry is recommended for long-term reef health and success.

III. Chapter 1: Effects of Oyster Castle Installation on Wave Attenuation and Marsh Morphodynamics

A. Introduction

Saltmarsh ecosystems are ubiquitous across the Atlantic coast of North America within intertidal areas. These ecosystems are characterized by frequent flooding, which mobilizes high amounts of fine sediments (Blum et al, 2021). The grass species that form the foundation of marshes impede the flow of water, and subsequently sediments, thereby building up the marsh platform and allowing for overall marsh edge expansion (Bertness et al, 1992; Stoorvogel et al, 2024). Often being positioned between the mainland and neighboring lagoons, saltmarshes form a vitally important buffer landscape, serving to protect the ocean from nutrient runoff and other pollutants, as well as protecting coastal communities from many of the destructive effects of storms (Leonardi et al, 2018). These marshes perform a variety of other important functions, including providing habitat for marine and avian species, sequestering carbon, and improving overall water quality. While the monetary value of such services is hard to define, some studies have placed the total value of salt marsh services, both in the context of sea level rise and ecosystem services, at $4,400 per acre annually (Mazzocco et al, 2022). In the context of Virginia's Eastern Shore, salt marshes play a key role in protecting many coastal communities, such as Wachapreague, from flooding and coastal storms, as well as sustaining local fisheries.

Salt Marshes are inherently dynamic ecosystems, and naturally undergo changes in shape, total area, and position relative to the mainland. However, a change in sediment supply or wave energy and frequency can result in a sediment imbalance (Townend et al, 2011). It is this balance in the sediment budget that allows salt marshes to change morphodynamically while still being sustained as an ecosystem. Additionally, the sediment budget dictates how marsh morphology changes over time, especially in the context of marsh migration and sea level rise. Salt marshes can build themselves up through a combination of trapping sediments on top of the platform and by creating organic root matter (Reed 2002). Within the VCR, it has been observed that low lying marshes can accrete vertically up to 4.9 mm/year, while high marshes accrete up to 3.3 mm/year (Blum et al, 2021). These differences in accretion rate are directly attributable to both tidal flooding time and rates of marsh grass root growth (Blum et al, 2021). However within Virginia's eastern shore, marshes may have difficulty accreting fast enough to keep pace with sea level rise and coastal erosion (Kastler and Wiberg, 1996).

Large scale sediment dynamics play an enormous role in sustaining coastal marsh ecosystems, especially in allowing them to dynamically adapt to various environmental factors. Coastal marshes naturally change spatially through several processes, such as marsh migration and marsh platform buildup, both of which are fueled by a balance between sediment erosion and accretion (Blum et al, 2021; Reed, 2002; Kastler and Wiberg, 1996; Matias et al, 2008). Since coastal marsh ecosystems frequently form the barrier between shallow lagoons and the neighboring mainland, sediment dynamics are coupled between the marshes and these other adjacent ecosystems (Marani, 2010). Subsequently, all incoming sediments to marshes are sourced from either the open ocean, lagoons, or the mainland, and all eroding sediments enter either the ocean or nearby bays (Lauzon et al, 2018; Reeves et al, 2020). It has been shown that up to 42% of sediments eroded from marshes settle in the nearby coastal bays and among the vegetation of marsh platforms, where it can then contribute to the sediment budget of nearby marshes (Donatelli, 2020). Similarly, it has been shown that storm events are important to creating sediment influxes, overwashing marshes and supplying sediments to the platform. The vast majority of sediments supplied during these storm events are originally sourced from mudflats and tidal creeks, and are remobilized and transported to the marshes (Pannozzo, 2023). The resulting sediment budget is a good indicator of marsh survivability amidst climate change. If a marsh cannot retain enough sediments, it will not be able to keep pace with sea level rise and erosional effects, eventually starving and drowning (Peteet, 2018).

Along the edge of the salt marsh, erosion is mainly driven by three factors: land subsidence, relative sea level rise, and wave attack (Day et al, 1999). In particular, it is this wave driven erosion that is of concern along Virginia's eastern shore. A model of various marsh morphologies at the VCR found that when waves reach the marsh platform at higher tidal levels, the associated energy dissipation causes sufficient shear stress to erode the marsh edge (Tonelli et al, 2010). This wave driven erosion can lead to salt marsh shrinkage, making it difficult for salt marshes to sustain themselves despite vertically accreting (Mariotta and Carr, 2014). McLoughlin et al found that at several marshes sampled within the VCR, lateral marsh erosion rates were 1.0-1.6 m/year at three of four marshes measured, and these erosion rates were consistent for the 50 year study period, albeit with spatial variability along the marsh edges (McLoughlin et al, 2015). Historically, salt marshes along Virginia's eastern shore have been able to sustain themselves in the face of wave attack. However, salt marshes face a variety of new pressures that worsen the effects of wave erosion and drowning. Relative sea level rise is approximately 5 mm/year at the eastern shore (Ezer and Atkinson, 2015), which, combined with other factors of climate change such as increased storm intensity (Hayden and Hayden 2003), as well as anthropogenic pressures, drastically changes salt marsh dynamics, consequently leading to both marsh erosion, migration, and ultimately shrinkage (Kirwan et al, 2016).

There are a variety of processes by which marshes can erode. At the VCR, however, a few processes tend to dominate. One of the most common is undercutting, in which the sediment underneath the marsh platform is washed away, leading to overhanging sections that eventually collapse. Another common process is block erosion, in which fissures, in part caused by bio-erosion, form along the edges of marsh platforms, leading to entire blocks of marsh breaking off and eroding (Priestas et al, 2015; McLoughlin, 2010). Regardless of the exact mechanism, marsh erosion is largely caused by wave action in the VCR. Prolonged marsh health and growth is dependent on controlling the extent to which waves can reach the shoreline. In the context of rising sea levels and increased storm impact caused by climate change, it is to be expected that these erosional processes may occur at higher rates, thereby causing coastal marshes to shrink faster than they can grow (Fagherazzi et al, 2020). Living shorelines may be implemented to mitigate increasing erosion rates due to climate change, and could serve as a key way to ensure coastal marsh health and function.

The Eastern oyster, *Crassostrea virginica,* was historically abundant along Virginia's coastlines, but the combined stress of overharvesting, disease, and habitat loss has led to an estimated ~95% reduction in population counts in the Chesapeake area between the 1800s and the present day (Rothschild et al, 1994; Mackenzie, 2007; Andrews et al, 1962). Suitable oyster habitat within the VCR has been characterized using LIDAR sensing, and typically is located within intertidal mudflats and along the barriers of marshes (Hogan and Reidenbach, 2019). Therefore based on modern data, historically oyster reefs would have grown into large reef structures in the mud flats of coastal lagoons (perhaps both inter- and sub-tidal), as well as along the shoreline of salt marshes and barrier islands (Bartol et al, 1999). However similar to oyster reefs, Virginia has experienced substantial loss of salt marshes due to both anthropogenic influences and climate change (Deaton et al, 2017; Burns et al, 2021). The long-term health of saltmarshes, as well as the areas they protect, depends on the ability of marshes to grow despite increased pressures from waves, storms, and sea level rise (Crosby et al, 2016; Pannozzo et al, 2021). In Virginia, wave attack, not storm surges, is the most common cause of marsh edge erosion (Tonelli et al, 2010; Leonardi and Fagherazzi, 2015). Thus, protecting marsh platforms from wave attack is a vital mechanism for increasing the long-term success of these ecosystems, and restoration and rebuilding of oyster reefs along the edges of marsh platforms could serve as a key way to lower incoming wave energy and reduce erosion rates. By virtue of being an intertidal species, oyster reefs may serve as a natural form of wave protection (Wiberg et al, 2019). Oyster reefs provide a structure of hard substrate capable of breaking incoming waves and reducing wave heights, in turn lowering wave energy propagation and potentially offering erosion protection to the shoreline during mid and low tides (Bieri, 2022).

Due to the widespread loss of oysters in Virginia’s coastal lagoon ecosystems, there has been growing interest in restoring populations. As both a keystone species and a prolific filter feeder, oysters provide a multitude of unique benefits and ecosystem services in these lagoon environments (Grabowski et al, 2012; DePiper et al, 2017). For example, oysters filter as much as 50 gallons per day per individual, working to clean what would otherwise be relatively stagnant water (CBF, 2024; Gawde et al, 2024). Additionally, the large reef structures formed by oysters provide vital habitat for crabs, juvenile fish, and various soft bodied invertebrates, in turn forming an important link in the coastal food web and increasing biodiversity (Henderson and Oneil, 2003). Finally, oyster reefs form an important physical barrier between the bays and marsh shoreline, helping to break and absorb waves before they make contact with the marsh edge (Wiberg et al, 2019).

Due to these benefits, there has been recent interest in constructing living shorelines out of oyster reefs. Concrete seawalls are frequently installed as a means of attenuating waves along shorelines (Mani, 2007; Kelletat, 1992). However, nature-based solutions, such as utilizing oyster reefs as a protective barrier, have recently been explored as an alternative to traditional seawalls (Vona et al, 2024; Perricone et al, 2023; Salatin et al, 2022). Preliminary work suggests that oyster reefs can reduce wave height by as much as 30-50%, but only at relatively shallow water depths of 0.5-1.0 m (Wiberg et al, 2019). However, given that oysters grow to maintain an intertidal depth in the water column, they have the potential to effectively absorb waves over time under the impact of sea level rise, even if the reef shifts or sinks in the substrate (Salatin et al, 2022). As incoming tidal currents and waves are attenuated, shear stresses will be lowered on the bed surface, potentially leading to lower rates of bed erosion, and even an increase in sediment deposition behind the oyster reefs (Stricklin et al, 2010; Bieri, 2022). Oyster reef based shorelines could therefore minimize marsh shorelines erosion, and encourage those shorelines to expand.

Oysters colonize on hard, rocky substrate, and often settle on other oysters, as well as natural rock formations and manmade debris (Whitman and Reidenbach, 2012). Populations have been reestablishing in recent decades, but progress is slow, with lack of suitable habitat often being the limiting factor in growth rates (Smith et al, 2022). Thus, the restoration of oysters depends on the presence of suitable habitat. Artificial rocky structures, called oyster castles, can be placed along shorelines to promote the establishment of new oyster reefs by providing suitable hard substrate (Theuerkauf at al, 2015).

The Nature Conservancy has recently been working to construct and restore oyster reefs across Virginia’s Eastern Shore through the installation of oyster castles, with one site at a historically eroding marsh near Wachapreague, VA (The Nature Conservancy, 2023). In addition to stabilizing the oyster population, this project has potential to protect marsh platforms from further erosion, as previously monitored restored reefs have been shown to lower both wave height and coastal erosion rates (Bieri, 2022; Wiberg et al, 2019; Hogan et al 2021). However, the long term implementation of oyster reefs as a living shoreline necessitates an understanding of how oyster reefs influence the hydrodynamics of flow immediately around them. There is a distinct lack in knowledge concerning how constructed oyster reefs can alter sediment dynamics and encourage sediment deposition in regions of the marsh that historically have eroded.

Specifically along Virginia’s eastern shore, several studies have investigated the protective and wave attenuating effects of oyster reefs along marsh edges in shallow coastal lagoons (Wiberg et al, 2019; Reidenbach and Timmerman, 2019; Hogan and Reidenbach, 2022). Experimental results from Hogan et al revealed that oyster reefs contribute to an elongation of marsh platforms (Hogan et al, 2021). Exposed marsh edges typically had a much steeper slope (11.4 degrees), while protected marsh edges had a shallower slope (6 degrees), suggesting that oyster reefs can protect the lower marsh platform from erosion, thereby reducing, and potentially preventing, marsh platform retreat over long term timescales (Hogan et al, 2021).

Traditionally, monitoring sediment dynamics in coastal environments has been difficult, both because common techniques are tedious and only provide discrete data points. Sediment plates may be placed to track sediment deposition, but they do not track erosion, and each can only provide one data point for sediment deposition (Bieri, 2022). Horizon marker layers of feldspar may be placed on the sediment surface, but these can wash away during storm events, and do not always provide a clear measurement when cored (Blum et al, 2021). Consequently, new data collection methods that yield higher frequency sampling are needed to thoroughly understand sediment dynamics as influenced by restored oyster reefs.

This project aims to quantify the impact of fringing oyster reefs on wave action, sediment transport rates, and salt marsh morphodynamics. Oyster reefs have been observed influencing flow rates and sediment transport, but no single project has investigated them in the context of detailed erosion trends and marsh morphology changes along Virginia's Eastern Shore. Thus, chapter 1 aims to quantify and understand what impact constructed oyster reefs have on coastal erosion rates and sediment dynamics. The questions this chapter will address are: to what extend do oyster castles alter erosion and accretion trends along a marsh shoreline; do restored oyster reef structures have an impact on morphology change at a historically eroding marsh; what are the long-term oyster growth rates and population densities on restored reefs.

B. Methods

i. Study Site

a. *Virginia Coast Reserve*

The Virginia Coast Reserve is a section of protected coastline that extends along 110 km of the east coast of the Delmarva Peninsula (Figure 1). The reserve is characterized by a series of lagoons, coastal wetlands, and barrier islands. Due to its vast size, history of continuous data sets, and vulnerability to climate change and sea level rise, the VCR offers an ideal system in which to study various coastal phenomena. In particular, the VCR is a study system that is relevant for answering how human communities and coastal ecosystems that are so heavily linked are affected by climate change.

Figure 1: A map showing the placement of Wachapreague and the ABCRC along Virginia's eastern shore

ii. Wachapreague

Wachapreague is a coastal town situated along the seaside portion of Virginia's Eastern Shore. Historically, Wachapreague has experienced significant and frequent coastal flooding. It is not abnormal for the town, especially near the marina, to entirely flood when coastal storms make landfall and bring storm surges. One of the main defenses against these storm surges are the various salt marshes and barrier islands that surround the town's coastline. Of particular concern is one main marsh, referred to in this project as Wachapreague Marsh. Wachapreague Marsh is the main feature separating Wachapreague from the neighboring Bradford Bay, and is the main marsh that mitigates storm damage. However, in recent years, these protective coastal ecosystems have receded at significant rates – up to several feet per year at some locations in Wachapreague Marsh (Figure 2).

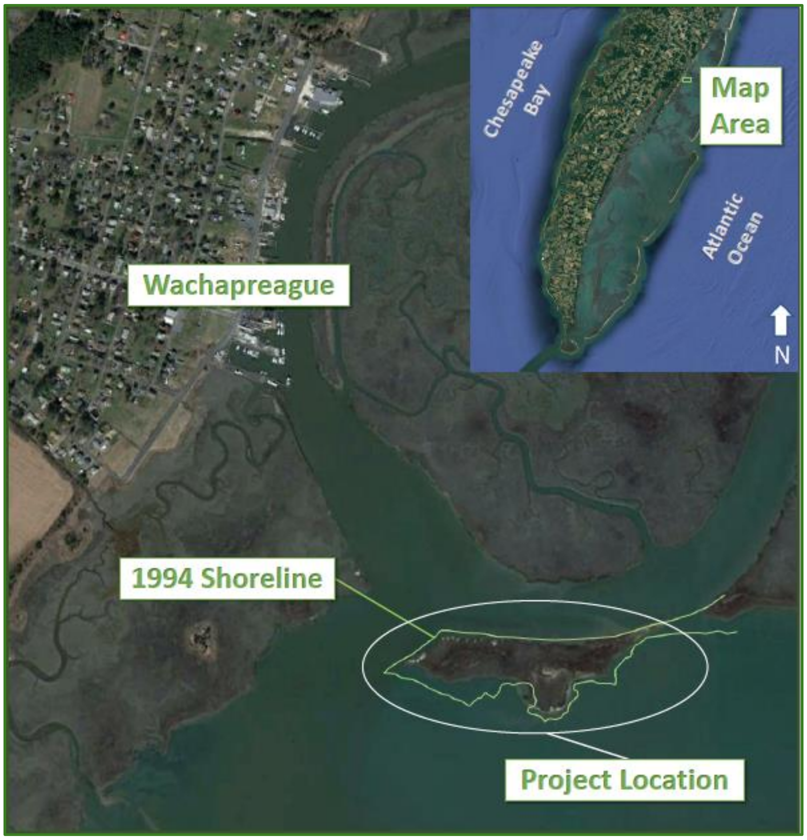

Figure 2: The position of Wachapreague Marsh relative to Wachapreague. Note that the 1994 shoreline was much larger than modern satellite imagery shows, with the addition of a new channel cut into the eastern edge of the island (Bieri, 2022).

The National Fish and Wildlife Federation and The Nature Conservancy are concerned with the disappearance of salt marshes, as such an event would only worsen coastal flooding and erosion in adjacent towns. Consequently, these agencies have been working to install artificial oyster reef substrate along the southern shoreline of Wachapreague Marsh. Substrate installation began in 2020, and installation of a completed protective substrate wall finished in 2024. The shoreline was divided into 9 subsections, and initial construction year of oyster reefs in each of those subsections is shown in Figure 3. Oyster reefs were constructed in a two wall configuration, as shown in Figure 4. Given that there are two parallel oyster castles lining Wachapreague Marsh's shoreline, they will subsequently be referred to as the nearshore and offshore reef, despite being positioned only approximately 1 m apart.

Figure 3: A map of Wachapreague Marsh showing all south facing shoreline sections, as well as initial year of oyster castle installation for each section. All deployments were done at sites 4 and 7 (Bieri, 2022)

Figure 4: The two layers of oyster reef that are typical to find around much of Wachapreague Marsh's southern shoreline

iii. Hydrodynamics

Between winter of 2023 and summer of 2024, various instruments were deployed at Wachapreague marsh to investigate various hydrodynamic and sediment transport trends as influenced by oyster reef presence. Specifically, a Ruskin® RBR Duo sensor and Nortek® Aquadopp HR 2 MHz sensor were deployed. The RBR Duo utilizes pressure and water temperature measurements to calculate significant wave height, water depth, and turbidity levels of the water. Likewise, the Aquadopp is an acoustic Doppler current profiler, capable of measuring water velocity throughout the water column. Sensor deployment locations are shown in Figure 5, and deployment configurations are shown in Figure 6. Aquadopps were deployed at SN4 and SO4 once in early 2023, while RBR sensors were deployed at SO7 during summer of 2024.

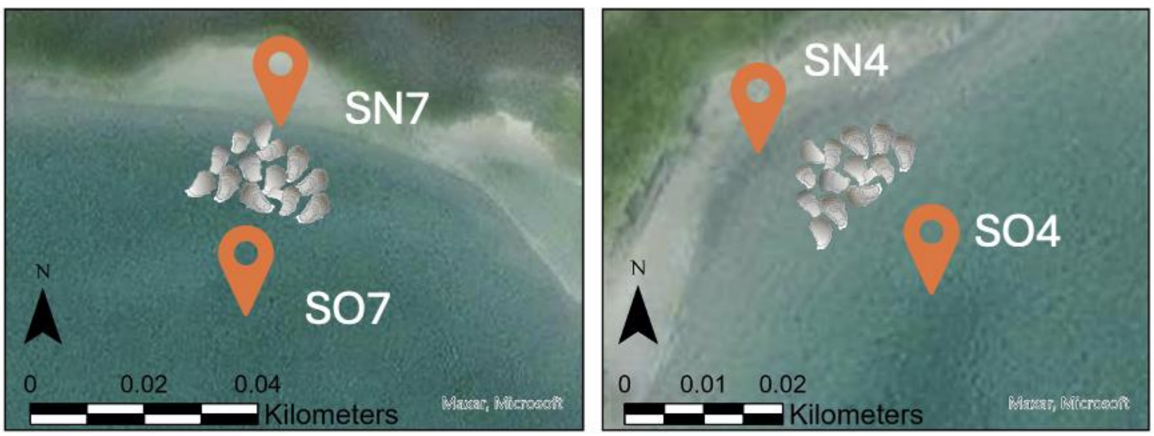

(a) **(b)**

Figure 5: A magnified map of sites 7 (a) and 4 (b), where all instrument deployments occurred. Sites are divided into nearshore and offshore sections, and are relative to oyster substrate location. GPS coordinates for the deployment sites are as follows: SN4 - 37.5980236° N, 75.6798882° W, SO4 - 37.5979734° N, 75.6798131° W, SN7 - 37.5977095° N, 75.6824565° W, SO7 - 37.5976213° N, 75.6824755° W

(a) (b)

Figure 6: A sample deployment of the RBR wave gauge (a) and Aquadopp velocity sensor (b)

The RBR wave gauges sampled at a rate of 4 Hz, and averaged data across 30 minute time intervals. They measure both wave and depth data with an accuracy of ± 0.05% total water depth. Likewise, the Aquadopp sampled at a rate of 1 Hz with an accuracy of ± 0.5 cm/s. The deployment schedule is shown in Table 1.

iv. Sediment Transport

To address issues with traditional field measurement methods, this project utilized Echologger® AA400 Acoustic Altimeters to accurately and continuously track sediment dynamics. These sensors were suspended approximately 0.5 m above the bed surface, as shown in Figure 7, and send out 5^{o} conical sound pulses at 2 Hz, averaging data over 10 minute intervals. The sensors measure the time to detect backscatter and calculate distance to the sediment surface, with a reported error of ± 1mm. However, the level of signal damping can significantly alter data precision. The sensors bin and discretize data in 7.5 mm increments, and interpolate more precise data points according to the strength of the backscattered signal. When the signal bounces off of a flat, hard substrate, the sensor records a strong, high confidence data point. These high confidence data points are then interpolated to yield the advertised ± 1 mm precision. However, water turbidity, bed forms, and soft substrate can all dampen the signal, causing the sensor to interpolate less with the collected values. If the environment is noisier, the sensor will only record data with a precision of ± 7.5 mm. While greater accuracy would be ideal, these sensors are capable of capturing long-term sediment trends and yield a fairly continuous data set that shows erosion and deposition rates. When paired with the temporal graphs of wave height, these data sets can portray sediment dynamics along the marsh edge. AA400 sensors were deployed at both site SO7 and SN7, with the deployment shown in Table 1.

Figure 7: Deployment of the AA400 unit. It is suspended 0.5 above the sediment surface via an aluminum frame

Deployment	Date	Location	Measurement	Instruments
1	Jan–Feb 2023	S4	Flow Velocity	Aquadopp (SN4, SN7, SO7)
2	Jun–Jul 2023	S7	Wave Height, Water Depth	RDR Duo (SN7, SO7)
3	May–Jul 2024	S7	Wave Height, Water Depth, Sediment Transport	RBR Duo (SO7), AA400 (SN7, SO7)
4	Jul–Sep 2024	S7	Wave Height, Water Depth, Sediment Transport	RBR Duo (SO7), AA400 (SO4, SO7)

Table 1: Deployment timeline for all instruments at Wachapreague Marsh

v. Marsh Boundary Morphology

As part of efforts to monitor morphological changes at Wachapreague Marsh, TNC has been monitoring and mapping lateral shoreline changes over time at Wachapreague Marsh. Bieri utilized historic satellite imagery and aerial photographs to create marsh perimeter outlines between 1994 and 2021. Between 2022 and April 2024, GPS survey rods were used to record the marsh perimeter. To continue this data set, the marsh platform boundary at Wachapreague Marsh was surveyed in July 2024 using a Trimble GPS Survey Rod. GPS data points were collected approximately every 10 m along the platform edge, as shown in Figure 8. These results were then superimposed on a satellite image of the marsh with the historic shoreline shapefiles provided by TNC. This provides easily visualization of changes in marsh morphology, as well as how those trends vary both spatially and temporally.

Figure 8: Use of the Trimble survey rod in the field. It was used to capture precise GPS coordinates every 10 m along the marsh platform edge

To quantify changes in marsh morphology, as well as lateral marsh retreat rates, the "AMBUR" R package was utilized. AMBUR is a quantitative tool developed to analyze shoreline change. Shapefiles are created to define historic shoreline footprints, and both an inner and outer baseline are drawn to define a "shoreline envelope". AMBUR creates a series of transects between these baselines going across the shorelines, marking each intersection point between shorelines and transect lines. The distance between points is analyzed, yielding various statistics and figures detailing net shoreline change, retreat rates, and overall morphology change. These results were then grouped according to shoreline subsection, and were used to quantify shoreline retreat rates relative to oyster reef presence. An example of how AMBUR constructs transects based on shorelines and baselines is shown below in Figure 9.

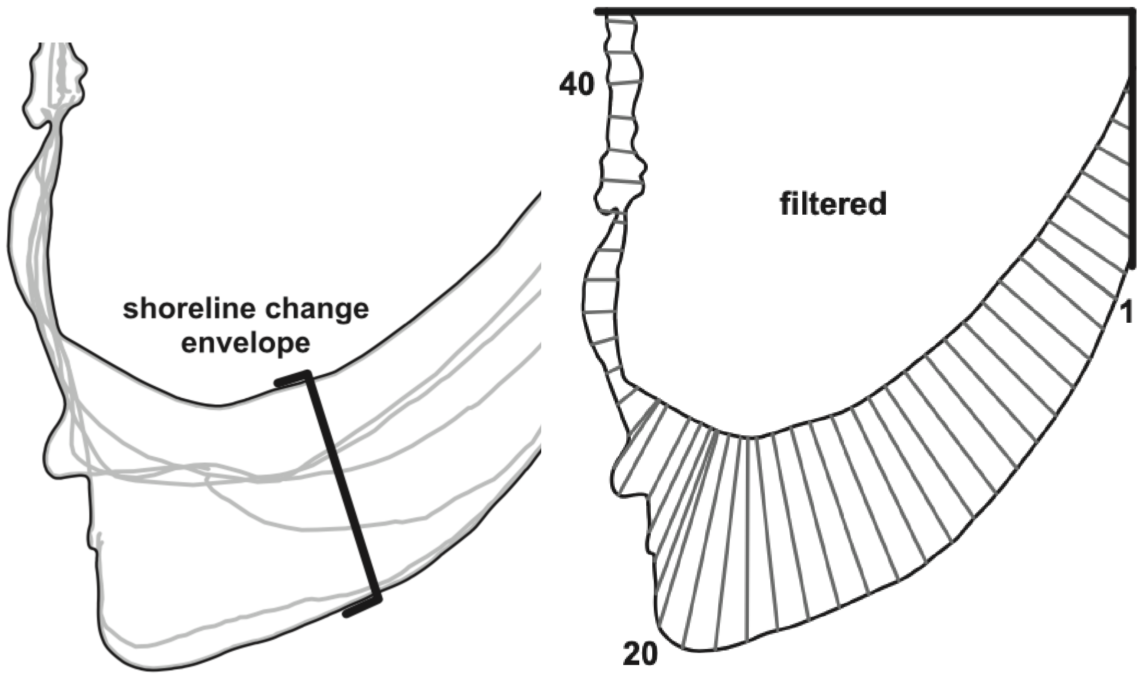

Figure 9: An example AMBUR shoreline analysis from Jackson et al. On the left, the shoreline envelope is established, with the shorelines shown in grey and the baselines shown in black. The transects between the two baselines are shown on the right (Jackson et al, 2012).

vi. Oyster Growth

To understand how effectively oysters grow on different installed substrates, Bieri conducted a series of oyster population and growth measurements between 2020 and 2022 at Wachapreague marsh (Bieri , 2022). To do so, 25x25 cm quadrats were randomly deployed on both the nearshore and offshore reefs. The total number of oysters larger than 2.5 cm within the quadrat was counted, and 15 random oysters were selected and had their length measured. From this, the density of oysters per square meter can be extrapolated, revealing the rates at which new oysters colonize reefs and existing oysters grow in size.

During both July of 2023 and July of 2024, these measurements of oyster density and growth rates were repeated at the S7 nearshore and offshore reefs using the same methods as Bieri et al. This reveals long-term reef health and growth metrics, showing how these trends may be changing as the reefs mature. Depending on flow characteristics and the reef's location relative to incoming flow, these trends may vary significantly.

C. Results

i. Flow

As detailed in Table 1, Aquadopp sensors were deployed both offshore and onshore at site 4, recording both water depth and velocity profiles over time. Offshore peak velocities were near the water's surface, and reached values of 20 cm/s, as visualized in Figure 10. However, velocities averaged approximately 12-14 cm/s throughout the water column. Nearshore velocities were heavily attenuated by oyster reefs, having an average velocity of approximately 4 cm/s, as visualized in Figure 11 and 12.

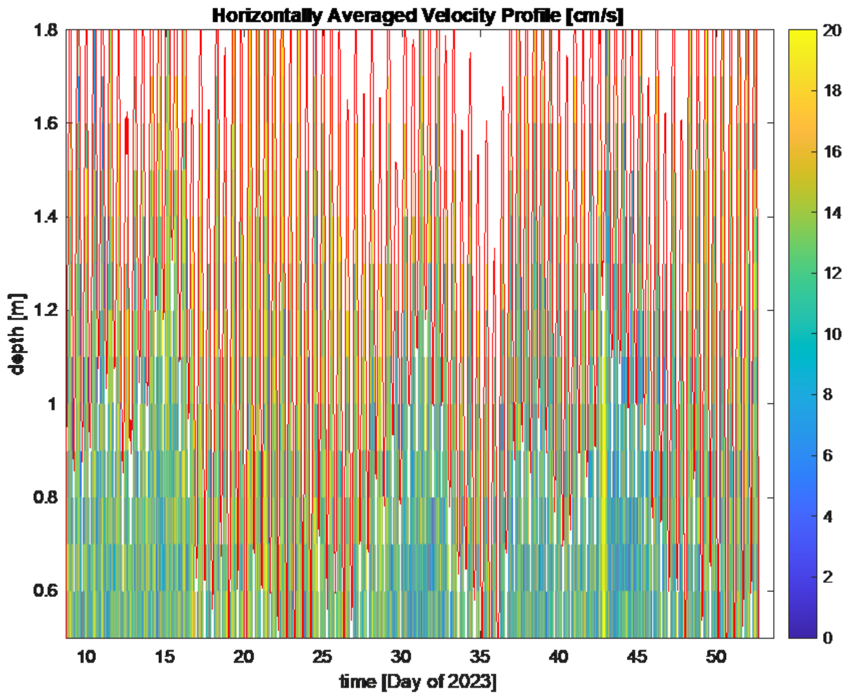

Figure 10: Offshore velocity throughout water column at site SO7. Velocity values are on average about 12-14 cm/s, with peak values being upwards of 20 cm/s. Average water depth was approximately 1.4 m across the dataset.

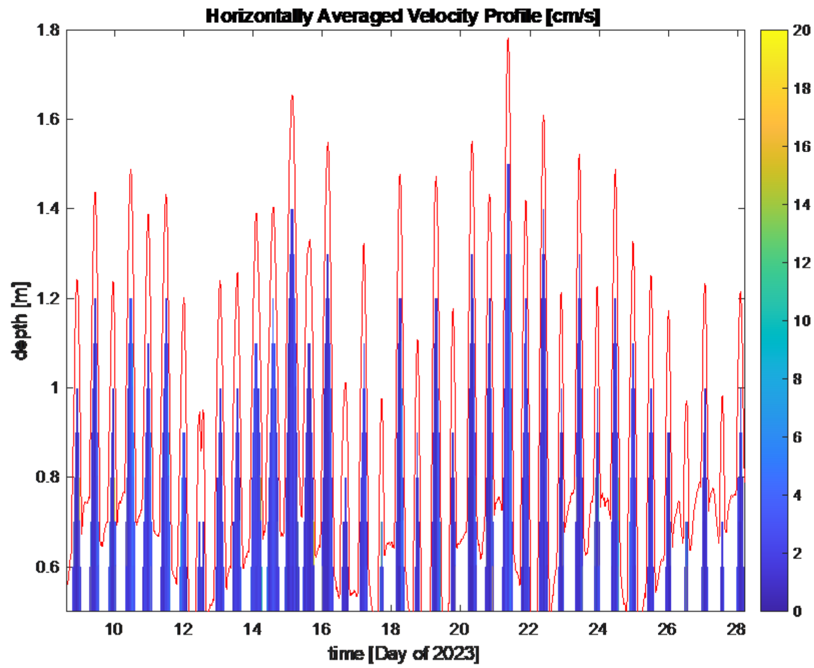

Figure 11: Nearshore velocities and water depths at SN7. Peak high tide water depths were approximately 1.5-1.8 m, and water velocities had peak values of approximately 4 cm/s. Average water depth was approximately 0.8 m across the dataset.

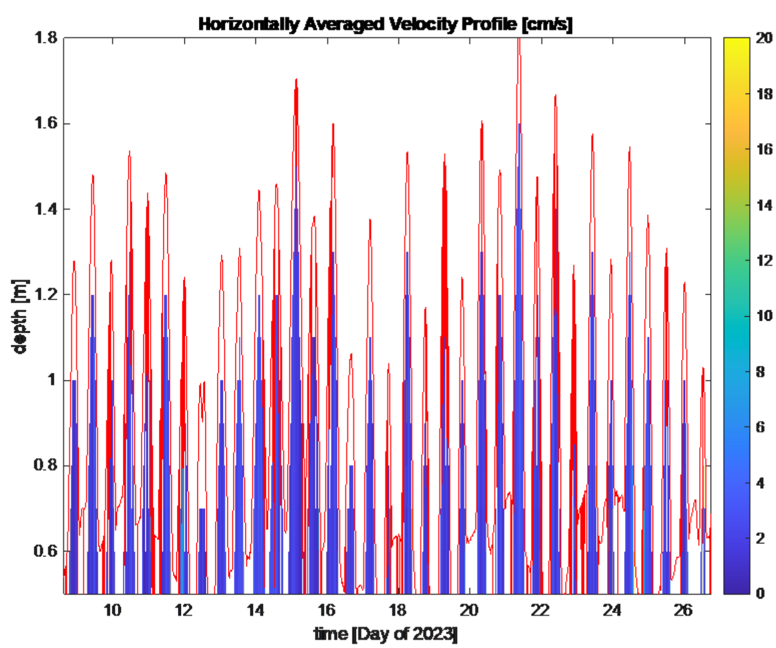

Figure 12: Nearshore velocities and water depths at SN4. Peak high tide water depths were approximately 1.5-1.7 m, and water velocities had peak values of approximately 4 cm/s. Average water depth was approximately 0.8 m across the dataset.

Figure 13 quantifies the reduction in flow velocity 50 cm above the bed surface due to oyster reef presence. It was found that reefs frequently attenuated flow between 70%-95%. While velocities will inherently be lower during slack tide, these attenuation effects are present regardless of tidal phase.

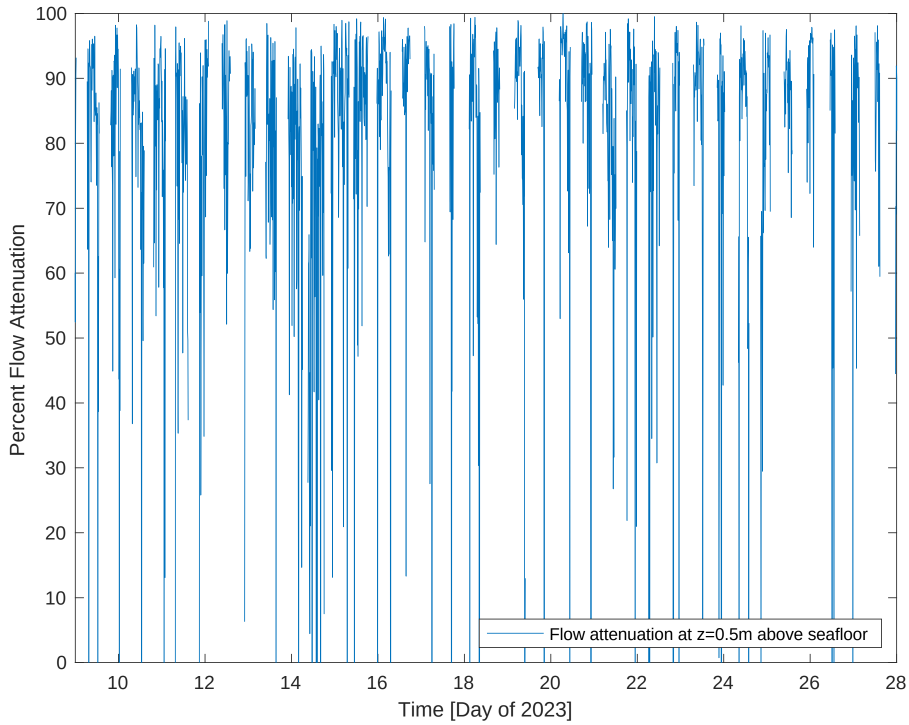

Figure 13: Percent flow attenuation when comparing flow rates at SO7 and SN7 50 cm above the bed surface

ii. Wave Height

Despite issues with biofouling, the Ruskin RBR Duo sensors successfully quantified wave height and water depth over time. Full datasets showing water depth and wave height are visualized in Figures 14, 15, 16, and 17. Peak high tide values varied between 1.5 and 2 m, while low tide varied between approximately 0.2 and 0.5 m. Wave height distribution was highly periodic, with condensed periods of both heightened waves and little to no waves. During these spikes, wave height frequently passed 0.2 m, with peak values reaching 0.32 m. To better interpret wave height and water depth variations across time, a small subsection of data is plotted in Figures 18 and 19 to visualize these high energy and low energy wave events.

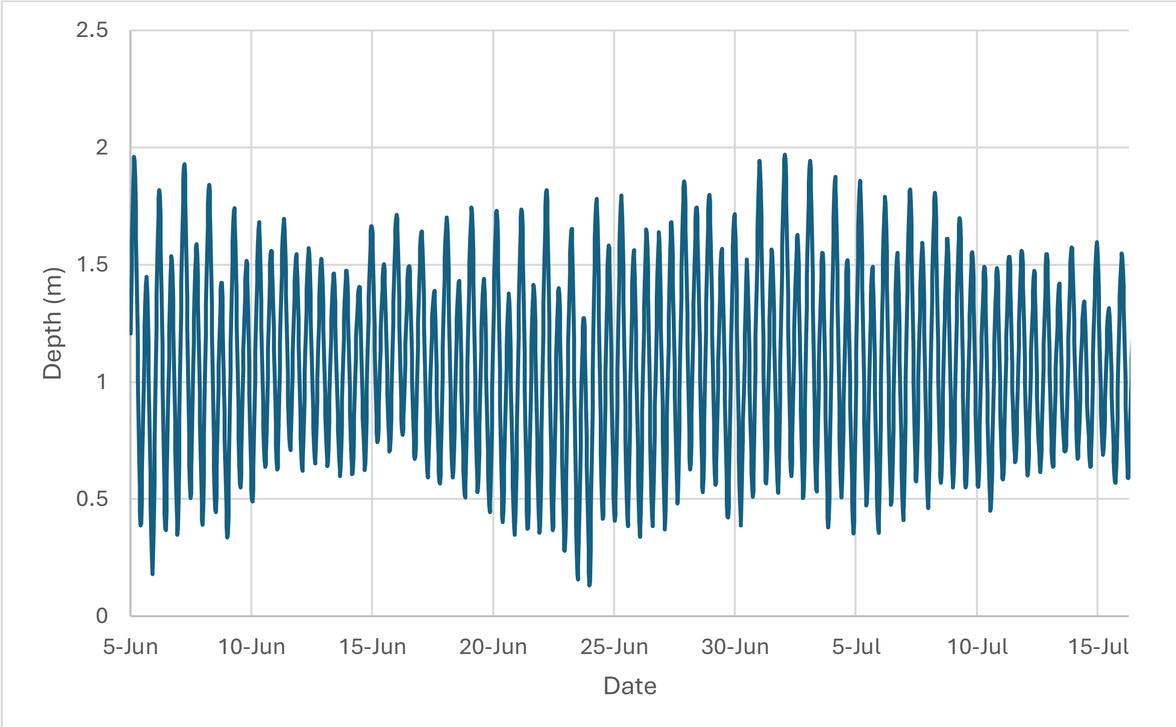

Figure 14: Water depth at SO7 during June-July 2024

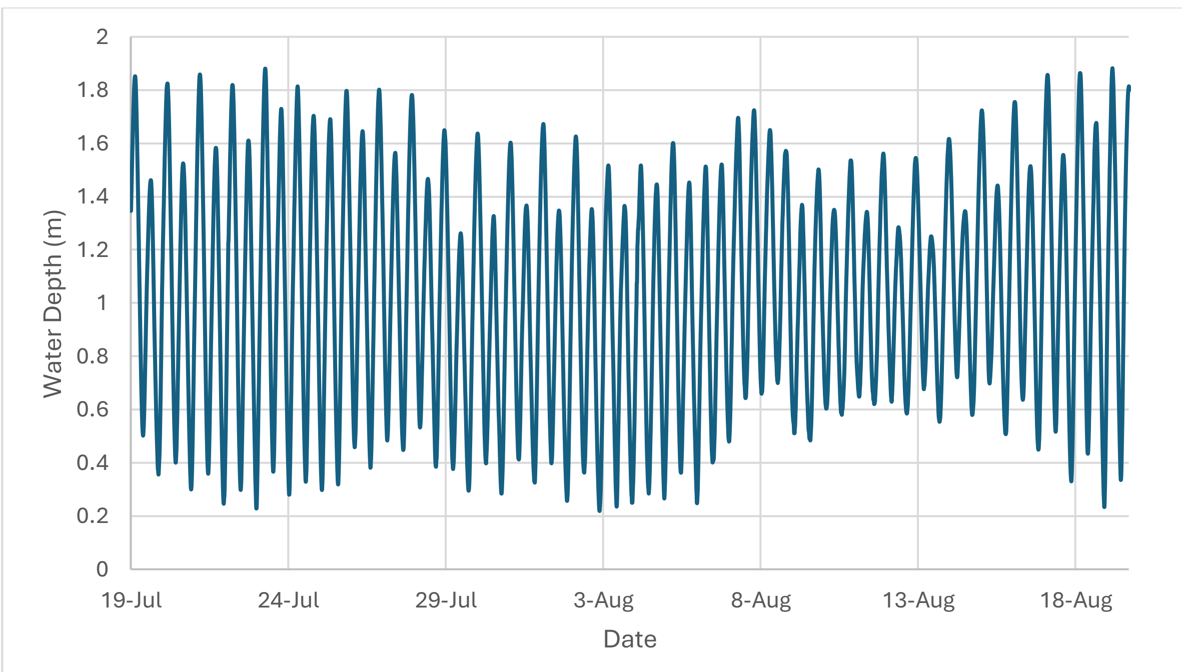

Figure 15: Water depth at SO7 during the July-August deployment

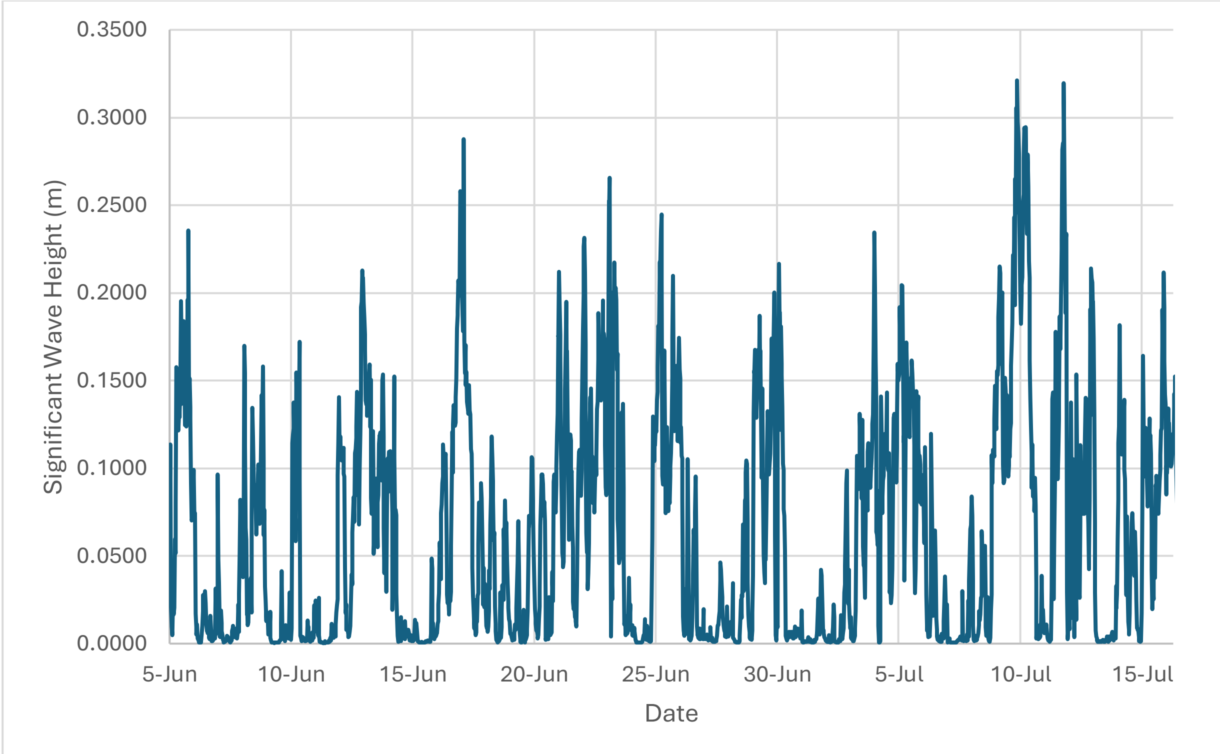

Figure 16: Significant wave height at SO7 during the June-July deployment

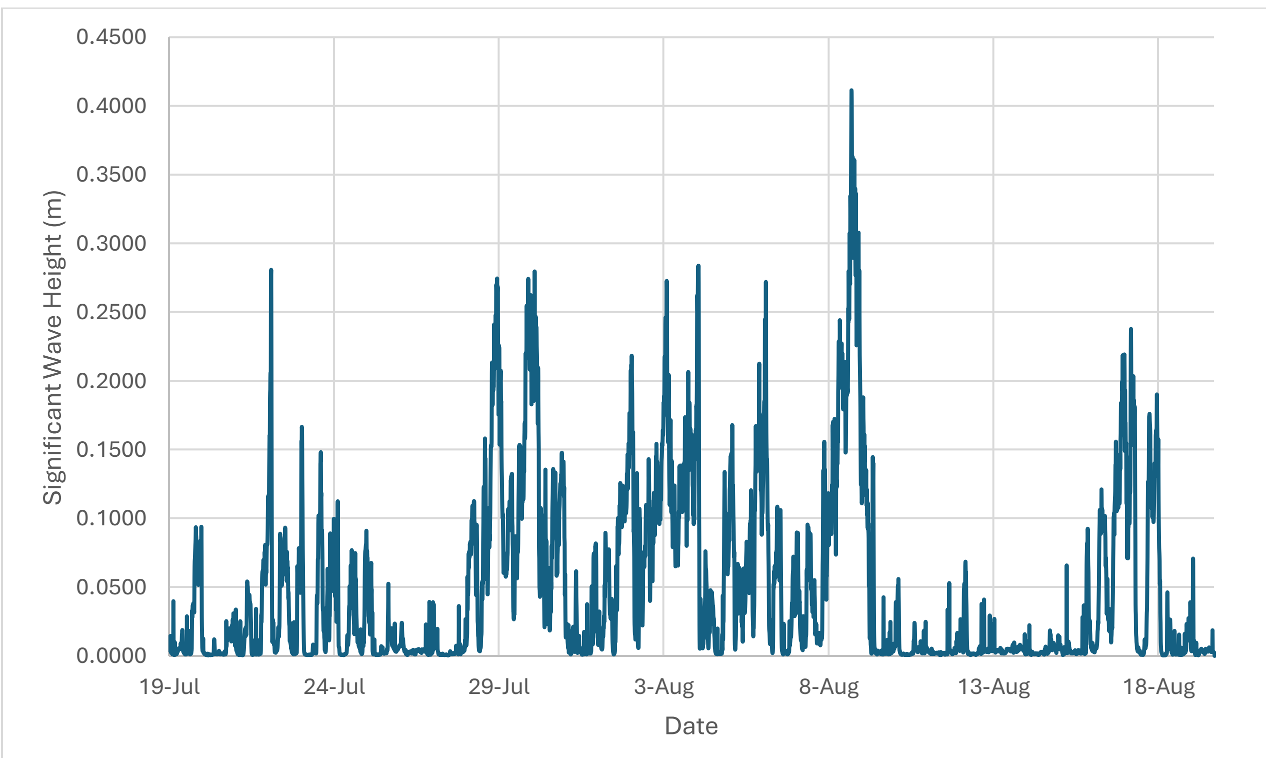

Figure 17: Significant wave height at SO7 during the July-August deployment

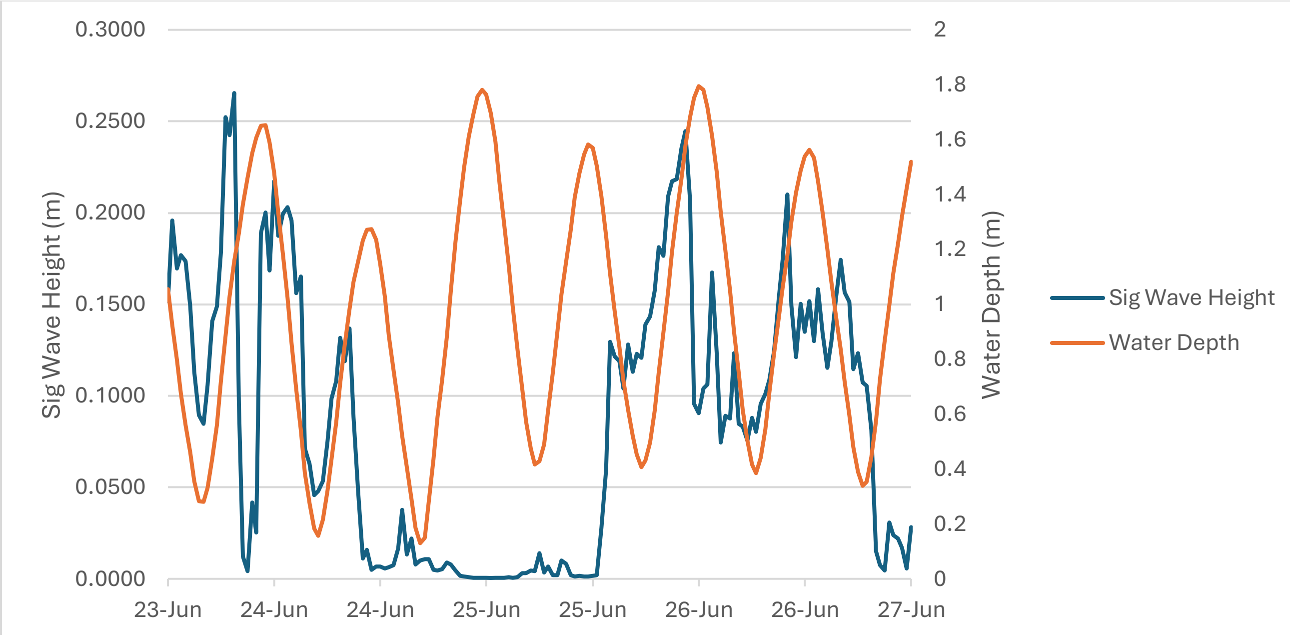

Figure 18: A high energy wave event captured at SO7. Peak wave height is approximately 0.16 m during this period

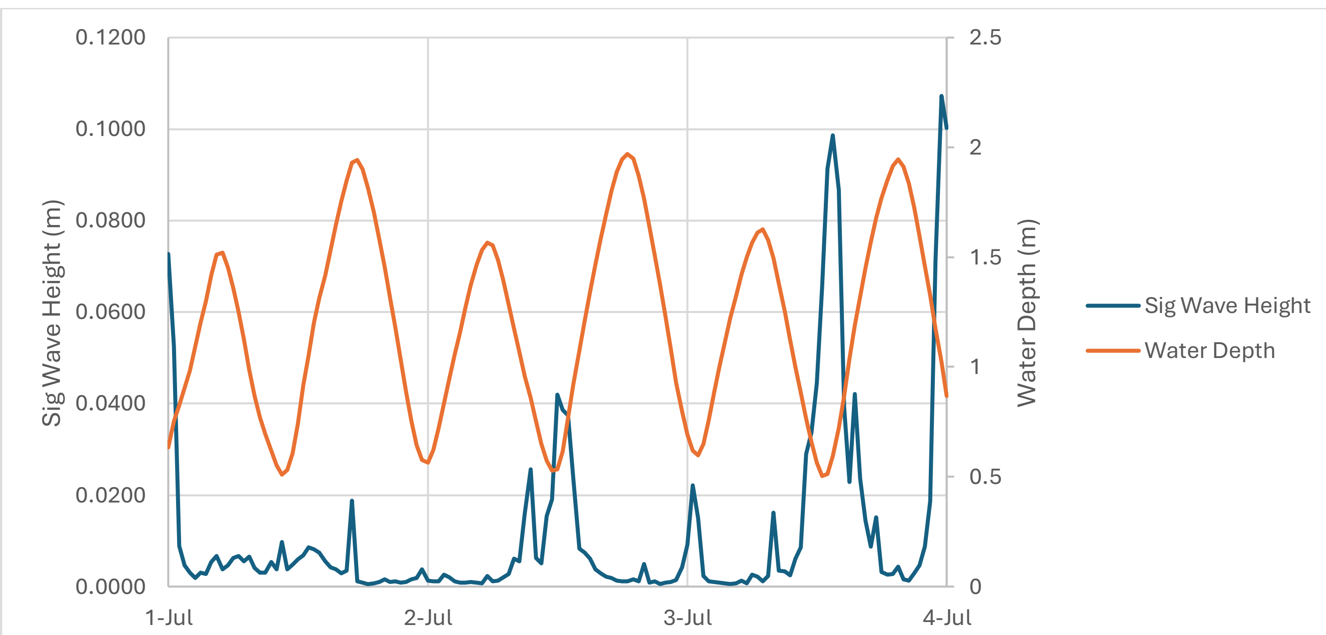

Figure 19: A low energy wave event captured at SO7. Peak wave height only climbs up to 0.06 m at the end of the dataset.

Significant wave height was plotted as a function of water depth at site SO7 as visualized in figure 20, revealing a positive correlation between the two. Deeper water depths are directly correlated with higher wave heights at Wachapreague Marsh, with waves over 30 cm in height occurring at depths greater than 1 m.

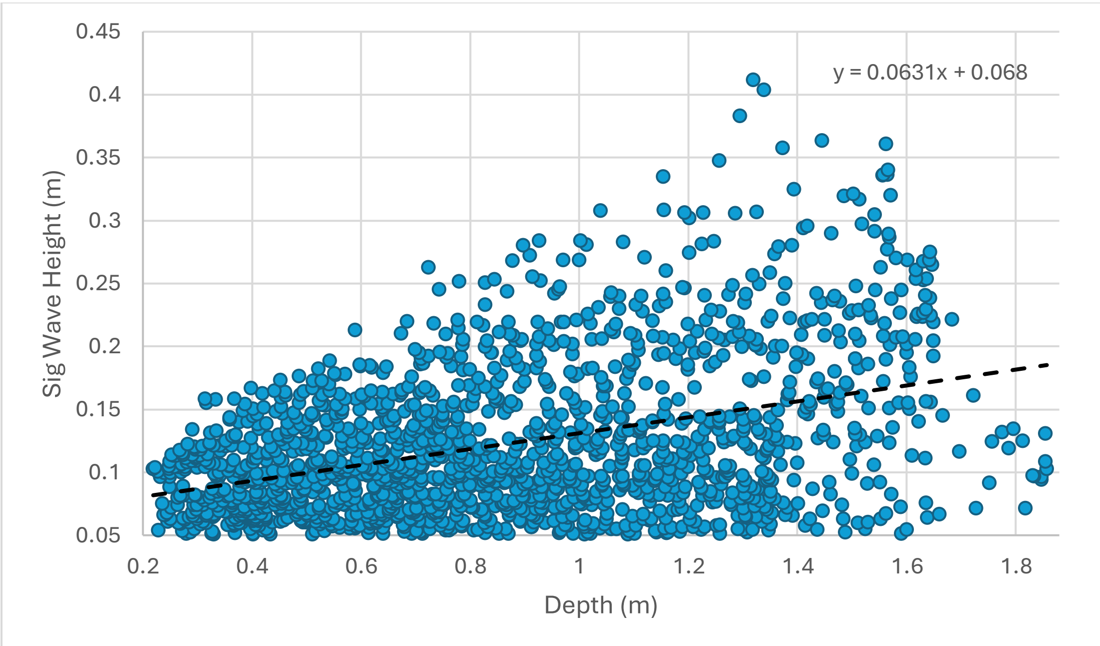

Figure 20: Significant wave height at SO7 as a function of water depth. Waves < 5 cm height were filtered from the dataset

Given the wave attenuating potential of oysters reefs, wave heights at SN7 were plotted against wave heights at SO7 to examine how waves change as they pass over the oyster reefs. Waves were grouped according to water depth above reef crest height, revealing the attenuating effects of oyster reefs on incoming waves across the tidal cycle. The data showing wave attenuation across various depths is visualized in Figures 21, 22, and 23. When water depth was less than 0.25 m, between 0.25 and 0.5 m, and greater than 0.5 m above reef crest height, there was always an increase in Hs as waves pass over the oyster reefs. This effect increases as water depth above crest height increases.

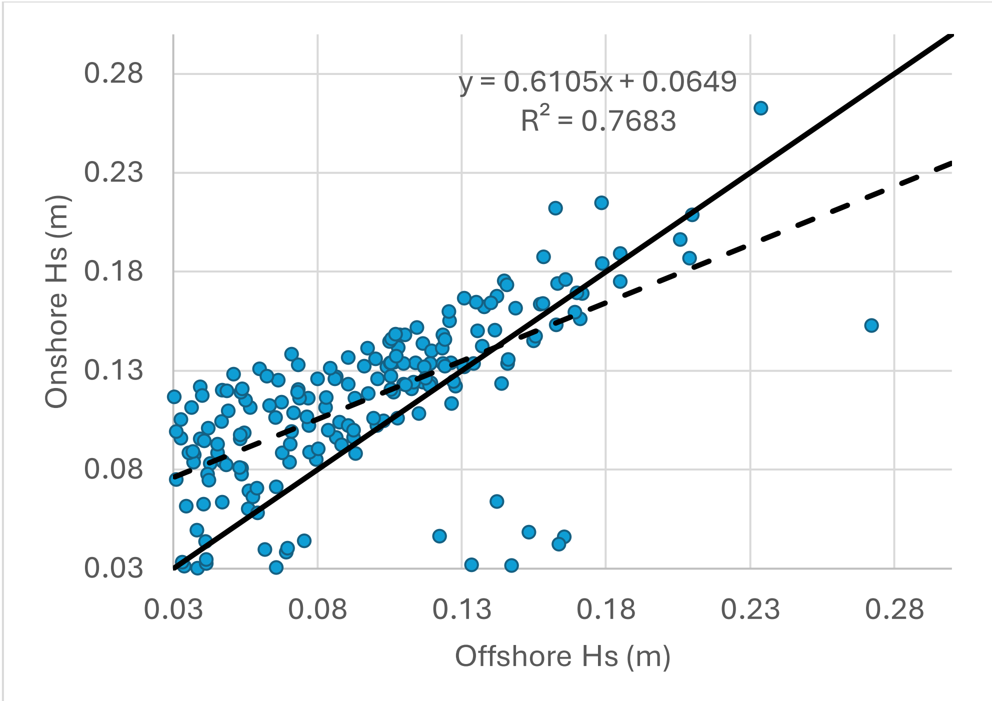

Figure 21: Offshore vs onshore significant wave height when water depth is < 0.05 m above reef crest height

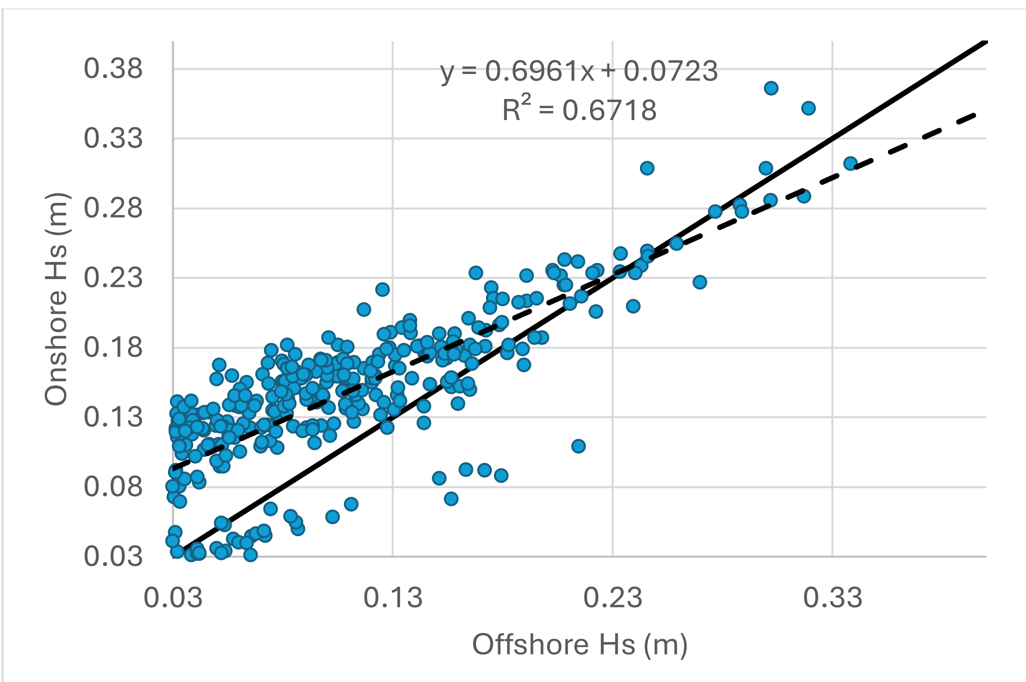

Figure 22: Offshore vs onshore wave height when water depth is between 0.05 m and 0.25 m above reef crest height

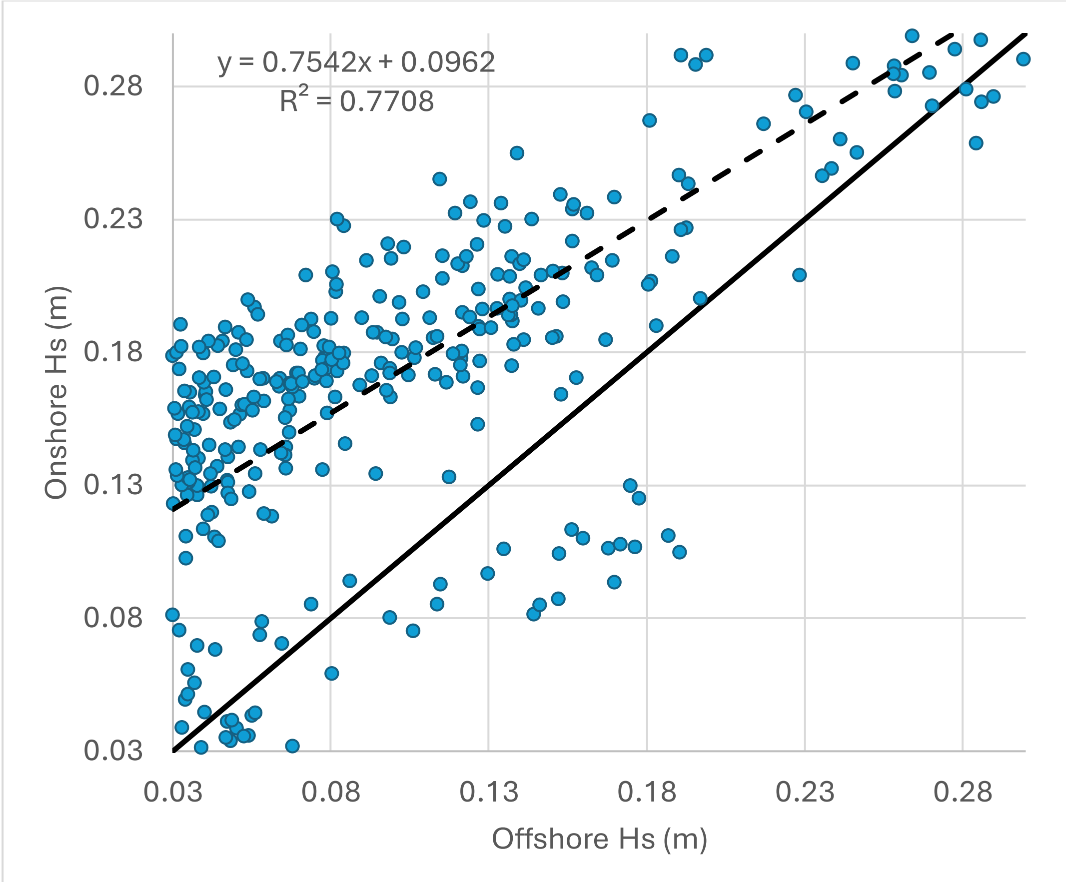

Figure 23: Offshore vs onshore wave height when water depth is greater than 0.25 m above reef crest height

iii. Turbidity and Sediments

In addition to measuring waves, the RBR Duo sensors measure turbidity as well. Turbidity was monitored both at SO7 and SN7 during summer of 2023, but was only monitored at SO7 during summer of 2024. 2024 data is visualized below in Figures 24 and 25. Generally, turbidity levels stayed at or near zero NTU, but high wave height drastically increased these values. During most high wave events recorded, turbidity rapidly increased as wave height increased, typically reaching values of anywhere between 150 and 300 NTU, depending on the severity of the spike in wave height.

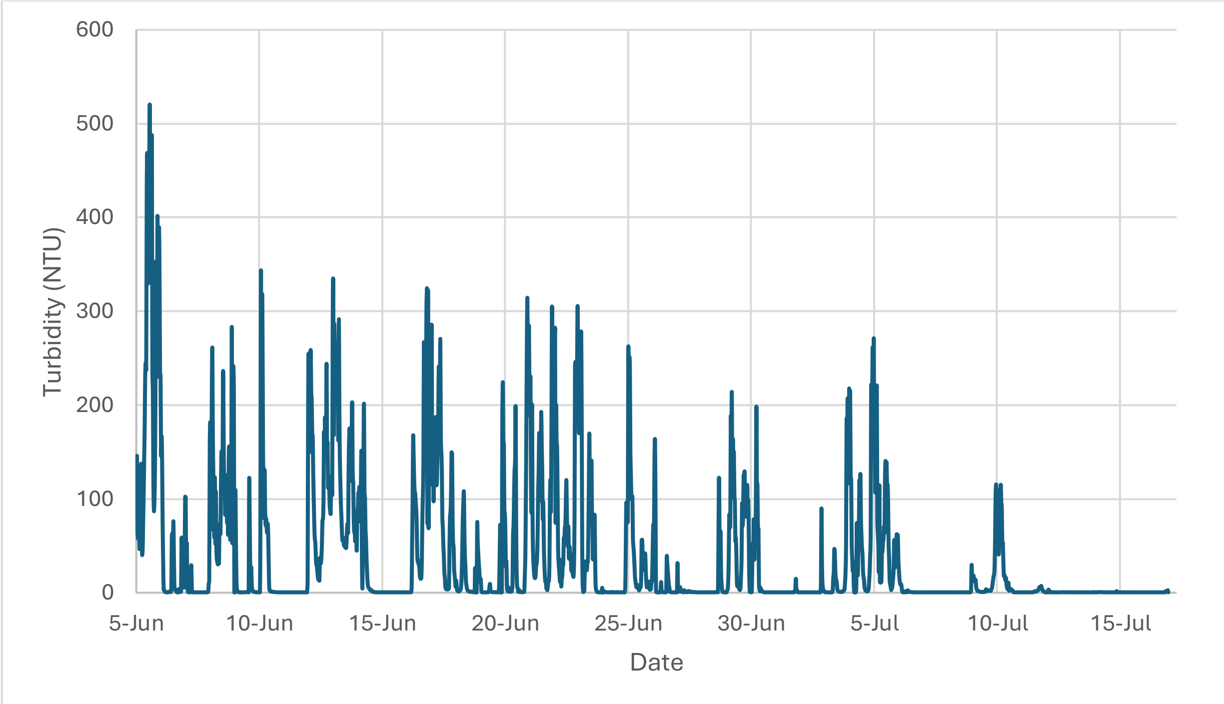

Figure 24: Turbidity from June to July of 2024 At SO7

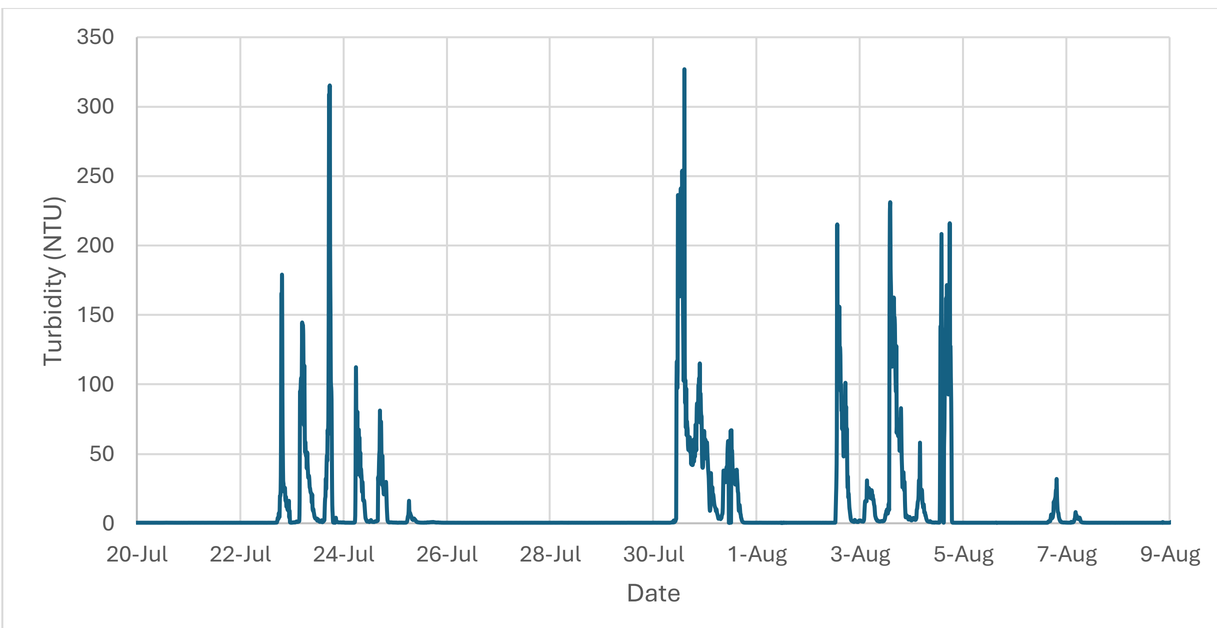

Figure 25: Turbidity from July to August of 2024 at SO7

Since it is theorized that turbidity levels at Wachapreague marsh are link with wave energy, turbidity was plotted as a function of significant wave height during summer of 2024, as visualized in Figures 26 and 27.

There is a clear correlation between the two values, with 0.3 m high wave creating an average turbidity of between 65 and 162 NTU.

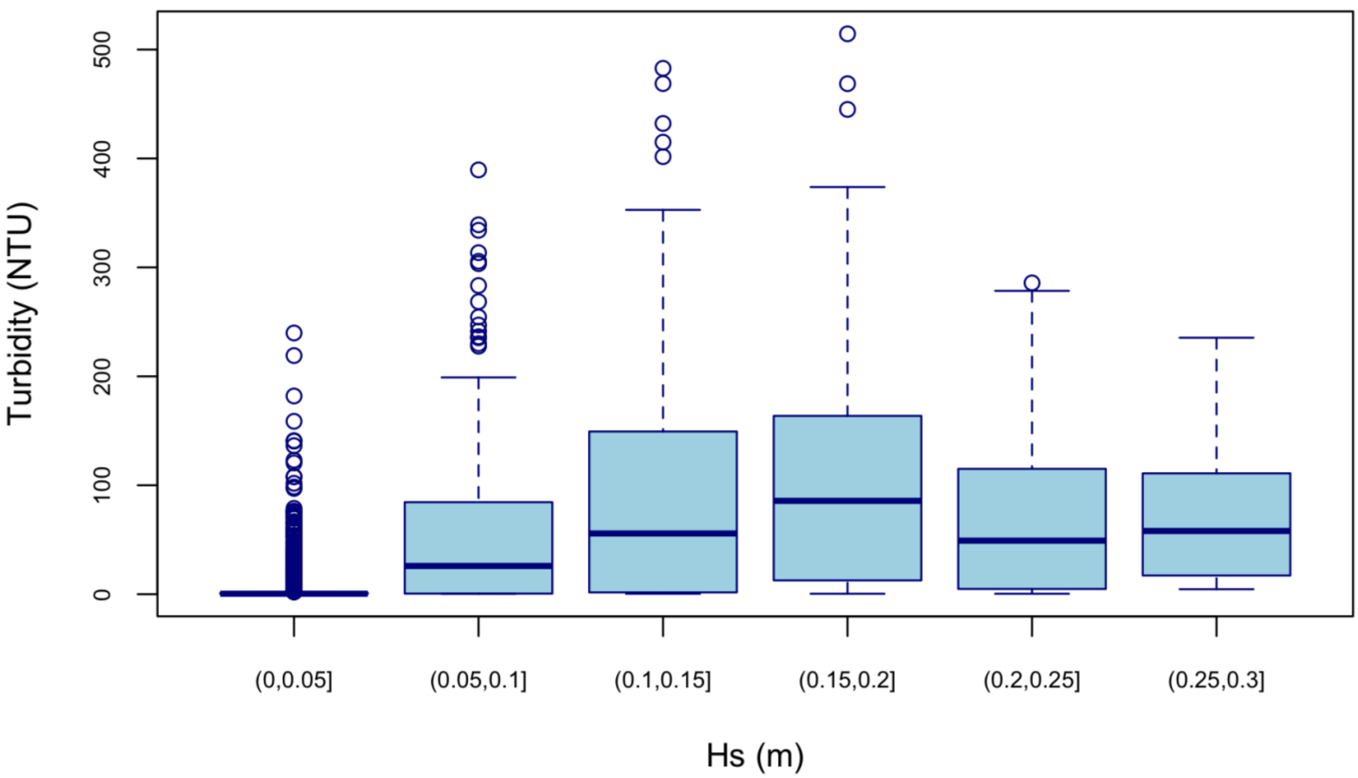

Figure 26: Turbidity as a function of significant wave height at SO7 during the July 2024 deployment. There is a strong positive correlation, with nearly 100 NTU being observed between 0.15 m and 0.2 m wave height

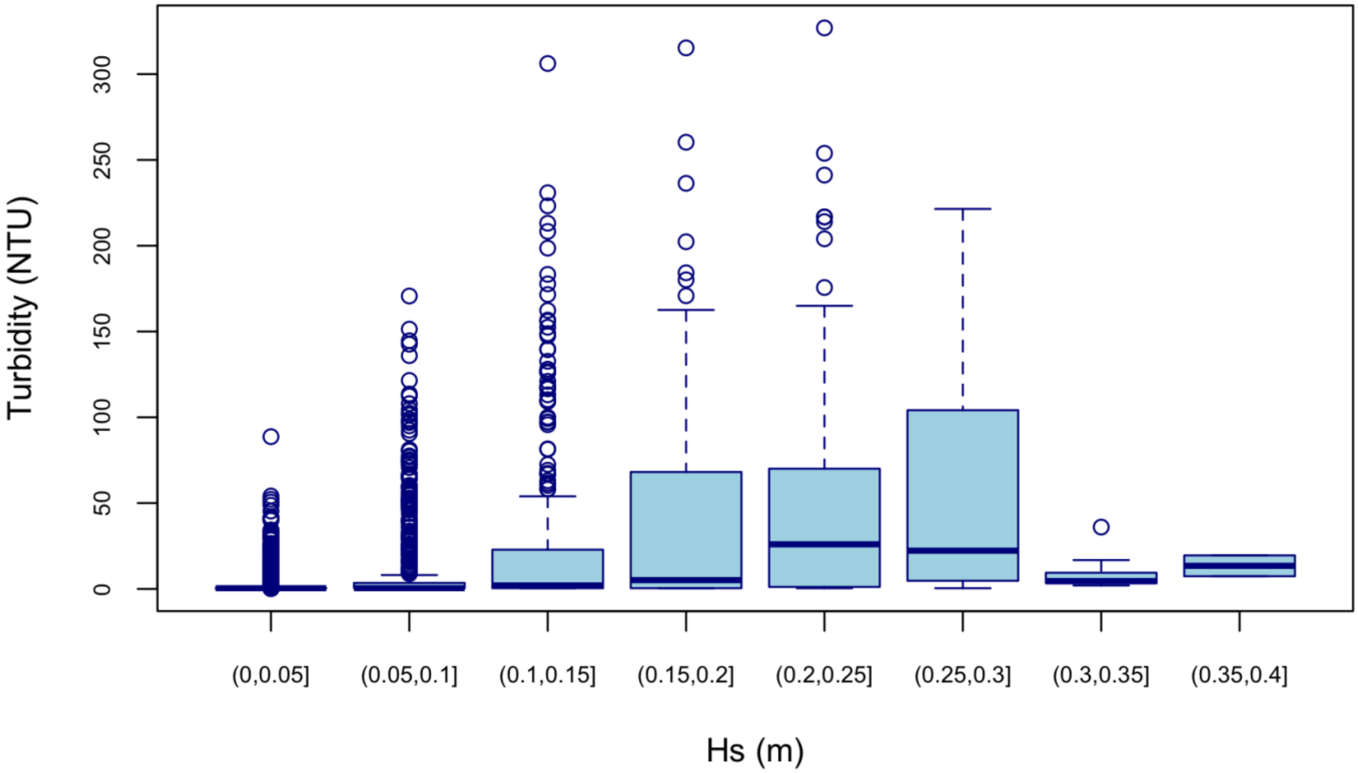

Figure 27: Turbidity as a function of significant wave height at SO7 during the September 2024 deployment. NTUs between 40 and 50 occur frequently at wave heights of 0.2 m to 0.25 m

Initially, there was significant concern regarding the reliability and accuracy of the Echologger sensors. It was unknown whether they would work in an intertidal area, as they are generally used in deep water locations where the sensor head is never exposed during low tide. Additionally, preliminary field tests yielded noisy data that was difficult to interpret. The sensors were tested in a controlled lab environment, with results visualized below in Figure 28 showing that the AA400 units can record depth with a precision of ± 1 mm under ideal conditions.

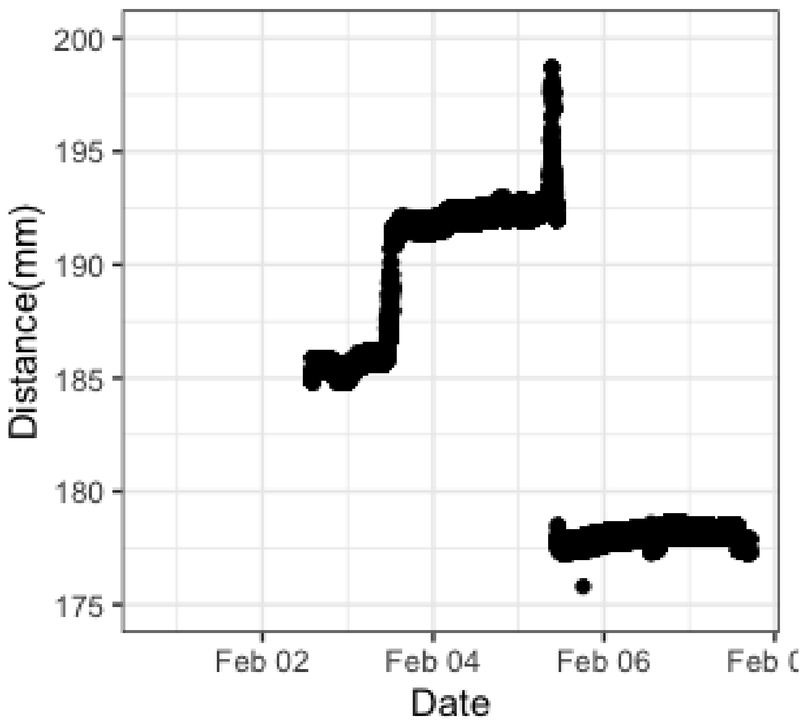

Figure 28: Lab tests of the AA400 sensor accuracy. The sensor was placed in a glass tank full of water, and sand was incrementally added or subtracted from the bottom. There is a very small amount of noise in the dataset, yielding accuracy of ± 1 mm

The Echologger altimeters were successfully deployed during the summer of 2024. Visualized below in Figures 29, 30, 31, and 32 are the sediment dynamics at both SO7 and SN7 at Wachapreague Marsh. The figures show distance between the sensor head and the bed surface, meaning that a positive trend indicates erosion, while a negative trend indicates deposition. From the figures, it can be seen that the nearshore site experienced nearly a centimeter of erosion between June and July, while the offshore site experienced approximately a 6 mm of accretion between July and September. The AA400 sensors did discretize and bin data in approximately 7.5 mm increments, which explains the sudden shifts in recorded bed height.

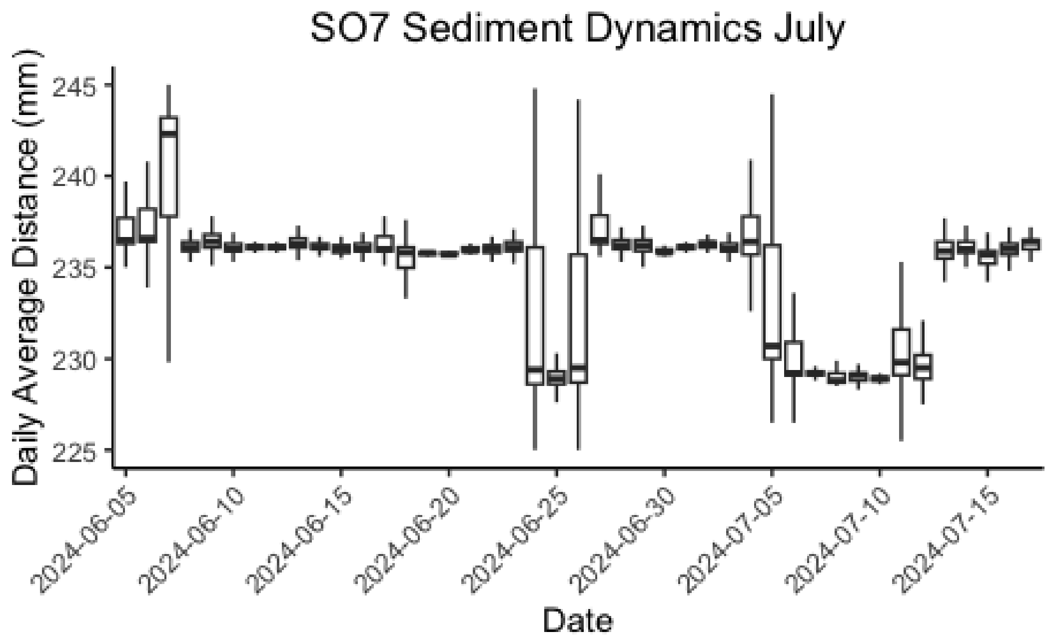

Figure 29: Offshore sediment dynamics between June 5 and July 17, 2024. There were periods of erosion and deposition, but no net change in bed height

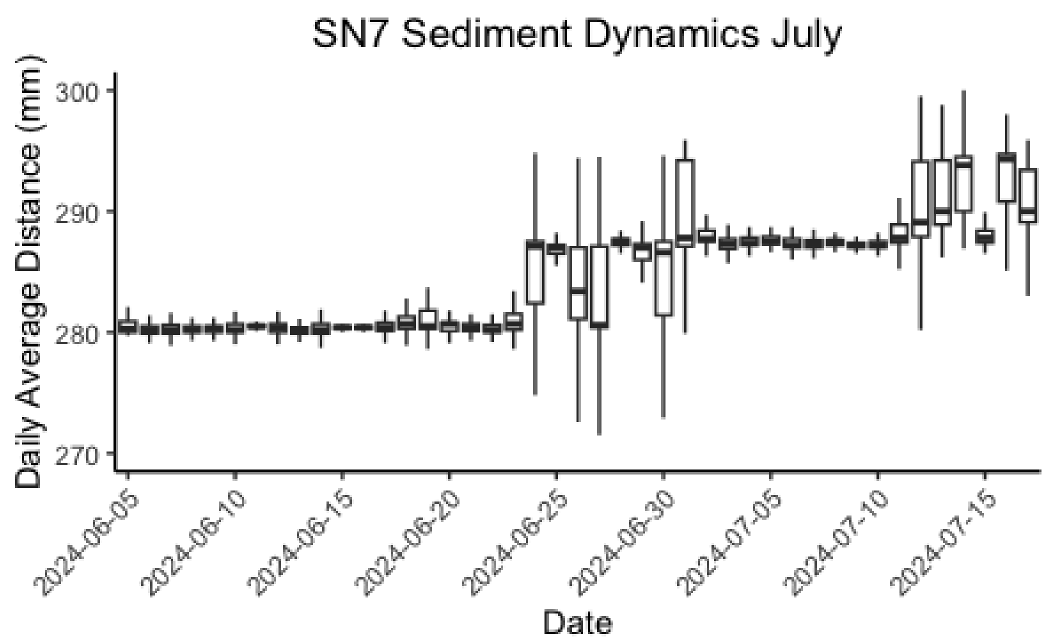

Figure 30: Onshore sediment dynamics between June 5 and July 17, 2024. There was approximately 1 cm of bed erosion observed

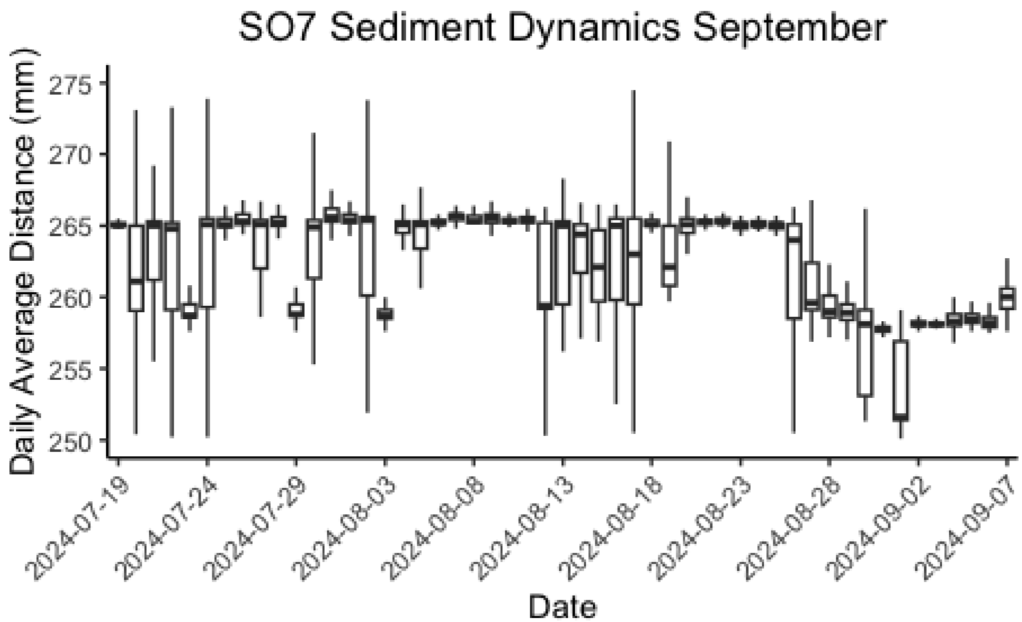

Figure 31: Offshore sediment dynamics between July 19 and Sep 7, 2024. There was approximately 6 mm of bed accretion observed.

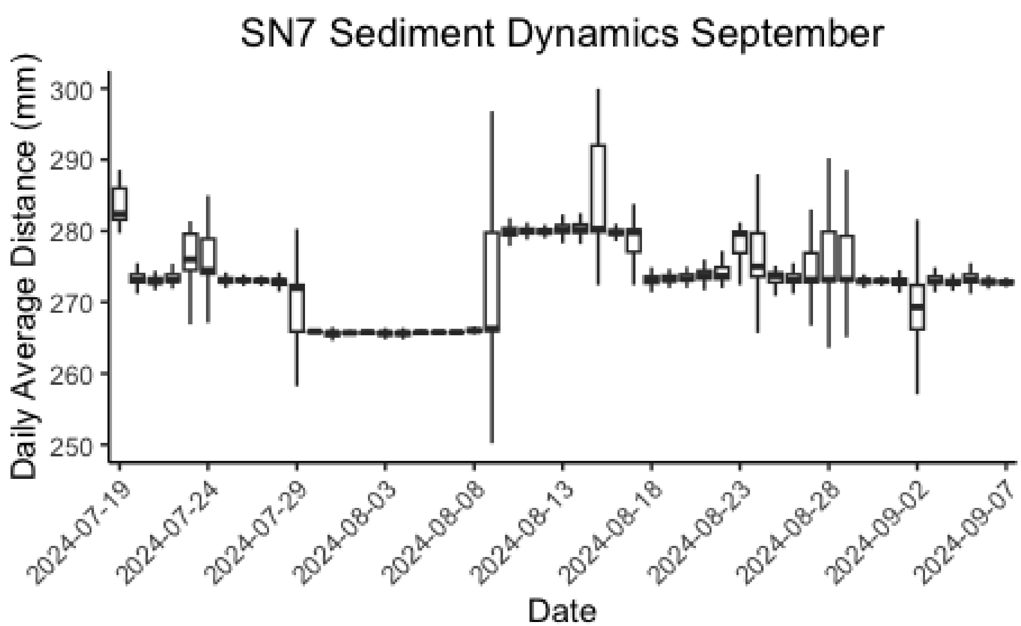

Figure 32: Onshore sediment dynamics between July 19 and September 7, 2024. Despite several shifts in bed height, there was no net erosion recorded

iv. Shoreline Morphology

The updated marsh perimeter shapefiles have been compiled together into a single GIS map, as seen below in Figures 33 and 34. These maps show Wachapreague Marsh's current perimeter as overlayed against historic shorelines dating by to 1994. There are notable spatial disparities in lateral erosion around the perimeter of the marsh. Particularly it is notable how the western portion has receded significantly more relative to other, more protected, parts of the island.

Figure 33: The first and last shoreline on record for Wachapreague Marsh. The town of Wachapreague is located to the north, and to the south is Bradford Bay, a large open lagoon.

Figure 34: A layout showing all the historic marsh shorelines on record.

Inner and outer baselines were established around the marsh perimeters, allowing an AMBUR analysis to be conducted. AMBUR yielded results quantifying overall lateral shoreline retreat, as visualized in Figures 35. On average, the northern boundary of the island experienced an average annual net erosion rate of ~0.64 m per year (not plotted), while the southern boundary experienced an average annual net erosion rate of ~1.37 m per year. However, it should be noted that both shorelines experienced interspersed instances of marsh growth, averaging about 0.20 m per year for the northern boundary and about 0.08 m per year for the southern boundary.

Figure 35: A representation of net shoreline change between 1994 and 2024. Red indicates net erosion, while blue indicates net accretion. The length of each transect line represents the amount of shoreline change.

As visualized in Figure 36, the southern shoreline experienced its highest amounts of erosion along its west bank, reaching a peak loss of about 120 m (std = 40 m) between 1994 and 2024. This trend is generally consistent across all transects – standard deviation at any particular point is approximately one third of its associated erosion value.

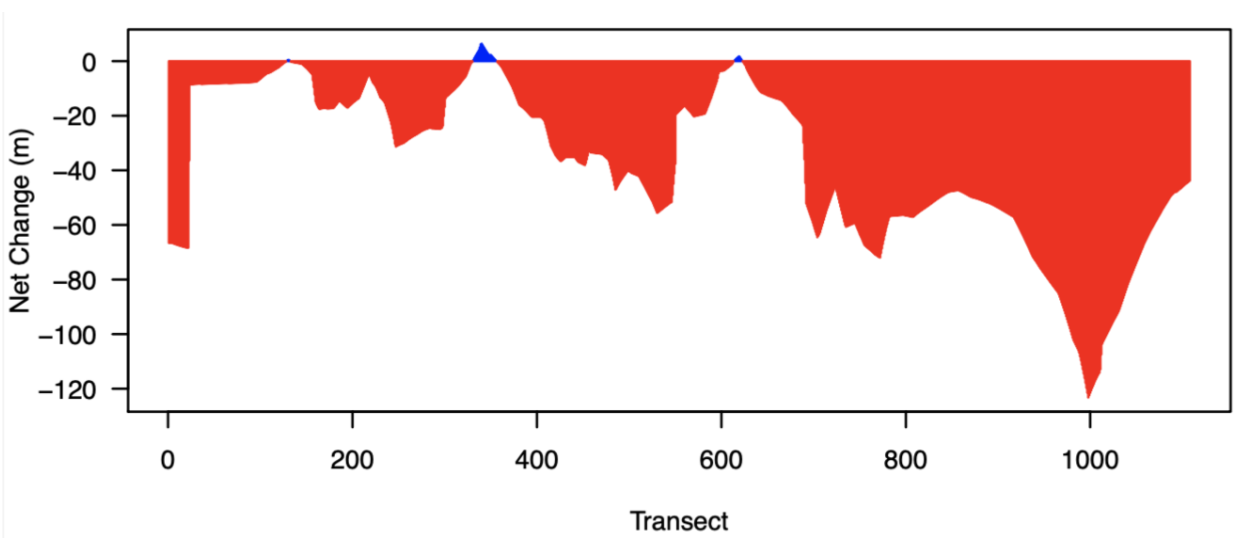

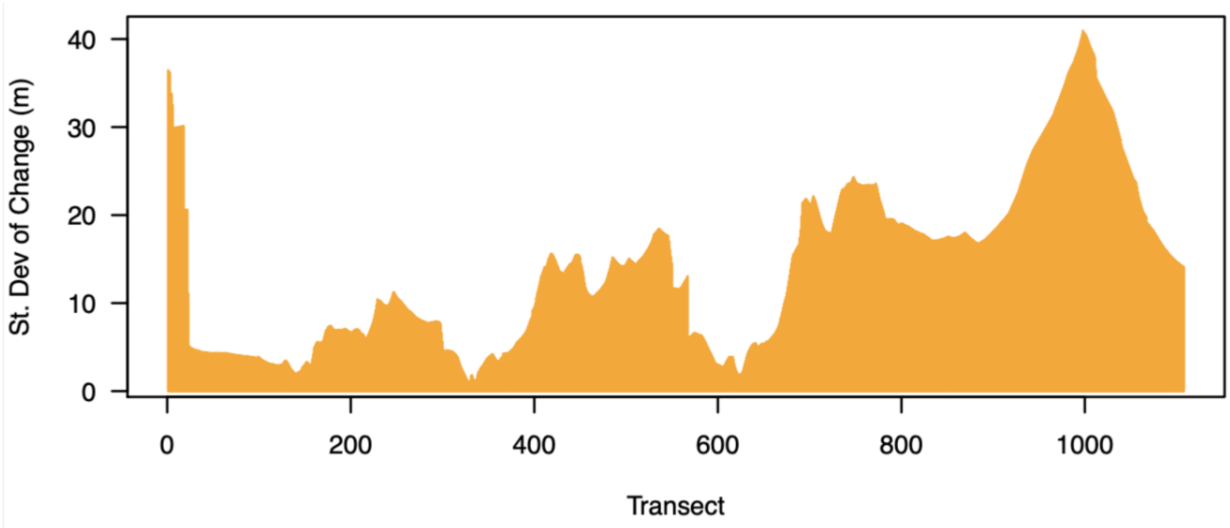

Figure 36: Total change in the southern shoreline across all 1100 transects, as well as standard deviation of those changes. Note that the transects start at the east side of the marsh, and move west in ascending order, meaning these graphs are flipped horizontally relative to cardinal directions.

Overall, the northern shoreline saw dramatically lower rates and amounts of erosion as compared to the southern shoreline, but it still experienced net marsh loss. Erosion peaked at the northwest portion of the marsh, with a total lateral loss of about 42 m between 1997 and 2024. This loss has an associated standard deviation of about 14 m.

Due to error introduced by tight geometric interfaces within AMBUR, data from sites 1 and 2 had to be clipped from the results to discern any meaningful trends. Below in Figure 37, cumulative shoreline loss at each marsh section post reef construction are visualized. Negative values represent marsh loss, and positive values represent marsh accretion. Initially after reef construction, section 9 and 8 showed no shoreline change, while sections 3, 4, 5, and 7 showed trends of up to 2 m of growth. However, erosion resumed at all sites between 2021 and 2023. To better quantify the effects of reef presence on erosion trends, Figure 38 visualizes normalized cumulative change from 1994 to 2020 (pre reef construction), and from 2020 to 2024 (post reef construction). Note that erosion rates are lowered substantially at sites 8 and 9 from nearly 2.5 and 2 m/yr of erosion, to 1.14 and 1.11 m/yr of erosion respectively. Similar trends manifest across the southern shoreline, with the exception of erosion rates worsening at sites 4 and 3.

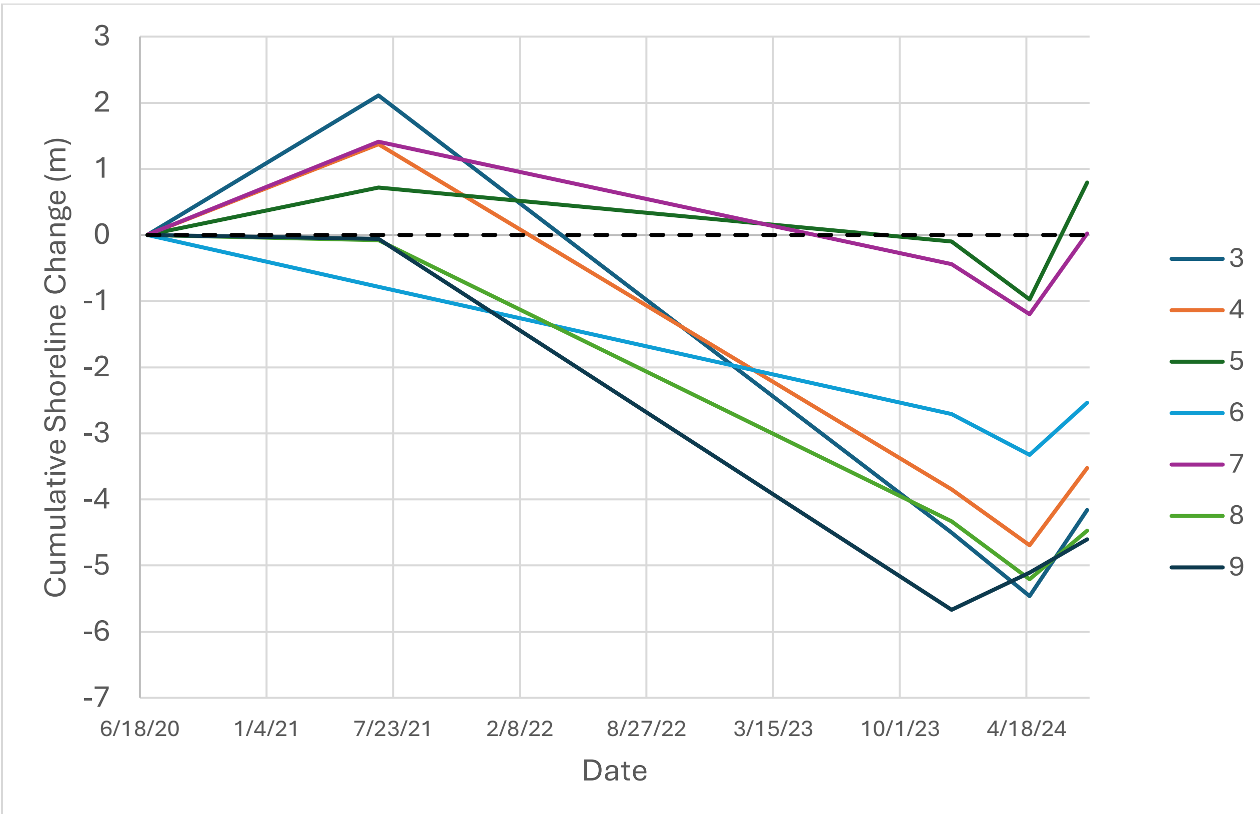

Figure 37: Cumulative shoreline change for each marsh section between 2020 and 2024. Oyster reefs were installed between the initial 0 values and first recorded data point.

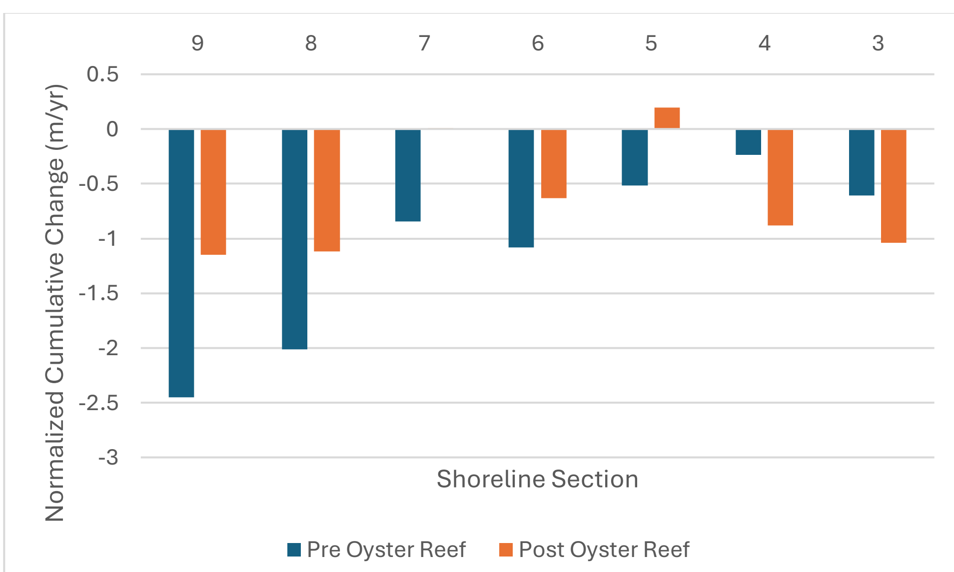

Figure 38: Cumulative shoreline change for each shoreline section normalized across time

v. Oyster Growth

Oyster growth trends can be seen below in Figure 39. Note that shell length seems to be relatively equivalent between 2023 and 2024 for both the nearshore and offshore reefs. While there are some minor trends showing shell lengthening from 62 (std ± 17.1 mm) to 71 (std ± 21.9 mm) mm at the nearshore reefs and shell shrinking from 67 (std ± 20.5 mm) to 64 mm (std ±19.1 mm) at the offshore reefs, the relatively high standard deviation indicates that these trends are not conclusive.

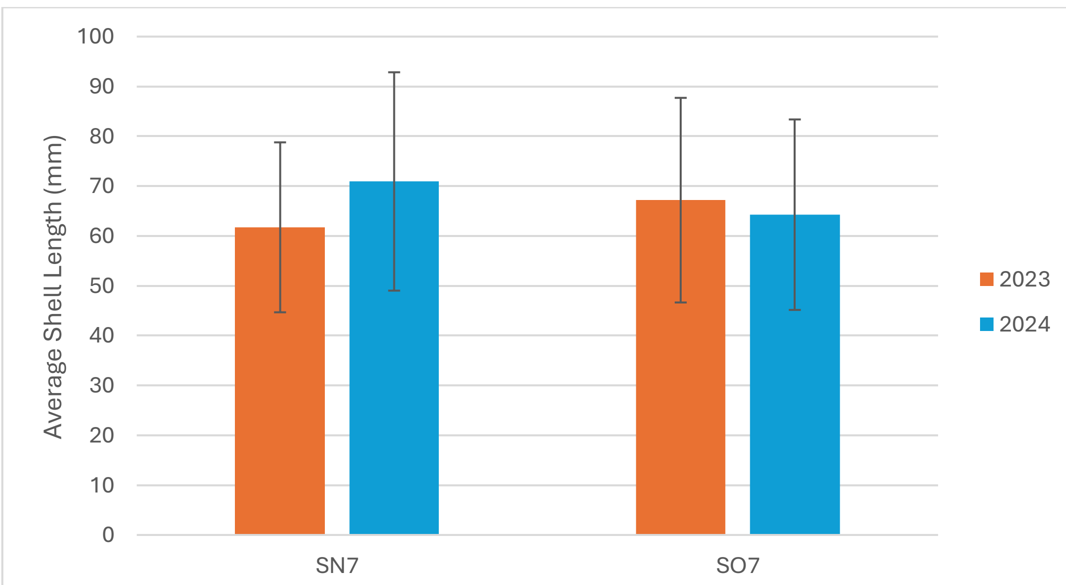

Figure 39: Oyster shell length at both nearshore and offshore reefs at site 7 compared between 2023 and 2024.

Similarly, trends are visualized below in Figure 40 for average oyster population densities at both nearshore and offshore reefs. However, these results are far more significant than those for shell length. Both the nearshore and offshore reefs saw over a doubling in population density between 2023 and 2024, with nearshore growing from 651 oysters/m^2 (std ± 177.0) to 1424 oysters/m^2 (std ± 136.7), and offshore growing from 661 oysters/m^2 (std ± 24.4) to 1301 oysters/m^2 (std ± 237.5). These trends can all be compared to those recorded by Bieri (Figure 41), and it can be seen that average shell length appears to have gone up by approximately 10-15 mm on average, while the population density appears to currently be within previously recorded amounts.

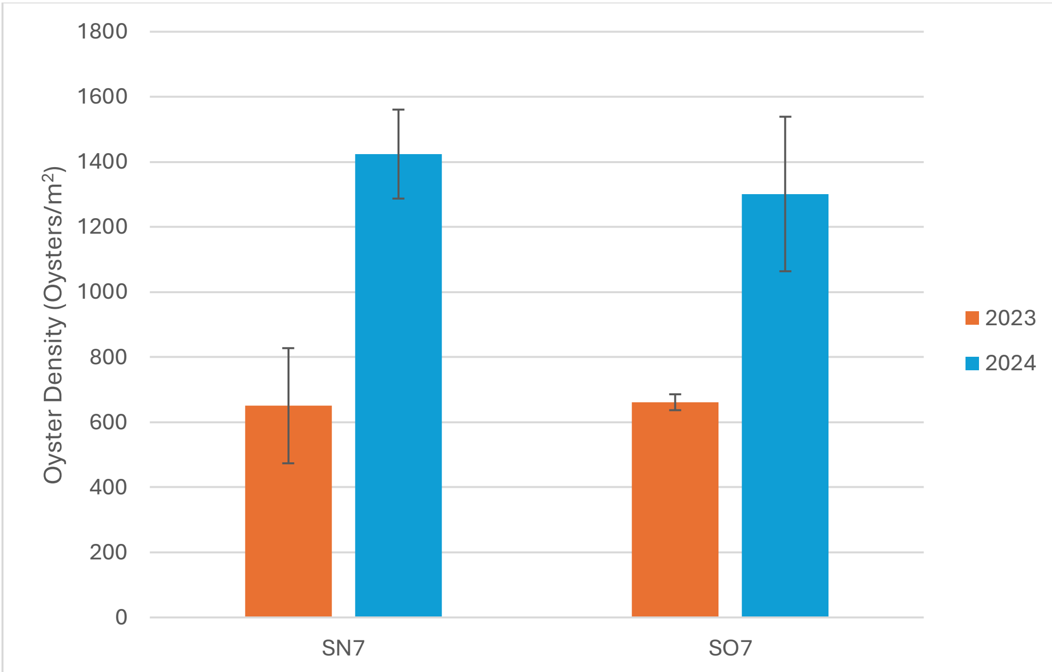

Figure 40: Oyster population density per meter squared at both nearshore and offshore reefs at site 7 compared between 2023 and 2024.

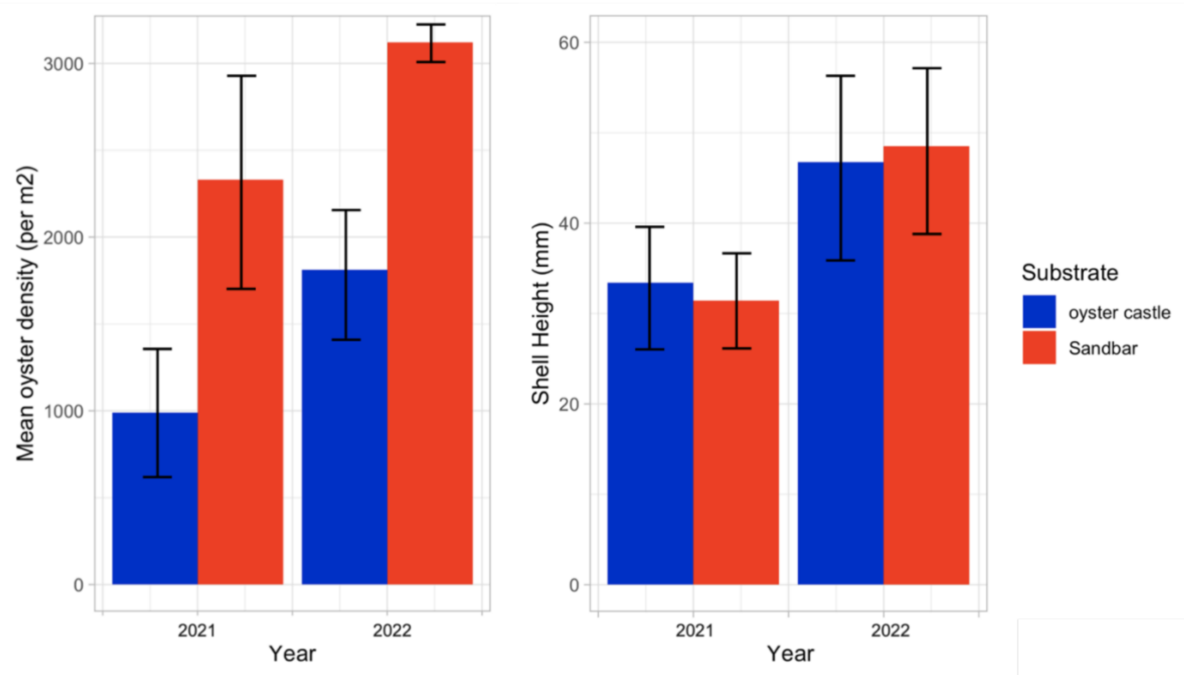

Figure 41: Oyster density and mean shell length at Wachapreague Marsh for 2021 and 2022

D. Conclusions

i. Wave and Turbidity Trends

Average wave height can vary anywhere between 0 and approximately 15 cm in height near Wachapreague marsh, but these higher wave periods tend to happen in consolidated periods of time. Within the back-barrier coastal lagoon system that characterizes Virginia's eastern shore, wind fetch is the main driving force behind wave development. Consequently, it is the windiest days that will have the highest associated wave height. Water depth is directly correlated with wave height, with waves over 30 cm in height appearing at depths over 1 m. This relationship between water depth and wave height agrees directly from wave theory, which states that tall waves form in deeper water (Bishop and Donelan, 1987).

Likewise, oyster reefs significantly alter flow as it approaches the shoreline, especially when grouped by depth above reef crest height. Regardless of depth above reef crest height, there is an increase in significant wave height observed as waves pass over the oyster castles. These trends are most significant when flow is greater than 50 cm above crest height, and decrease in strength as the water depth lessens. Previous work has shown that reefs do have little-to-no attenuation during deep water events (Hogan and Reidenbach 2021, Wiberg et al, 2019; Bieri, 2022). However, it is surprising that there is no attenuation at all during the shallow depth events. This may be due to natural wave shoaling, in which waves increase in height as they approach the shoreline. However, since the Ruskin units collect data via pressure sensors, they will have more difficulty measuring values at the surface when placed in deeper water. The offshore sensors may therefore not be capturing wave data as effectively as the onshore sensors, potentially skewing the datasets.

Since this data suggests that wave attenuation will exclusively be significant when reef crest is at the water surface, oyster castles will be most effective at absorbing wave energy when assembled as taller structures. However, the height of oyster castles is largely limited by the scope of tidal fluctuations, as oysters must be submerged for a sufficient amount of time to ensure adequate growth and survivability. Future oyster castle research should therefore explore the effectiveness various oyster reef assemblies, and project managers are encouraged to construct castles as tall as possible to best absorb waves.

ii. Sediment Transport

Wave height is strongly associated with higher water turbidity, with waves 30 cm in height being capable of producing average turbidities upwards of 161 NTU. The exact relationship between turbidity and suspended sediments depends on sediment grain size, but it has been shown that higher turbidity directly correlates with higher SSC in aquatic environments (Gallegos, 2001). Peak turbidity values during high wave events were recorded reaching 500 NTU, indicating that waves are actively mobilizing sediments at Wachapreague marsh, but during relatively short periods of time. These high, periodic values are in line with SSC trends from previous studies (Bieri, 2022; Lawson, 2003). Since waves are primarily wind driven within the eastern shore's coastal lagoon system, wind speed is likely directly contributing to sediment mobilization at Wachapreague marsh. Once mobilized, it is far easier for currents to transport sediments elsewhere. These high wave events therefore may be associated more with sediment transport, either in the form of sediments being brought into Wachapreague marsh's shoreline or marsh platform, or being eroded away from the marsh's shorelines and into the surrounding lagoons.

Long term Echologger deployments helped reveal how sediments behave along the bed surface. There are two specific trends showing bed height change that are of interest. First, between June 5 and July 17, there was a net bed height loss of approximately 1 cm at SN7. The bed height was stable for nearly three weeks after data collection began, until the sediment surface drastically eroded approximately 6 mm on June 24. Similarly, there was approximately 6 mm of sediment deposition at the offshore site between July and September.

Most of the significant changes in bed height, especially regarding erosion, typically occur over a period of one or two days, and the only trends that occur more gradually are sediment deposition. The AA400 sensors discretize and bin data in 7.5 mm increments, especially when collecting data in high noise environments. There are several instances in the data where bed height can change significantly, but then immediately revert back to its original value after one or two days. Despite lab tests showing that the sensors can record with the advertised precision of ± 1 mm, data collection in the field may suggest that the sensors can only record with 5-6 mm precision. However, despite the lack of desired precision, the sensors still describe general sediment trends, and show the high degree of variability in sediment transport. Despite the variability in sediment trends, the Echologger data reveals the rate of sediment fluxes along the shoreline. Sediments at Wachapreague marsh may be prone to rapid erosion, and may experience gradual sediment deposition over several days. This shows how marsh shoreline may be prone to rapid loss, while restoration efforts may take considerable efforts over longer timescales.

iii. Morphodynamics

Over the course of the entire geospatial dataset, there is a clear pattern of marsh erosion across Wachapreague Marsh's southern shoreline. However, these trends vary in strength both spatially and temporally. For instance, the western portion of the island is receding at dramatically higher rates than the eastern portion. Additionally, this trend is consistent; the western portion of the marsh is always eroding at the fastest rate throughout the dataset. Conversely, the portions of the island with the lowest rates of erosion are the two coves near the base of the island's central peninsula. These two sections are naturally protected from wave energy, as they have a relatively shallow angle of exposure that waves can attack.

TNC did not begin installing oyster reefs until 2020, and did not finish surrounding the southern shoreline until 2024. Additionally, the reefs were not installed at the same time, and were rather installed in patches. Thus, it is a bit difficult to discern the exact effects of oyster reefs on marsh retreat and growth. Therefore, to simplify the results, the data has been grouped according to erosion before the installation of oyster reefs, and erosion after TNC began installing oyster reefs at each respective section. When the data is grouped this way, there are a few trends that can be seen in the dataset. First, there is a clear effect of oyster reefs on marsh retreat. At sites 5, 6, 7, 8, and 9, normalized marsh platform retreat was noticeably lowered after oyster reefs were installed. However, sites 3 and 4 showed higher normalized erosion rates post reef construction.

Marshes constantly are undergoing opposing processes of erosion and expansion. Prior to this, it was unknown if Wachapreague marsh was simply growing along its north shoreline, and its southern shoreline loss was merely representative of a normal marsh phenomena. However, the AMBUR analysis reveals that while the north shore of the island is eroding significantly less than the southern shore, it still is eroding at an average rate of 0.64 m per year, compared with the southern shore's rates of 1.42 m per year. It is difficult to say why the island is not growing enough to keep pace with shoreline loss. The most likely candidate is a combination of sea level rise and changing storm intensity. While marshes can grow vertically, they can be outpaced by SLR and ultimately drown. Additionally, since marshes depend on storms to bring in new sediments, changing storm intensity and frequency can easily change the rates and amounts of sediments being transported onto the marsh platform. Anecdotally, However, another possible candidate is the result of changing waves, especially those human generated. The northern shoreline of Wachapreague marsh borders a small channel often used by local boat traffic. As these boats drive by, they can easily make waves comparable to those made by wind fetch, potentially explaining why the northern shoreline is eroding at its current rate. However, exploring this hypothesis would necessitate further data collection and experimentation.

iv. Reef Growth and Health

While TNC began installing oyster reef substrate at Wachapreague in 2020, they continued to do so well into 2024. When installed, the castles are initially barren, and it takes time before oysters are able to colonize and grow to a respectable size. As such, the reefs are constantly experiencing a mixture of oyster colonization, growth, and death, with new oyster additions frequently growing over top of the old oysters. Monitoring the growth rate and population of these oysters, especially in reference to previous datasets, can be used to monitor overall reef health, which can reveal the long term health of the reefs.

Between 2023 and 2024, there was no significant difference observed in average shell length for the oysters growing at site 7, neither at the offshore or nearshore reefs. In some ways, this was slightly surprising, as oysters do have the potential to grow to extremely large sizes when allowed to do so. However, larger oysters do face a larger risk of predation, particularly from crabs, rays, and shorebirds (Tedford and Castorani, 2022). Therefore, this may be representative of natural population dynamics, with predatory pressure restricting oysters above a length of 70 mm. However, there is a difference with population density. In 2023, the Wachapreague reefs at site 7 showed oyster densities of about 650 oysters per m squared at both the onshore and offshore reefs. However, 2024 data revealed densities of approximately 1400 and 1300 oysters per m^2 at the nearshore and offshore reefs, respectively. This would suggest that both the offshore and nearshore reefs experienced nearly a doubling in population density in just one year. However, trends from prior years have shown oyster population densities of approximately 1000 and 1600 oysters per m squared for 2021 and 2022, respectively. Therefore, while this data may be genuine, the 2023 data may also be indicative of an error in data collection.

Based on the collected data, both offshore and onshore reefs have healthy rates of oyster growth, both in terms of individual size and total oyster recruitment. And given that many of these reefs are nearing 4 years old, this data is a good indicator that these reefs are resilient across time, suggesting that they will likely still be healthy and functional many years from now, assuming that the substrate itself does not collapse. Oyster castles therefore offer a viable option for long-term reef growth, providing a catalyst for larger reefs to eventually form.

v. Future Trends

Based on all of the data collected and analyzed throughout this experiment, the oyster castles installed along Wachapreague Reef's shoreline are having a positive impact on shoreline erosion rates by virtue of attenuating incoming wave energy and flow rates. However, the constructed oyster reefs have not been successful at stopping marsh loss, but rather slowing the rate at which it occurs. Thus, these oyster reefs should not be treated as the main solution to stopping marsh platform erosion; rather, they should be treated as an important piece in the ultimate solution to stopping coastal erosion. There is potential that the reefs will better attenuate flow as oyster populations continue to grow. Therefore, a better understanding of the interaction between oyster reefs of various ages and flow attenuation is needed.

Continued monitoring of Wachapreague Marsh's perimeter will be important to help better predict future erosion and accretion trends. A model's predictive capabilities are only as accurate as the historic data it is based on, and this has indeed been true of AMBUR. In particular, it has been difficult to sift through the results and predictions of future trends when data collection is so temporally inconsistent. In order to better train the model to predict future trends, continual annual surveying of the marsh perimeter is strongly advised.

IV. Chapter 2: Modeling The Effects of Oyster Castle Topography on Flow Attenuation and Sediment Resuspension

A. Introduction

To ensure the long term success of oyster reefs as living shorelines, they must be constructed such that they effectively attenuate waves, foster healthy oyster growth rates, successfully recruit new oyster larvae, and are not inundated with high quantities of sediment. Successful reef designs must meet the biological needs of oysters, as well as the physical needs of the ecosystems they are protecting (Morris et al, 2019). Various oyster reef configurations have been investigated at the VCR, and studies have shown that wave attenuation and oyster growth are most influenced by reef height, with high elevation reefs having oyster densities of ~2000 per m^2 during year 1 recruitment (Hogan et al, 2022). Consistently, high elevation reefs contain nearly double the oyster density of low elevation reefs, with 1.2 cm longer oysters on average (Hogan et al, 2022). Additionally, high elevation reefs attenuate waves by as much as 41%, compared to only 6% for low elevation reefs (Hogan et al, 2022). Reef width, and number of substrate rows are not nearly as influential on the previously mentioned ecosystem services, but reef orientation is vital for long term health, as reefs oriented parallel to tidal flow may be more susceptible to sediment burial and suffocation (Colden, 2016). Even partial burial, if not cleared by wave action and storms, can prove detrimental to oysters, forcing higher rates of shell growth and vertical migration, but thereby damaging metabolism and reproductive success (Colden, 2015). However, oyster larvae recruitment may also depend on sedimentation rates, with reefs >50% buried being more successful at recruiting larvae, despite not being as effective at attenuating waves (Morris, 2021). It may prove difficult for restoration efforts to balance these different effects of burial on reef health and function, but reef position and configuration could prove key to maintaining reef health and functionality. Consequently, investigating sediment and flow dynamics around restored oyster castles is vital to understanding how reefs can be built to be more resilient under sediment induced stress.

While it is known that oyster reefs can influence the hydrodynamic properties of fluid flow near coastal marshes to attenuate waves and reduce sediment resuspension, it is not well understood exactly what effects oyster reef topography has on local drag, shear stress, and turbulent development. Studies have found that oyster reef topography increases the drag coefficient by as much as 5-6 times relative to bare mud, drastically lowering the amount of shear forces present and helping to reduce sediment resuspension (Reidenbach et al, 2013; Styles, 2015). However, no studies have modeled fluid flow over a detailed oyster reef topography, and therefore no studies have examined fine scale changes in drag and fluid dynamics over time at the reef-flow boundary. Finite Element Methods (FEM) computational fluid modeling offers an effective and robust method to analyze changes in drag, turbulence, and subsequent fluid properties, such as velocity and pressure, within flow over an oyster reef. Such a model can offer insight into these fluctuations within the interstitial spaces between individual oysters, as well as show fluctuation profiles across space above and around the reef.

Given that oyster reefs attenuate flow, they also have an impact on shear stresses, and therefore sediment suspension (Fagherazzi and Furbish, 2001; Shi et al, 2015). Understanding how oyster reefs interact with flow is therefore critical for anticipating how they will impact coastal sediment dynamics and erosion trends. Models are needed to characterize the hydrodynamic influences of oyster reef topography on drag and turbulent development, especially in the interior and wake of oyster castle structures. These models can then be used to quantify flow attenuation throughout the model domain and resultant bed shear stresses along the reef and bed surfaces, informing several other relevant questions. For example, using calculated velocities, the models can answer questions regarding fluid circulation in an oyster reef's wake. It has been shown that oyster larvae preferentially settle on substrate based on pressure fluctuations, so pressure fluctuation calculations can theoretically be used to predict larval settlement trends (Lillis et al, 2015; Eggleston et al, 2016). The resultant shear stresses calculated using these models can then answer questions regarding sediment transport, deposition, and resuspension. All sediments, depending on their size, density, and level of compaction, will have a critical shear stress at which they will be suspended by flow (Reidenbach and Timmerman, 2019). If shear values within the model's bed surface exceed a particle's critical shear stress, then that particle is predicted to erode. Critical shear stresses for the fine mud particles present around oyster castles are hard to predict, mostly due to sediment flocculation and compaction. However, previous studies have estimated the critical shear stress of sediments in Hog and South Bay to be t = 0.04 Pa, while the critical shear stress of oyster larvae is predicted to be approximately 1 Pa (Hansen and Reidenbach 2012, 2013; Reidenbach and Timmerman 2019).

Previous models have analyzed flow over farmed oyster baskets, have utilizied simplified 2D rather than 3D models, or have used heavily idealized geometry (Gaurier et al, 2011; Stanley et al, 2024). However, no studies have analyzed the fine scale trends of tidal flow over oyster reefs using 3D computational modeling. When running fluid mechanics simulations using models sourced from real world topography, there are often issues with balancing model accuracy and model running time. However, similar models have analyzed turbulent development and flow characteristics over 3D scans of corals, yielding precise and accurate data from those organic scans (Stocking, 2021; Stocking 2018). Thus the same methods can be extended to modeling flow over oysters, and scanning and quantitatively analyzing flow over oysters is both viable and practical.

The long term effects of artificial oyster reefs on salt marsh edge erosion, as well as the long term health of these reefs, is not fully understood within the VCR. Some datasets pertaining to preliminary marsh edge erosion and oyster reef health at Wachapreague have been collected (Bieri, 2022). However, these datasets must be expanded upon to better reveal the sustainability of oyster reefs as a nature-based solution to coastal erosion, and especially their interaction with flow during high tide. This leads to the questions this chapter will address: How do oyster castles interact with tidal flow and influence flow attenuation, sediment resuspension, and bed shear stresses; how do these effects change as oysters colonize and grow on the castles; and what key differences in flow attenuation are there between an restored oyster reef vs a natural reef?

B. Methods

i. ANSYS Computational Fluid Dynamics Model and Validation

To quantify the fine scale influences of oyster reef growth on flow attenuation, bed shear stresses, wave height, and sediment resuspension, ANSYS was chosen as the primary computational fluid dynamics (CFD) software. ANSYS is a robust and widely used engineering software, which offers a variety of CFD packages.

The CFX package was chosen, primarily because other similar research projects have utilized it in past experiments, and thus much of the methods can be easily adapted from those prior simulations.

ANSYS has not been widely used to examine fluid flow over biological structures, including scanned oyster reef topography. Thus, ANSYS required validation to show that it is suitable for answering these research questions. Lowe et al conducted a series of flume experiments in which various arrays of vertical cylinders were assembled, and flow attenuation was measured at various points in those arrays under steady flow conditions (Lowe et al, 2005). Lowe et al intended to use the cylinder arrays as analogues for coral reefs, and created a series of vertical profiles of velocity attenuation throughout the array. Since flow around cylinders is well understood, replicating the results from these experiments within ANSYS can verify that it is an appropriate tool to examine more complicated flow regimes around oyster reefs. The experimental setup of the flume assemblies from Lowe et al is shown below in Figures 1 and 2.

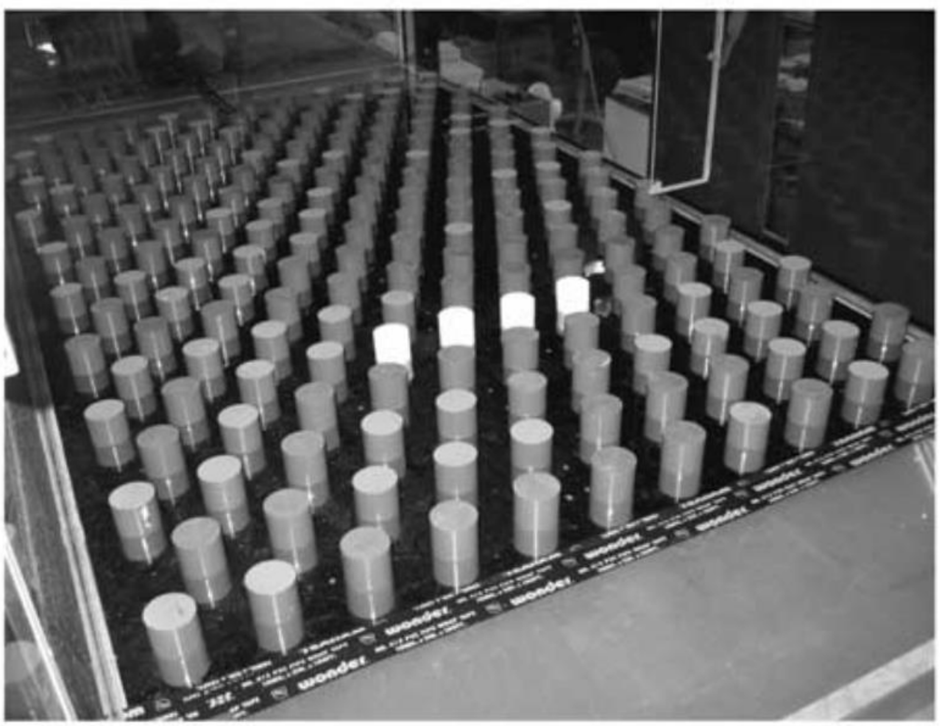

Figure 1: Arrangement of the cylinder array as detailed in Lowe et al. The cylinders have a diameter of 5 cm, height of 10 cm, and are placed in a flume with 43 cm deep water, although cylinder arrangement changes between trials. The full cylinder array has dimensions of 1.2 x 1.8 m in the streamwise direction.

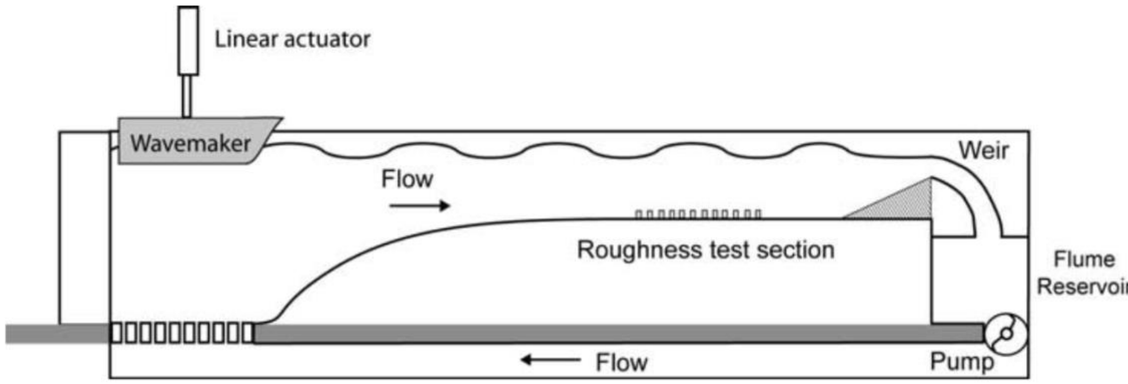

Figure 2: The flume setup from Lowe et al, with the cylinder array being placed in the portion labeled "Roughness test section". For simplification purposes, the ANSYS model does not include either the weir, surface waves, or the upstream deep water section below the wave maker.

All of the various cylinder spacings and flow configurations used in the Lowe et al flume experiments are shown below in Table 1. For the purposes of validation, the U1 experiment was replicated within ANSYS. The cylinder array was digitally created according to the specifications reported by Lowe, and all flow conditions were matched and modeled until steady state convergence occurred. However, the model was simplified by only recreating the flat portion of the flume, and it was assumed that the surface of the flow was perfectly flat and uniform.

Run	Geometry	S/d	$U_{\infty,c}$, cm/s	$u_{*c}/U_{\infty,c}$	C_f	α_c
U1	staggered	1	4.8	0.10	0.019	0.12
U2	staggered	1	9.2	0.09	0.017	0.10
U3	staggered	1	12.4	0.10	0.018	0.10
U4	staggered	2	4.5	0.12	0.031	0.22
U5	staggered	2	9.1	0.12	0.030	0.23
U6	staggered	3	4.3	0.13	0.032	0.32
U7	staggered	3	8.5	0.12	0.029	0.33
U8	unstaggered	1	4.4	0.09	0.018	0.12
U9	unstaggered	1	9.4	0.09	0.017	0.11

Table 1: The specifications for all unidirectional flow trials.

Lowe et al created a graph showing flow attenuation throughout the cylinder array (Figure 3). Using the ANSYS model, these same vertical profiles were generated and analyzed, and flow attenuation data was output. The flow attenuation relative to surface velocity from the ANSYS experiment can be seen in Figure 4.

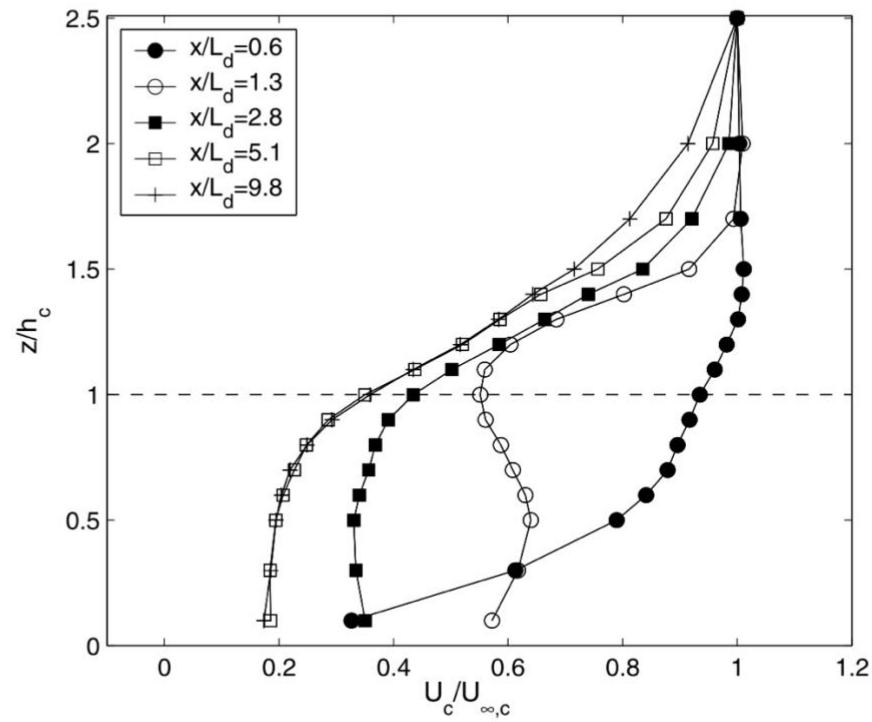

Figure 3: Relative flow attenuation at various points from the leading edge of the cylinder array for trial U1 from Lowe et al. This is the data the CFX model replicates. Height (z) is normalized by array height, and velocity (U) is normalized by surface velocity

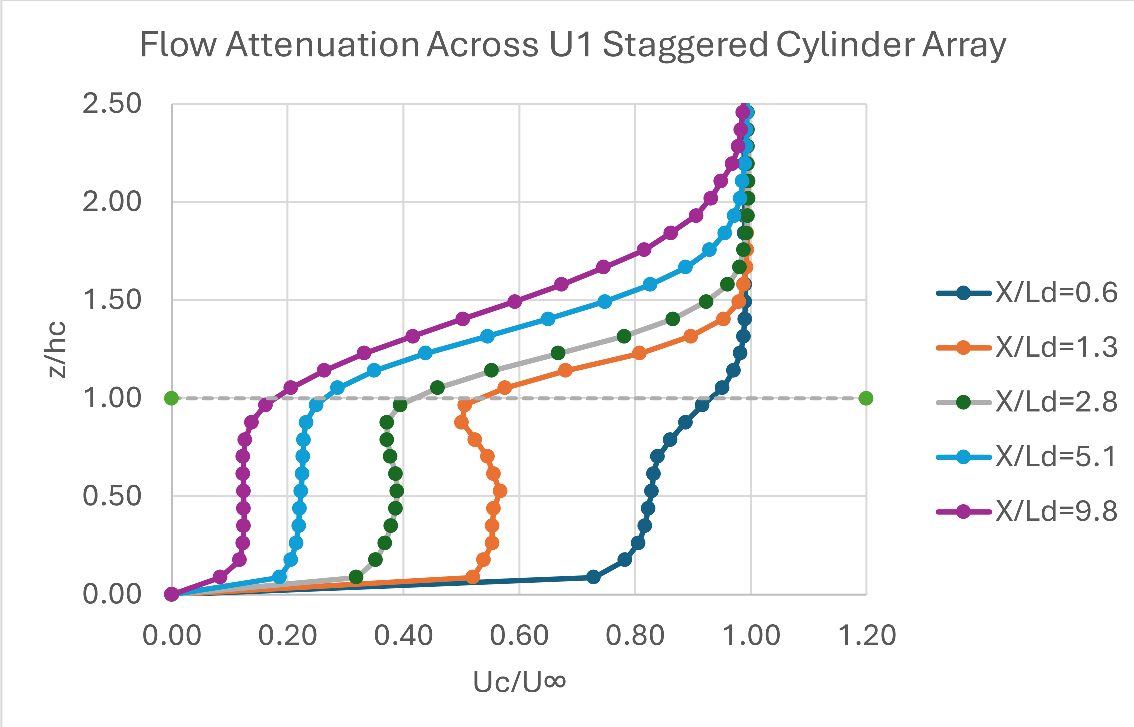

Figure 4: Relative flow attenuation as output by the ANSYS model. The trends from Lowe et al were recreated within 80-90%

The ANSYS model does correctly predict all of the major trends shown by Figure 3, specifically the sharp change in slope associated with X/Ld = 1.3, as well as attenuation trends below reef height. ANSYS was able to correctly recreate the results from Lowe et al. with up to 90% accuracy for some profiles, and correctly predicted all major trends in flow attenuation. This validates ANSYS as a suitable tool for analyzing the effects of oyster reef topography on flow attenuation.

ii. Oyster Castle Model

Utilizing ANSYS requires creating a model with the desired geometry. For this research project, three different initial model geometries were created: an empty oyster castle, an oyster castle with juvenile oysters, and an oyster castle with adult oysters. These three models can then be compared under the same flow regime to examine how flow attenuation changes with oyster reef maturity. The oyster castle structures are a series of concrete blocks stacked into a larger structure (TNC, 2024). The base model of one individual block is shown in Figure 5, while the assembled and colonized oyster castles are shown in Figure 6.

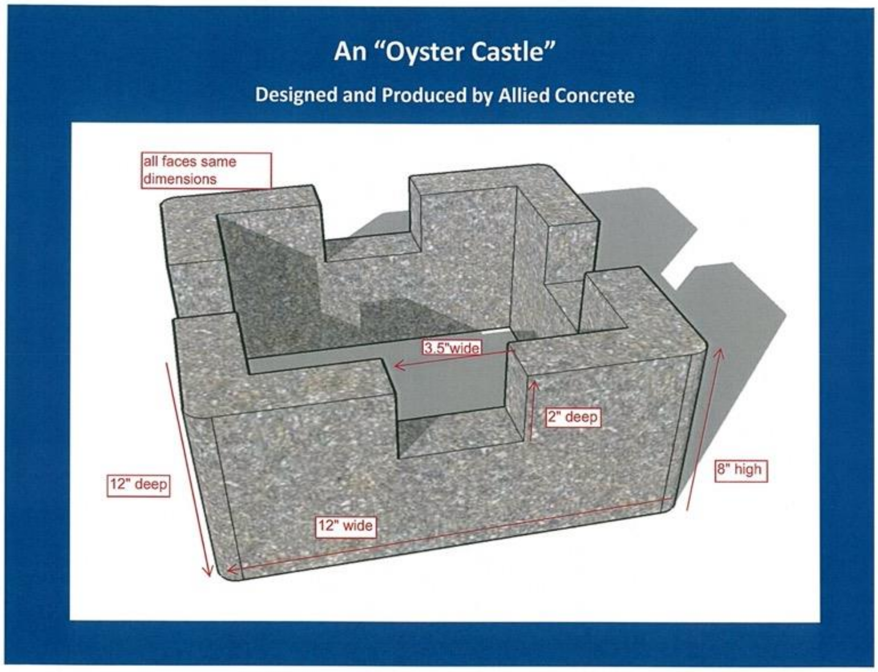

Figure 5: The dimensions for one oyster castle block. Multiple blocks are stacked into a wall that is two blocks wide on the bottom layer, and one block centered on the top layer. This pattern is repeated to form walls of any desired length.

Figure 6: The ANSYS oyster reef model is based on the constructed oyster reefs found at Wachapreague marsh.

All relevant geometries were created using Spaceclaim, the built in geometry editor included with ANSYS. To most accurately portray the influence that oyster castles have on flow, the ANSYS geometry was created to model a subsection of the constructed reef found along Wachapreague marsh. This yielded a model with 4 castle blocks on the bottom, and one full block and 2 half blocks centered on top, giving a final model geometry of 24 in width, 24 in depth, and 16 in height. A fluid domain was created around this subsection, with 8 ft of water modeled on the front and backside of the castle, 0 m of water along the sides, and 0.305 m of water above the model (Figure 7). This large expanse in front and behind the model allows ANSYS to stabilize the incoming flow, and 0.305 m of water above is a value representative of high tide over the oyster castle.

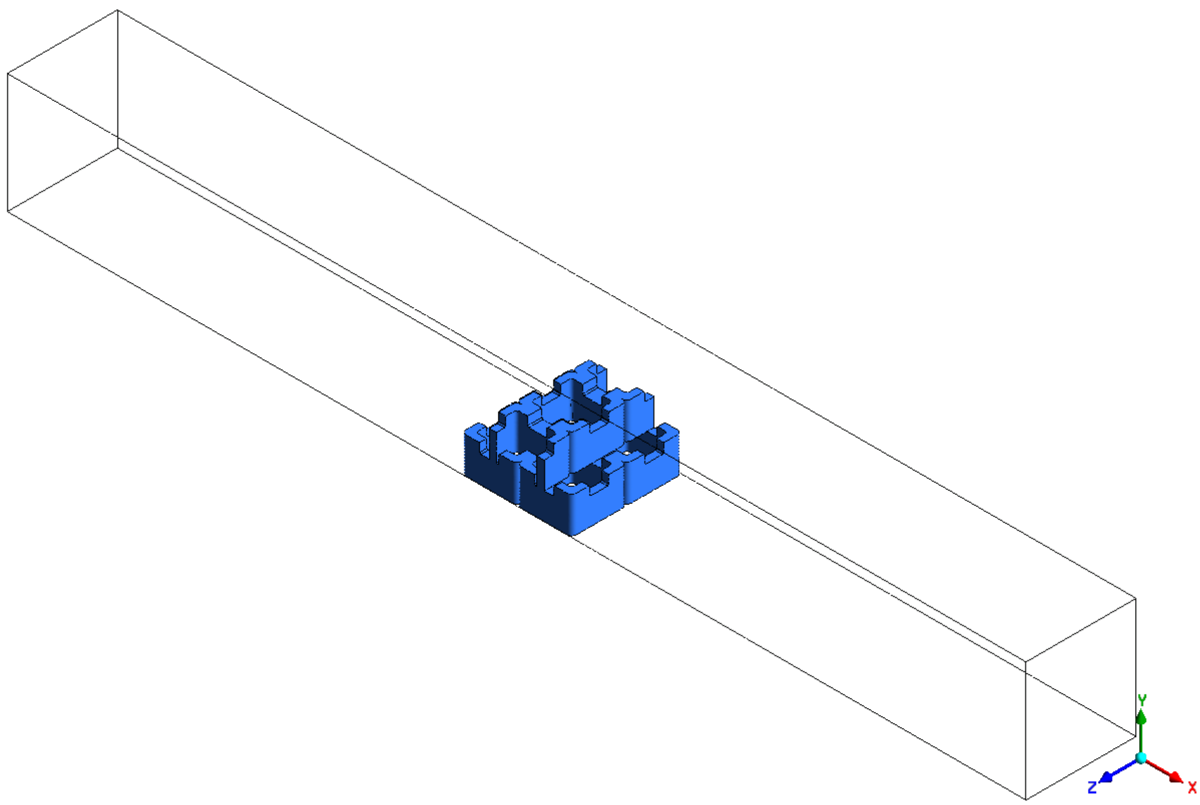

Figure 7: The fluid domain for the empty oyster castle. There are four blocks underneath, and one full block and two half blocks on top (24 x 24 x 16 in).

This fluid domain was meshed (Figure 8) and was initialized with an incoming horizontal fluid velocity of 10 cm/s, which is an approximation of tidal flow velocity. To appropriately replicate the conditions under which this wall subsection would experience tidal flow, specific boundary conditions were applied to the model. The top was defined as a zero shear surface, which replicates a flat and waveless free surface, and the sides were defined as symmetry boundary conditions, indicating to ANSYS that the model is mirrored on either side of the defined fluid domain. This model was run under steady state conditions until it converged, yielding time averaged results for all relevant metrics.

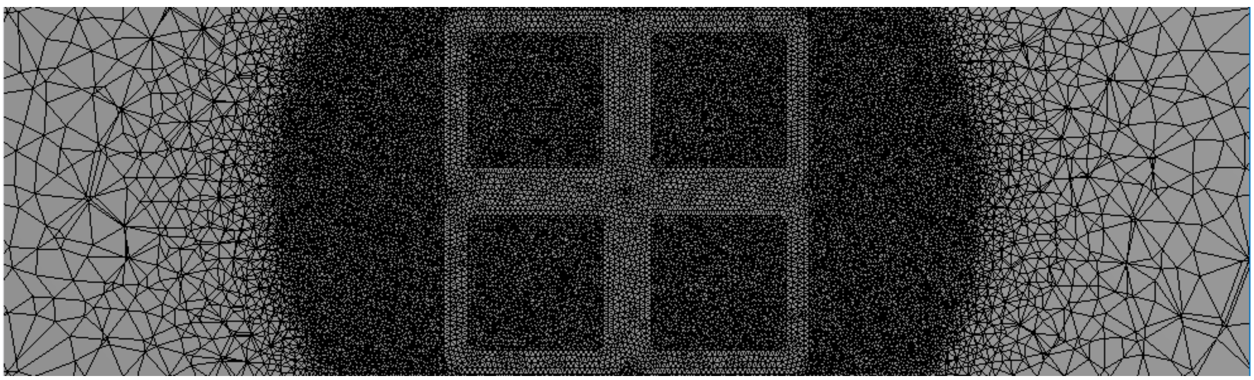

Figure 8: An example mesh of one of the oyster castle models. The finest mesh elements are 7 mm in length.

Once this initial model was successfully run, the same flow conditions were applied to and modeled over the juvenile and adult oyster castle models. Specifically within this project, juvenile oysters are defined as having 3-6 cm length, and adult oysters as having 7-13 cm length, with these parameters being based on field measurements from the Wachapreague oyster castles. A series of 3D scans were generated from both juvenile and adult oysters at Wachapreague marsh. Oysters were scanned using the PolyCam 3D scanning software, yielding hollow body stl files. These stl files were imported into Spaceclaim, simplified to ensure model stability, converted to solid models, and assembled onto the empty oyster castle geometry to recreate the Wachapreague oyster reefs at various growth stages. The oyster models were assembled onto the oyster castles at the maximum allowable density at which the simulations would converge, approximately 400 oysters/m^2. All other dimensions and parameters of the fluid domain and model initialization were kept identical, and these two models were run until steady state convergence was achieved. An example of these models, and the reef they are replicating, is shown below in Figure 9. Populating the castle model with adult oysters unfortunately resulted in small gaps being generated between the sides of the model and the fluid domain boundaries, allowing a small amount of flow to leak around the side of the model. The adult reef therefore is less representative of reality in terms of reef wake zone trends; however, trends within the reef are still useful. Additionally, these models represent a specific and idealized flow scenario. Live reefs are subject to more complex flow regimes, and likewise generate more complex attenuation and shear stress trends. However, the models reveal invaluable results when interpreted in the context of their associated assumptions.

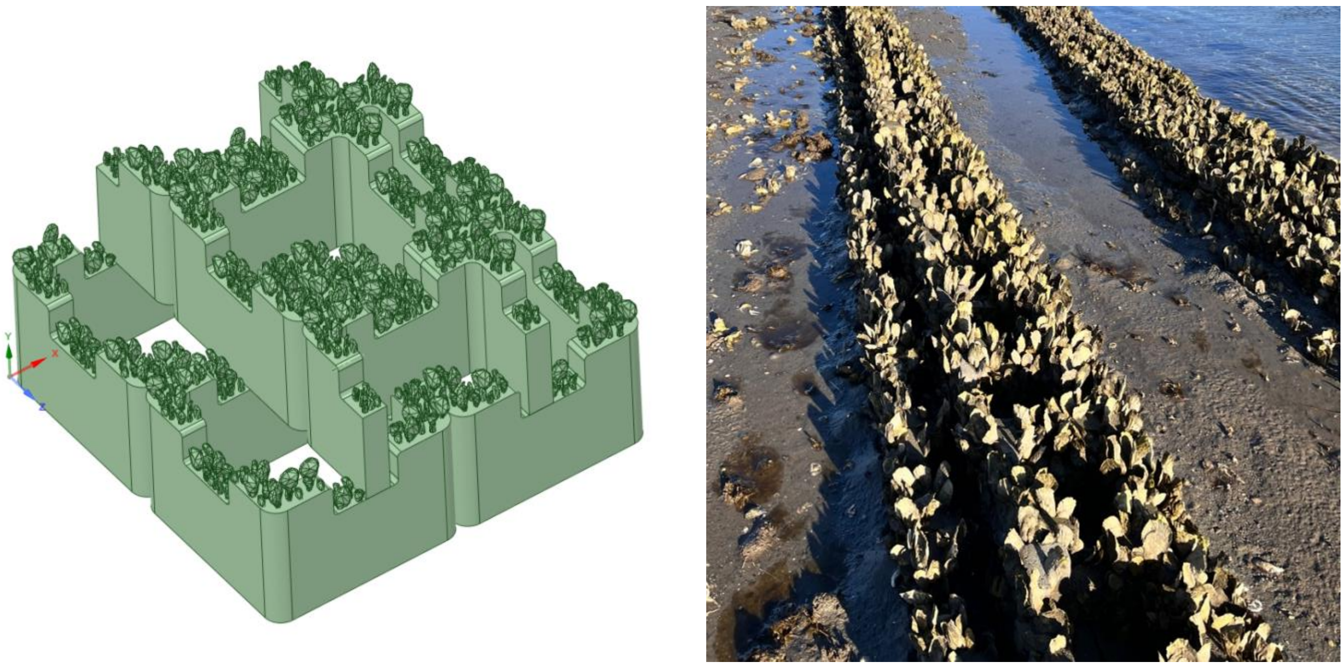

Figure 9: The oyster castle with juvenile oyster scans attached, compared with the Wachapreague oyster castle the model is based on.

To investigate how an oyster castle and a natural reef differ in attenuating tidal flow, a model approximating a natural reef was created. This was done by deleting the oyster castle block geometry and rearranging the remaining oyster models into a flat 0.6 x 0.6 m reef with the same footprint as the oyster castle model, providing an approximation of a natural reef with the same oyster geometry and density as the oyster castle models. This was done for both the juvenile and adult oyster castle models, yielding two natural reef models. An example of a natural reef these simulations are approximating is shown below in Figure 10.

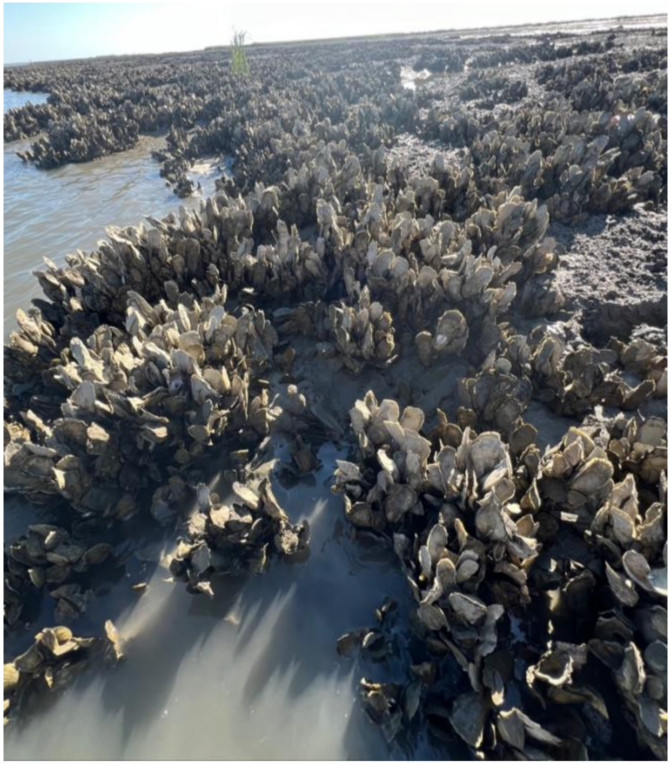

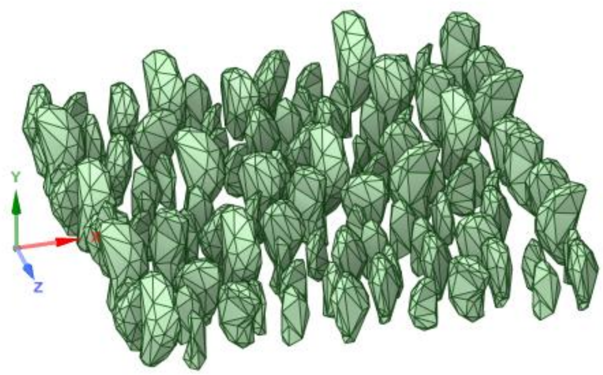

(a) **(b)**

Figure 10: A naturally occurring oyster reef found neighboring one of the marshes at Virginia’s eastern shore (b) compared with an ANSYS geometry approximation (b)

A series of XY planes and vertical profiles were established throughout the castle models to analyze flow attenuation. These profiles allow for comparison between models, altering only oyster presence and size. ANSYS provides included post processing tools, which allow for easy data analysis and visualization along the desired point or profile in space. The vertical profiles were created to best show the specific effects of oyster castle geometry on flow as it moves over and across the reef. Of particular interest are areas within the oyster castle, as well as immediately in front and behind. Therefore, one profile was created in front of the model, three within, and one behind. Note that to most clearly visualize how trends change across each simulation, all directly compared graphs were generated using identical scaling. As a result, colors are comparable between graphs. Other figures utilizing local scaling are attached in Appendix B.

C. Results:

i. Oyster Castle Planar Velocity

Velocities were plotted along the XY plane exactly halfway across each model, visualized in Figures 11, 12, and 13. These figures show the development of clearly defined recirculation zones in the model's wake when oysters are present. Additionally, as these oysters grow in size, this recirculation zone becomes more pronounced, reaching a length of approximately 0.92 m between the bed surface and oyster castle height with peak velocity values of 0.07 m/s. The results also show an increase in velocity above the model, sharply increasing from input levels of 0.1 m/s to between 0.25 and 0.27 m/s for all three models. Thus, the models do attenuate flow below reef height, but increase velocity by over 150% above reef height, regardless of oyster presence or size.

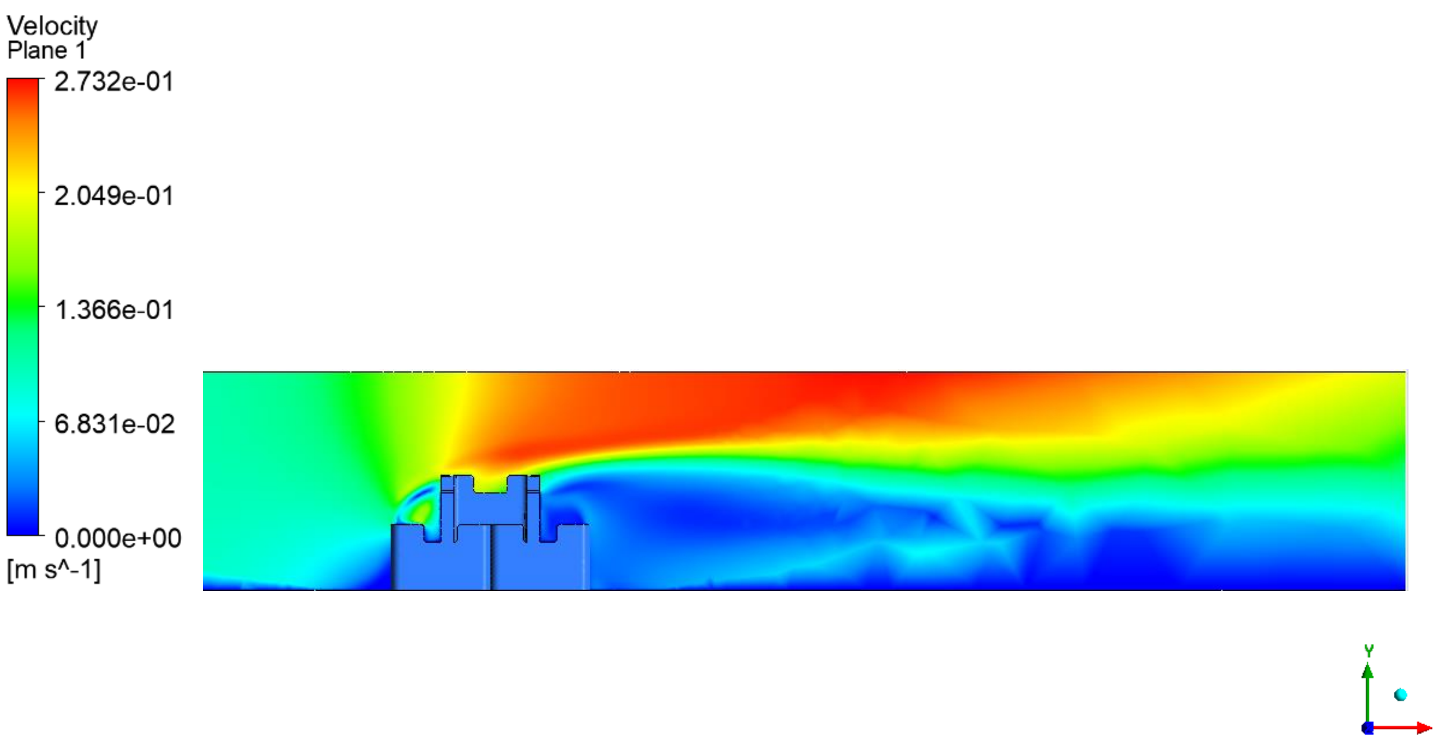

Figure 11: XY Plane velocity for the empty oyster castle

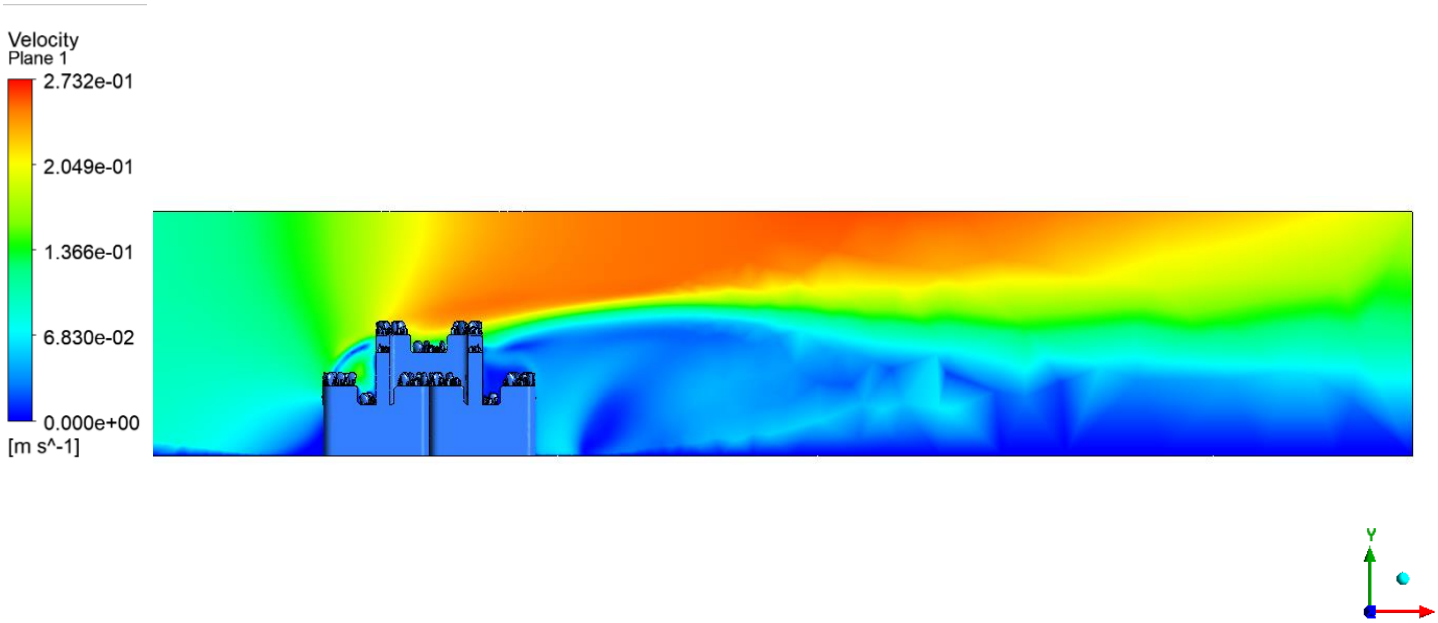

Figure 12: XY plane velocity for the juvenile oyster castle

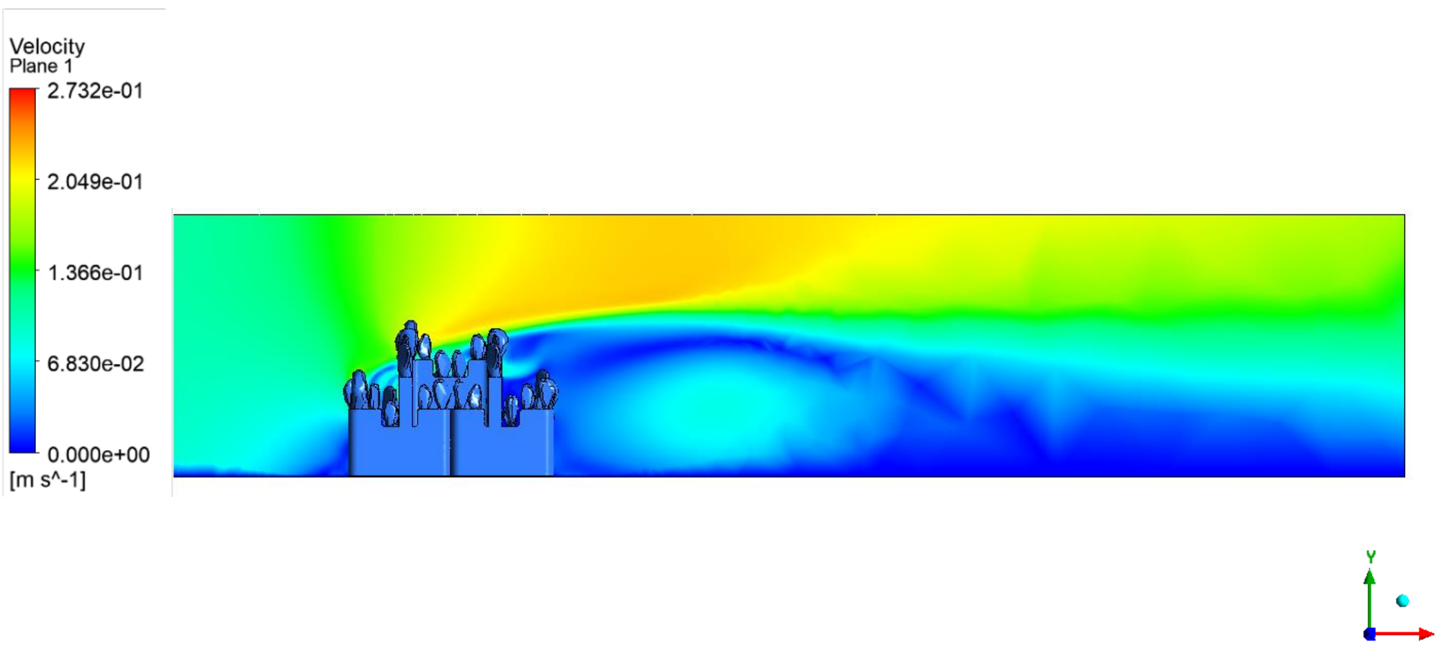

Figure 13: XY plane velocity for the adult oyster castle.

ii. Oyster Castle Velocity Attenuation Profiles

Flow velocity was output along five profiles (one in front, three within, and one behind) within the three oyster castle models, and three of the five generated plots are visualized in Figures 14, 15, 16. Compared to the empty castle, the large oyster castle reef had up to 10% better flow attenuation in front of the model, between 10% and 58% within the model, but up to 39% worse attenuation behind the model. The juvenile oyster castle saw similar trends as the large oyster castle, only providing 40% of the flow attenuation that the large oysters provided; however, the juvenile oysters increased flow by as much as 52% compared to the empty reef behind the model. These increases in flow velocity indicate an area of recirculation behind the model below a height of 0.30 m.

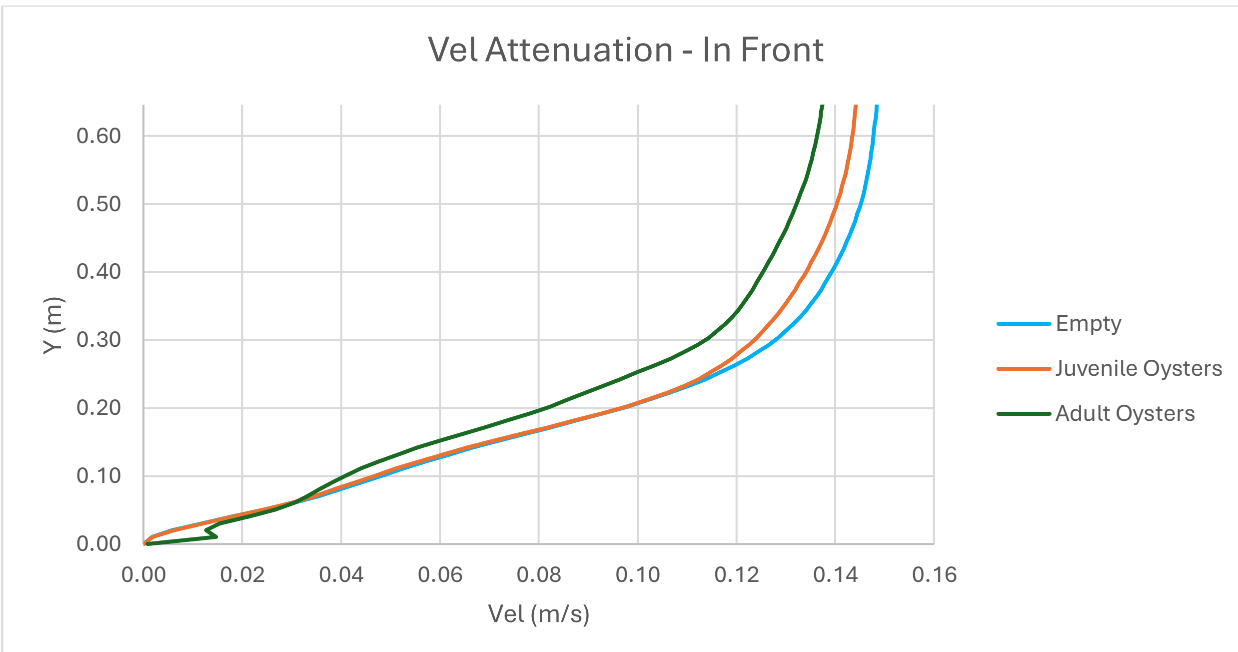

Figure 14: Velocity profiles of the three different oyster castle simulations at the ‘Front’ profile

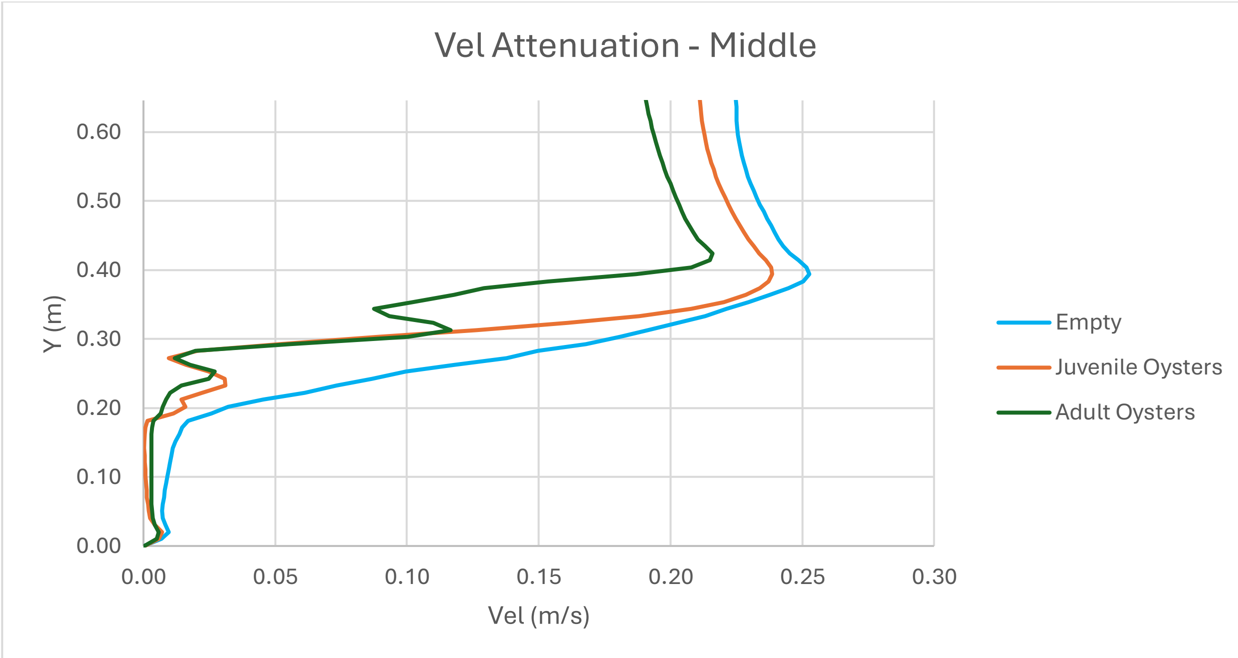

Figure 15: Velocity profiles of the three different oyster castle simulations at the 'Middle' profile

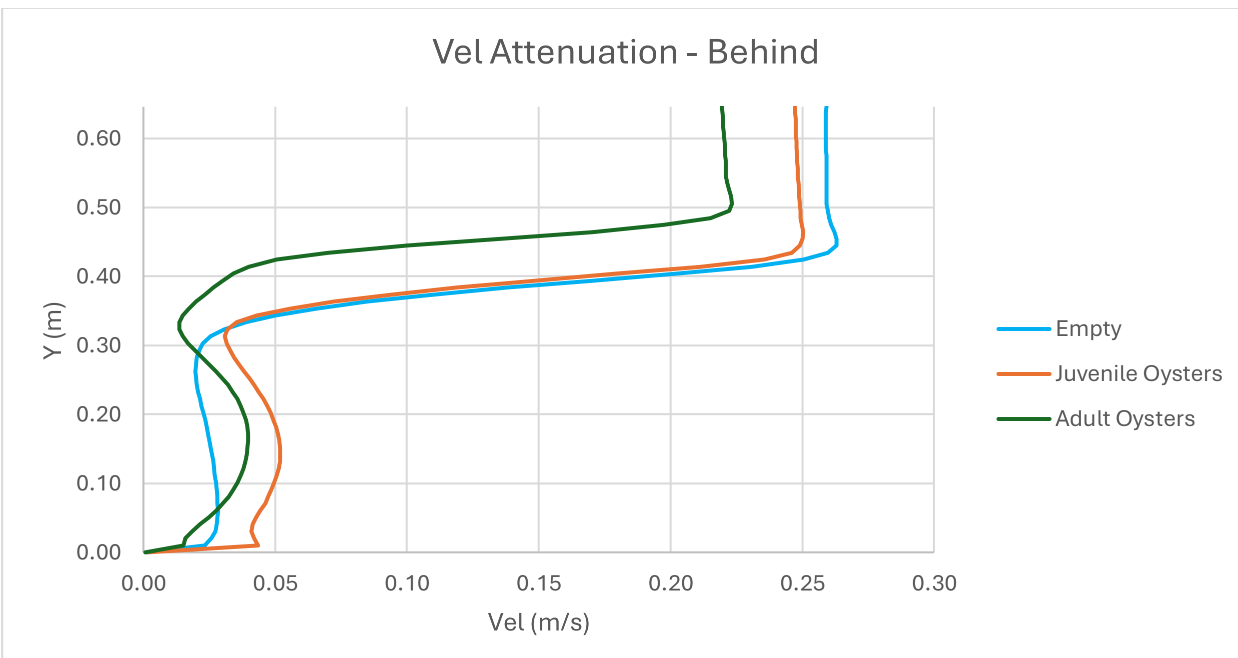

Figure 16: Velocity profiles of the three different oyster castle simulations at the 'Back' profile

iii. Oyster Castle Surface Shear Stresses

Shear stresses were plotted along both the surfaces of the models, as well as along the bottom of each fluid domain, analogous to the bed surface, visualized in Figures 17, 18, 19, and 20. In the case of surface shear stress on the model surface, note that the areas of highest stress are on the upper portions of the front side of the model, peaking at approximately 0.33 Pa for the empty reef, while the areas of lowest shear are towards the back side of the model, peaking at approximately 0.2 Pa. Shear stresses along the bed surface peak within the front chamber of the model, reaching values of approximately 0.065 Pa, 0.094 Pa, and 0.04 Pa for the empty, juvenile, and adult reefs, respectfully. Some models also have a region of high erosion approximately 1.5 m behind the model, peaking at 0.05 Pa and 0.04 Pa for the empty and juvenile reefs.

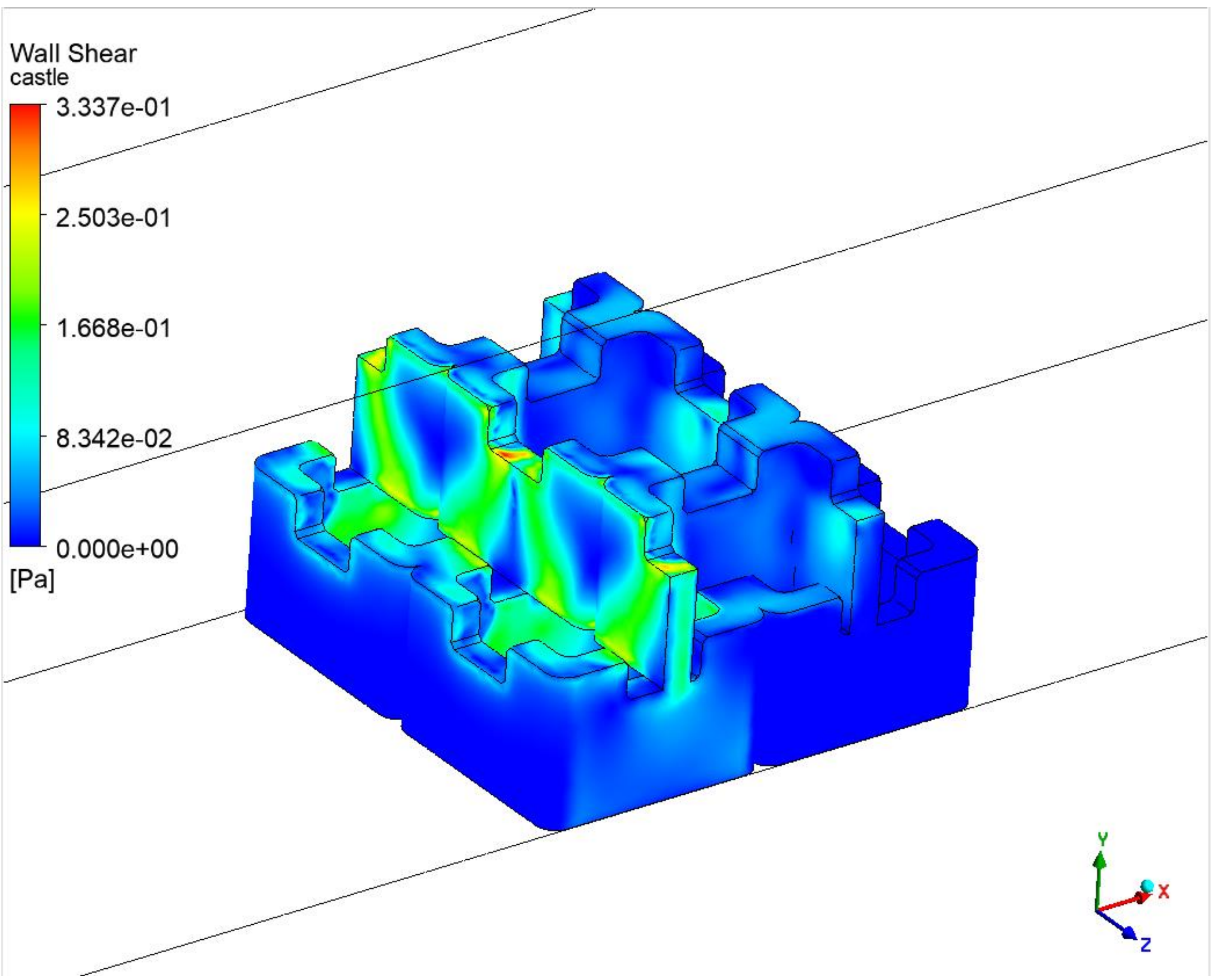

Figure 17: The shear stresses present on the surface of the empty oyster castle

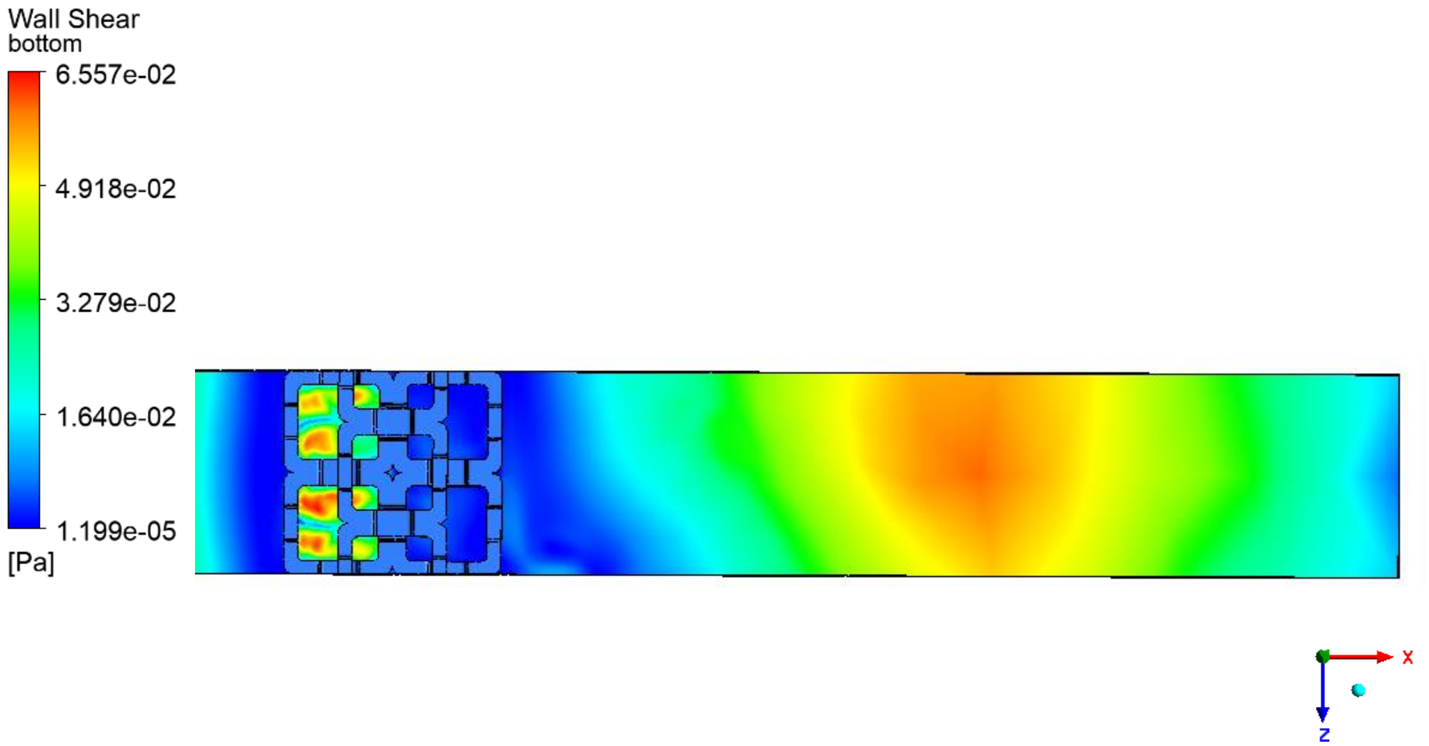

Figure 18: Shear stresses along the bottom surface of the empty oyster castle flow domain.

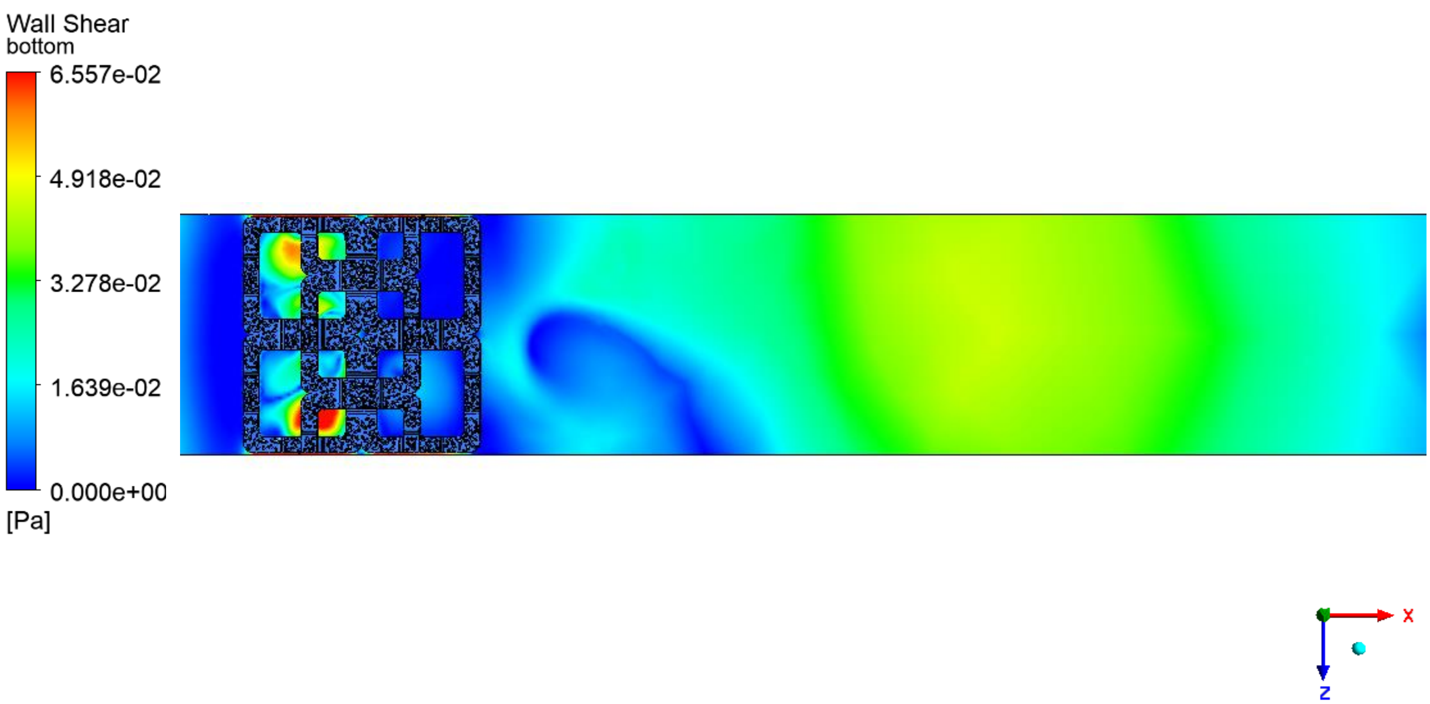

Figure 19: Shear stress on the bottom of the juvenile oyster castle reef model

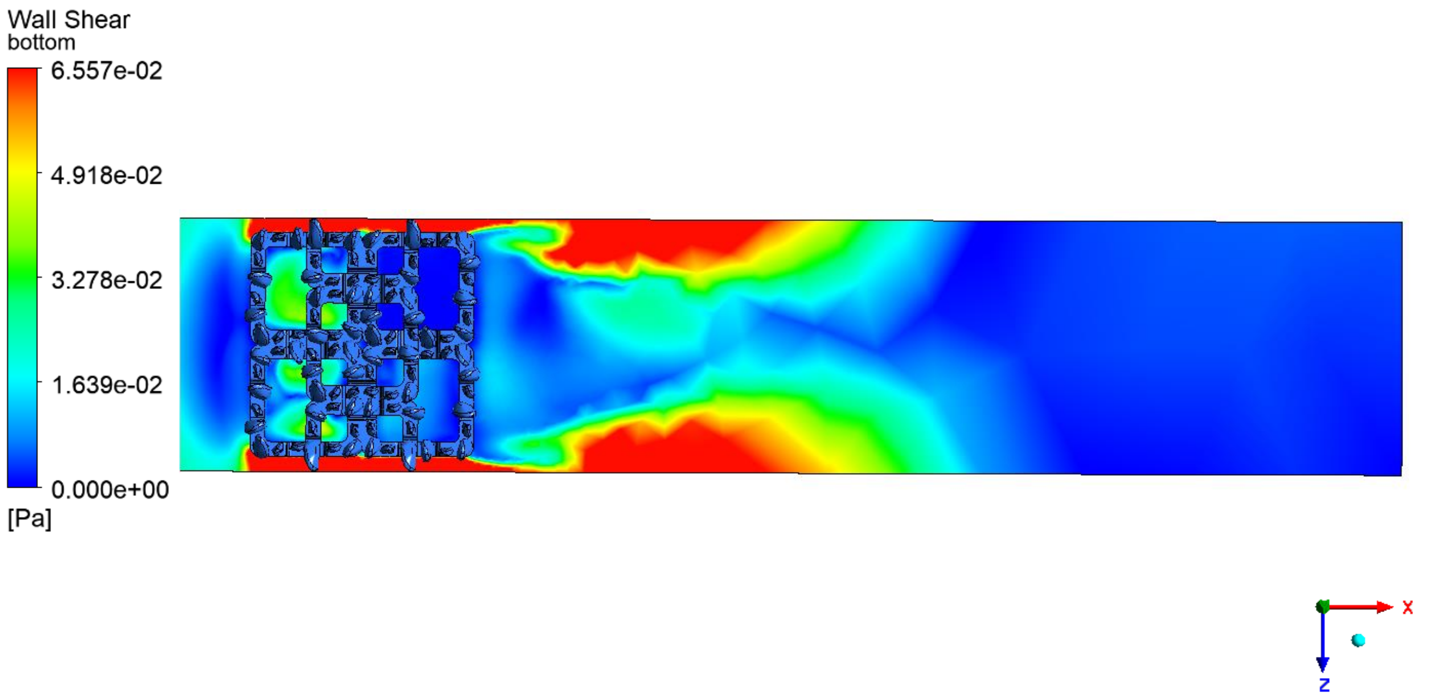

Figure 20: Sediment surface shear stress in the adult oyster castle simulation. Unfortunately, CFX limitations caused gaps along the side of the model, allowing flow to leak around the model boundaries.

iv. Oyster Castle Energy Dissipation

Turbulent kinetic energy (TKE) was also plotted along the central XY plane, as visualized in Figures 21, 22, and 23. TKE describes the kinetic energy present per unit mass, and is a metric of turbulence within the model. The empty reef experiences distinct arcs of higher TKE just above its leading edge, as well as behind the upper edge of the model's tailing end. These arcs are most prominent for the empty and juvenile reef, peaking at 0.0046 m^2/s^2 and 0.003 m^2/s^2 for each model, respectfully. The presence of small oysters vs the empty reef has no significant impact on TKE, only slightly widening the tailing arc of higher TKE and lowering values by approximately 30% both at the leading and tailing edge. However, large oysters dramatically change TKE dynamics. The large oyster reef has a large wake zone of moderate TKE, approximately 0.001 m^2/s^2, surrounding a pocket of high TKE, approximately 0.002 m^2/s^2. This shows a region of large eddy formation and zone of high turbulent mixing.

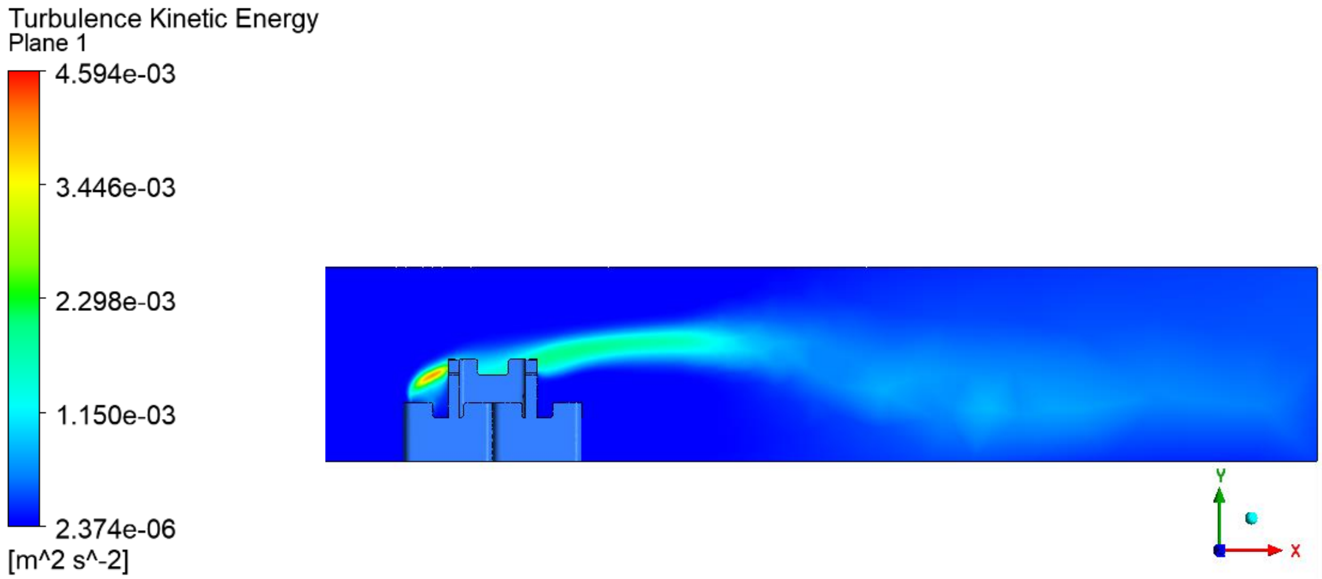

Figure 21: The TKE of the empty castle along its central XY plane

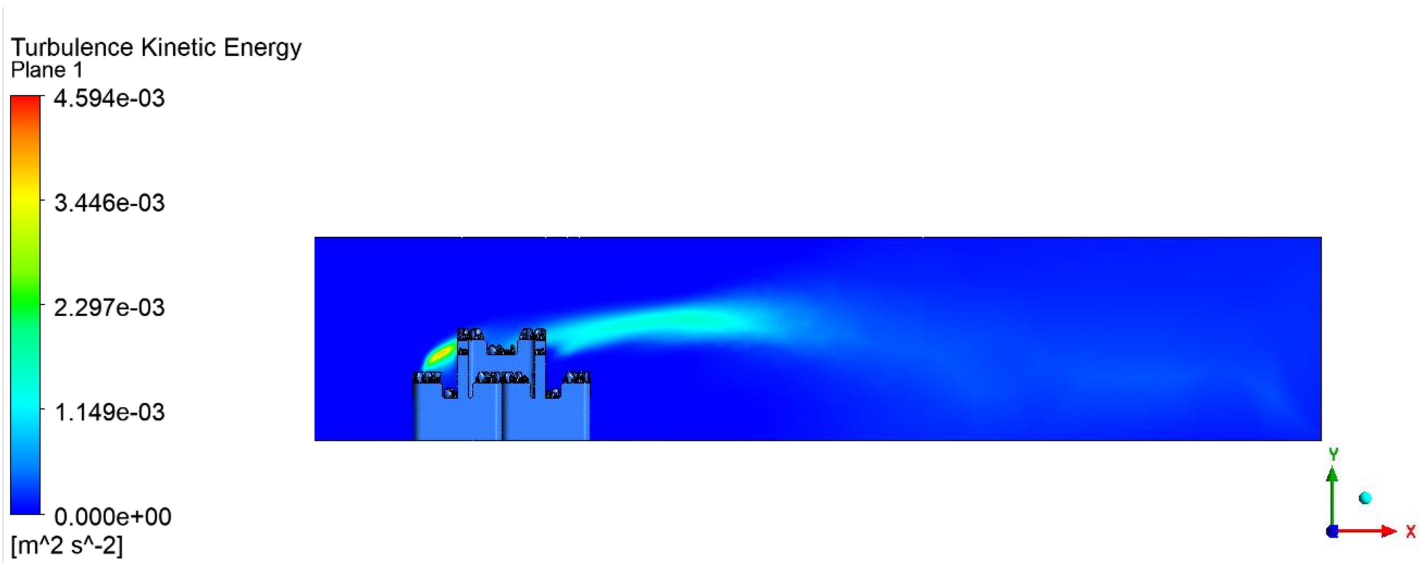

Figure 22: The TKE of the small oyster castle along its central XY plane

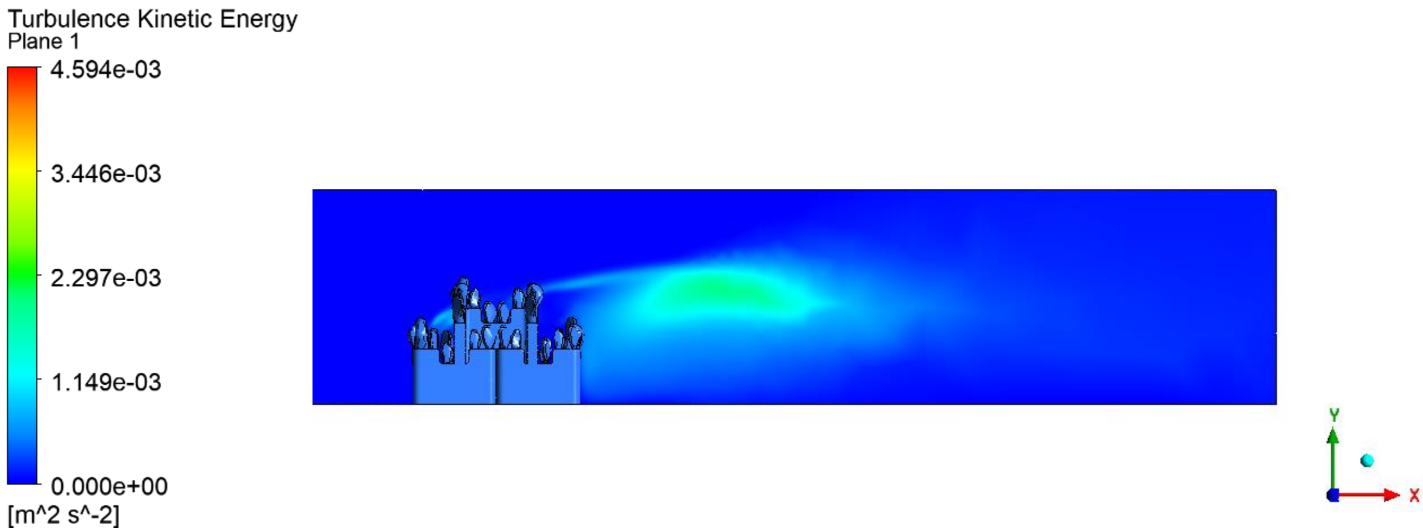

Figure 23: The TKE of the large oyster castle along its central XY plane

v. Natural Reef models

Similar graphs were created from the models of flat oyster reefs, and center plane velocity profiles were used to visualize velocity attenuation data, shown in Figure 24. The zone of attenuated flow is much smaller than in the oyster castle models, and is generally limited to a height of 10 cm above the sediment surface, similar to the reef height. Velocity values were attenuated to near 0 m/s near the bed surface, but above the reef were increased to peak values of 0.14 m/s. The natural reef has a more minimal impact on flow compared to the oyster castle model, with flow below the reef height only being reduced 30-50% in most places. Comparatively, the oyster castle frequently reduced flow speed by upwards of 30-70%, and in many more locations spatially.

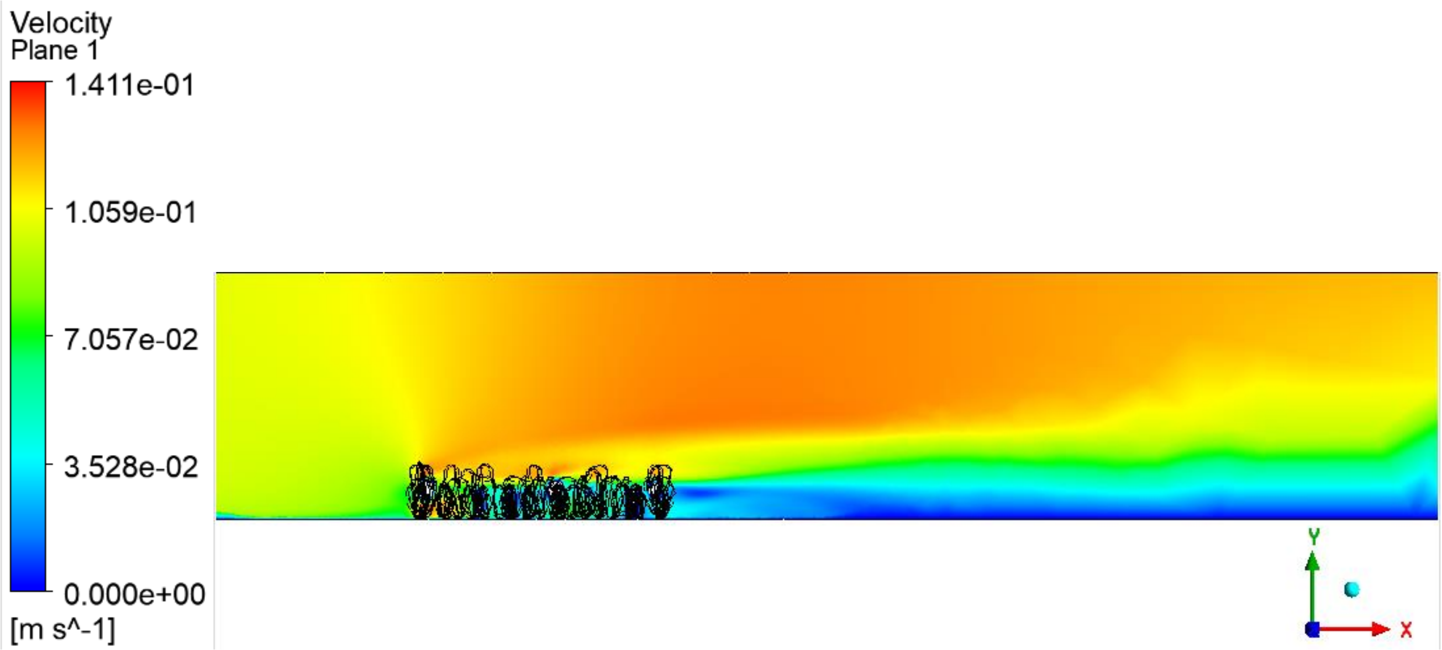

Figure 24: The velocity trends present along the central XY plane of the flat adult oyster reef

Shear stress was also analyzed in the natural reef model, visualized in Figures 25 and 26. Similar to the oyster castle model, shear stress is highest on the leading edge of the reef, and declines in strength towards the back of model. Shear stress peaks at 0.11 Pa near the leading edge of the model, and reaches values of 0.055 Pa near the back of the model. Additionally, shear stresses are much higher along the bed surface near the front third of the reef geometry, reaching peak values of 0.077 Pa. The back half of the reef's bed surface has much lower shear stresses, but they do not fully attenuate until in the reef's wake zone.

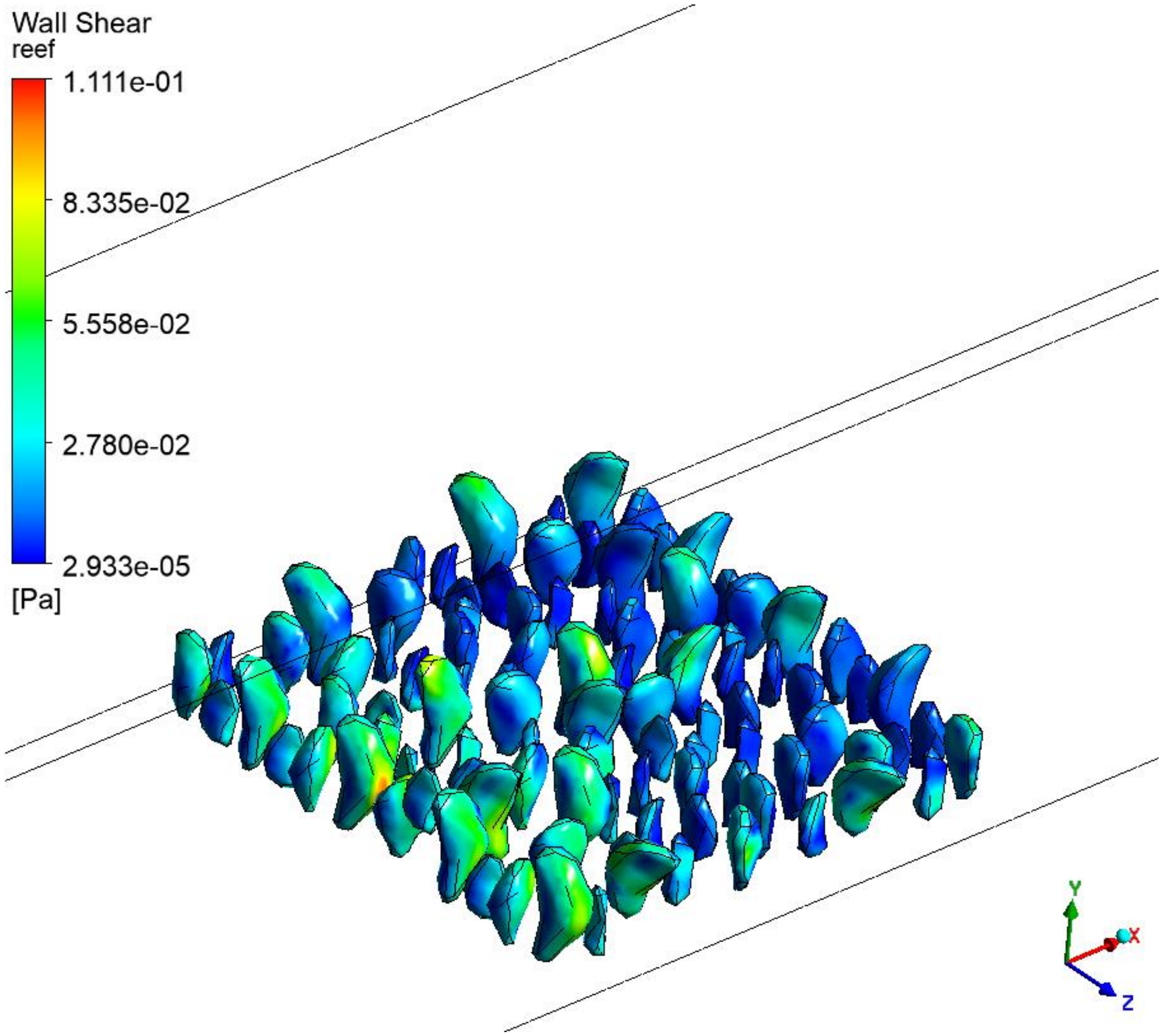

Figure 25: The shear stress present along the oyster shell surface of the flat adult oyster reef

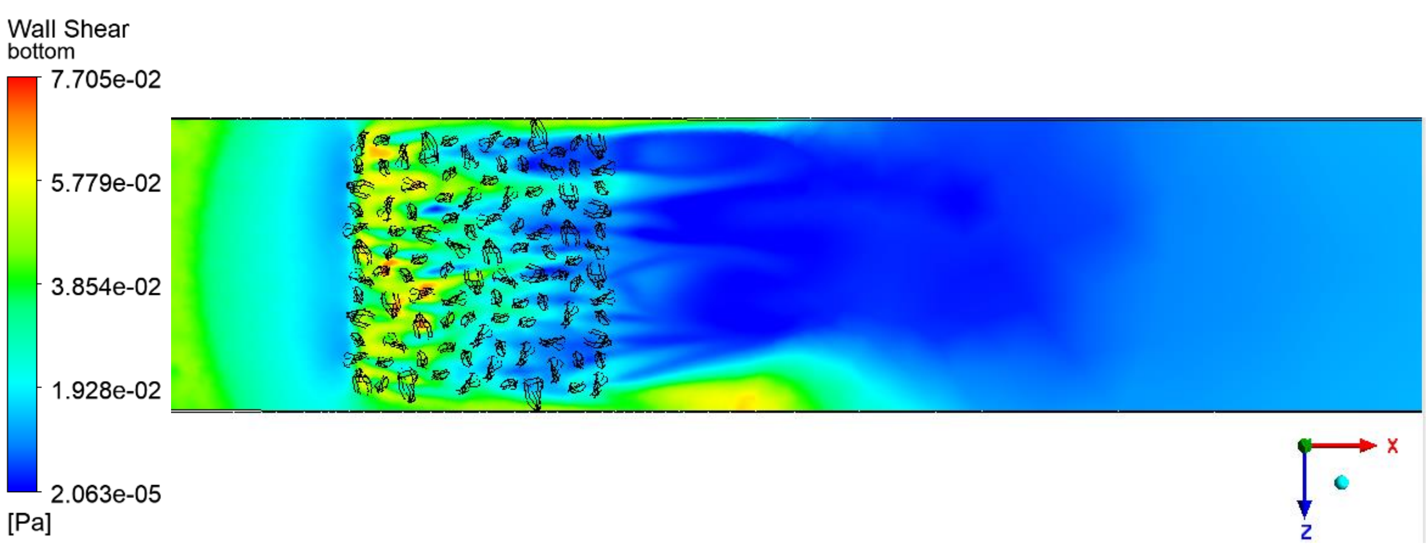

Figure 26: Bed shear stress for the flat oyster reef. Values peak in the front third of the reef's bed surface

Finally, TKE trends for the natural reef, visualized in Figure 27, reveal similar zones of recirculation in the reef's wake, reaching peak values of 0.0003 m^2/s^2. As compared with the oyster castle model, these values are significantly smaller, and also represent a mixing zone that is approximately 40% along the Y axis. Note that the zone of high TKE is also significantly closer to the bed surface and model geometry as compared to the oyster castle model.

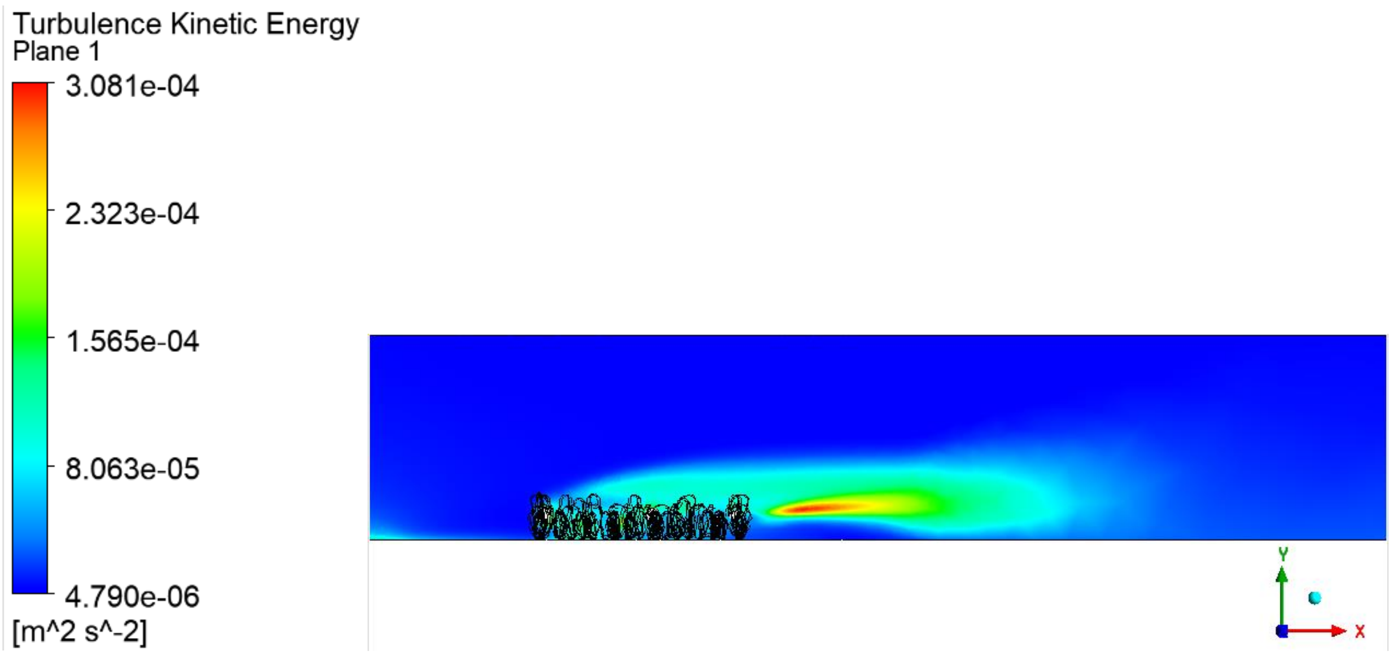

Figure 27: The TKE present along the central XY plane of the flat adult oyster reef

D. Discussion:

i. Oyster Castle Flow Attenuation

All three oyster castle models exhibit the ability to attenuate flow, but to varying degrees. Figures 11, 12, and 13 visualize attenuation trends across the reef model topography. As oysters colonize the castle and grow to adult size, they increase velocity attenuation when compared to the empty castle up to 58% within the reef, and up to 10% in front of the reef. Juvenile oysters provide similar improvements to attenuation, but only have about 40% the impact that adult oysters have. Additionally, all models attenuate flow to 0 m/s near the bed surface in the model's wake. The presence of oysters on the castle increases surface roughness and add obstructions to the flow, introducing friction and drag to slow down velocity. The results show that larger oysters that further obstruct flow also increase drag when compared to juvenile oysters. Thus, oyster growth can directly be attributed with greater flow attenuation within, far behind, and in front of the model.

However, oyster presence causes in increase in flow rather attenuation at many points within the fluid domain, specifically above the model and in the model's wake. Behind the model, oysters of any size increase velocity by up to 40%-52%. This suggests that the presence of oysters on the castle creates an area of recirculation immediately behind the reef. In particular, this is evident from the XY planar velocity profiles (Figures 14, 15, and 16), which visualize an increase in vortex definition and strength behind the model that is proportional to oyster size. The empty castle has no turbulent recirculation, while the juvenile oysters introduce scattered velocity values of approximately 6 cm/s, and the adult oysters create a fully defined zone of turbulent mixing, with velocities of approximately 6 cm/s. Larger oyster obstructions exert more drag on incoming flow, but inadvertently may create a large pocket of negative pressure behind the model, pulling flow down out of the water column and creating these observed vortices.

Above the model, flow rates reach peak values of approximately 27, 26, and 23 cm/s for the empty, juvenile, and adult reefs, respectfully. Due to conservation of flow, incoming fluid will be forced over the top of the structure, drastically increasing velocity compared to input rates of 10 cm/s. Despite all models demonstrating this increase in flow rates, larger oysters do result in a slower flow rate above the model, with adult oysters lowering velocities by up to 15% compared to the empty reef. However, due to the small amount of flow leaking around the sides of the adult reef model, this decrease in surface velocity may actually be due to flow simply taking an alternative path around the model. These increased ambient flow rates continue along the entire portion of the fluid domain above the vertical height of the reef surface, with velocities lowering to approximately 13 cm/s at the end of the domain for all three models. This suggests that oyster castles, regardless of oyster growth, actually increase ambient flow rates above the reef height, potentially increasing the velocity of the water colliding with the marsh platform. Thus, exposed marsh edges that are growing above reef height could experience flow that is 30-50% larger than ambient flow rates if castles are placed adjacent to the marsh edge. When combined with wave shoaling, these effects of oyster reefs on surface flow are likely to increase wave height as flow approaches the shoreline. Projects that plan to utilize oyster castles should account for flow attenuation to largely be below crest height, and should expect to see an increase in surface flow. This may be especially relevant if the oyster castles are to be used as shoreline protection, as deep water conditions will allow fast water to reach the shoreline.

ii. Oyster Castle Shear Stresses and TKE

The erosion and sediment suspension potential of flow can be quantified through trends in shear stress and turbulent kinetic energy. All three oyster castle models exhibit high shear stress inside the confines of the model geometry near the front walls. These shear stresses reach peak values of 0.065 Pa for the empty castle, 0.094 Pa for the juvenile castle, and 0.04 Pa for the adult castle. These shear stresses, however, decrease in magnitude with larger oysters, instead shifting to a trend where there are high shear stresses farther behind in the model's wake. Additionally, all three models show high shear stresses, between 0.1 and 0.3 Pa along the leading edge of the model topography. As oysters exert drag on the flow, they slow down flow velocities until surface shear is decreased to nearly 0 Pa along the backside of the models. These decreases in shear stress are more directly proportional to oyster size, as larger oysters exert more drag on flow rates. All models lower shear stress by over 80% as flow moves behind the model. However, the high shear stress within the model poses a threat for long-term castle health. Since shear stresses are much higher within the front model chambers relative to its backside, the castles are predicted to undergo differential erosion trends. The castles will lose sediments withing these front compartments, while the backsides will experience no erosion, or even some degree of sediment deposition. The result is the front of the castle may subside, while the backside may get buried with new sediments, potentially causing the castle to topple and collapse over time. Projects utilizing oyster reefs should be aware of these risks with reef toppling, and should potentially alter reef construction so as to minimize this front region of high shear. This may require asymmetric reef construction, or a complete overhaul of the castle design.

TKE is the variable most representative of turbulence and turbulent mixing. Consequently, areas of relatively high TKE reveal where reef topography is inducing heavily turbulent flow. In the empty and juvenile castle models, there is a clear zone of high TKE just above the leading edge of the model, reaching peak values of 0.0045 and 0.003 m^2/s^2 for the empty and juvenile reefs, respectively. Additionally, the adult oyster reef creates a zone of high TKE approximately 0.6 m behind the model and situated approximately at reef height. This zone has peak values of approximately 0.02 m^2/s^2, and is approximately 0.3 m in length and 0.12 m in height. Since the adult reef causes this region of high TKE, there will be high amounts of mixing and turbulence in its wake zone. These higher rates of mixing as oysters develop may actually be helpful for infauna and invertebrates at the sediment surface, as both oxygen and nutrients will more easily cycle from near the surface of the flow towards the bed surface. Similarly, these higher rates of mixing may encourage more oysters to develop in the reef's wake over time, as they will flux out hypoxic water from the spaces inbetween individual oysters.

iii. Oyster Castle Particle Transport and Reef Health Implications

The trends in shear stress have several implications for particle motion, in particular oyster larvae and sediments. Shear stresses greater than 0.04 Pa are sufficient to dislodge and erode flocculated mud sediments commonly found in oyster reefs along Virginia's eastern shore. Therefore, any point in the model that experiences shear stress greater than 0.04 Pa will experience sediment erosion. Oyster larvae, however, will actively swim towards suitable substrate in response to turbulence, and therefore a higher shear stress of 1 Pa is needed to wash them away from the reef. In these models, there are no clear regions with shear stresses above 1

Pa, and thus oyster larvae are at no risk of being washed away. However, the models reveal several distinct regions with high potential for sediment erosion. First, the bed surface within the front chambers of the oyster castles consistently experiences shear stresses between 0.04 Pa when adult oysters are present on the reef and 0.065 Pa when the reef is empty or has juvenile oysters. Similarly, 4 ft behind the empty and juvenile oyster models, there are large regions of the bed surface with shear stresses of approximately 0.06 Pa (Figures 18 and 19). The results reveal these to be the two primary regions of sediment erosion in each reef scenario, and demonstrate how oyster growth is tied to shear stress trends. Larger oysters may limit the rate of sediment erosion within the oyster castle by lowering bed shear stress from 0.09 Pa to 0.04 Pa; however, this is still above the threshold for flocculated sediment erosion, and thus the front of the castle is still at risk of losing sediment.

The model results suggest a pattern of differential sediment erosion within the model domain, with sediments preferentially eroding from the front chambers of the oyster castles, as well as approximately 4 ft behind the model. This is consistent regardless of oyster presence, potentially showing a means of oyster castle failure over time. Given the predicted trends in shear, the leading chambers and front edges of the castle may subside relative to the castle's backside. If this differential erosion of sediments continues over time, the castle may eventually collapse. Oyster castle burial and collapse is a relatively common issue that restoration projects face, and these models help show the mechanism that may govern oyster castle failure.

iv. Natural Reef Trends

The natural reef model exhibits all flow attenuating trends that are present in the oyster castle models, but these trends are weaker in strength and smaller in scope. For example, flow attenuation is largely limited to a vertical height at or below that of the reef surface, or below a height of 10 cm above the bed surface. Velocities in this region are attenuated to values of between 3-7 cm/s within and immediately behind the reef, and flow values reach near 0 cm/s along the bed surface in the reef's wake. However, there is little effect from reef topography on fluid velocity at the free surface, with values being increased to 12-14 cm/s, as compared with the input value of 10 cm/s. Additionally, while there is some flow recirculation happening in the wake of the flat adult oyster reef model, it is to less of a degree than in the wake of the oyster castle reef, and occupies a smaller space. Peak TKE values behind the flat reef are approximately 0.0003 m^2/s^2, compared with the oyster castle's peak values of 0.002 m^2/s^2. This further supports that natural reefs have less of an influence on incoming tidal flow compared with restored reef structures, as turbulence generation is an order of magnitude lower in the natural reef's wake zone.

Additionally, like the oyster castles, the leading edge of the flat reef experiences much higher shear stresses than the trailing edge, reaching peak values of between 0.07 Pa along the bed surface and 0.1 Pa near the top edges of the oyster shells, both well above the threshold of mud's critical shear stress. However, shear stresses quickly decrease across the reef, and pass under the critical shear stress for mud approximately halfway through the reef. It has been theorized that natural reef size is limited by the ability of flow to flush out hypoxic water and sediments from the surface of oysters. This model may show why that is the case, as oysters may attenuate flow enough a reach a point where adequate water and sediment cycling is not occurring. Oyster castles may offer an interesting advantage over natural reefs – they may be constructed in such a configuration to encourage sufficient turbulent mixing and water cycling throughout the water column over a large space. Previous studies have created multiple layers of oyster castle walls next to each other, but the castles could be constructed into a larger structure featuring more dramatic topographical changes. If done correctly, the castles should theoretically encourage high rates of turbulence near the reef surface, therefby allowing the formation of larger reefs than are naturally viable.

v. Model Limitations

Given that these models are approximating tidal flow, flow conditions will constantly be changing in intensity and direction. Thus, any directionally focused trends and conclusions from these simulations, such as preferential erosion and castle toppling/burial, may not be as strong as these figures would depict. However, incoming flood flow is generally stronger than outgoing ebb flow, especially owing to the presence of wind fetch and waves. Thus, these trends and conclusions still accurately describe this system's behavior.

Additionally, the inherent limitations of these ANSYS simulations must be considered when interpreting results. All geometries present are highly idealized. Each individual oyster scan initially had hundreds of faces, but was simplified to only have approximately 20. Since each model has hundreds of oysters, this was necessary to ensure efficient model runs, but unfortunately results in unavoidable accuracy loss. Additionally, since oyster geometry extended over the sides of the base oyster castle model, small gaps formed along the outer edges of the colonized oyster castle models, which increase in size as larger oysters are modeled. This does introduce error along the model's edges, but trends within the reef are still accurate relative to incoming tidal flow. Finally, since the top boundary of each fluid domain is fixed at a certain height, the model does not account for wave action or changes in water depth. Thus, since conservation of flow is forcing water through the models rather than above in the form of waves, the predicted shear stresses and flow velocities are likely lower in reality.

vi. Model Implications

The trends predicted in these models agree well with field observations. Along marsh edges monitored by TNC, beaches generally have a much shallower slope and finer particle size behind areas with oyster castles as opposed to unprotected sites. These CFX models show that oyster castles can significantly alter shear stresses, velocity, and TKE present just above the sediment surface, and these observed shallower bed slopes and grain sizes are likely the direct result of those flow attenuating effects. However, oyster castles and natural oyster reefs have not succeeded in stopping marsh platform erosion. This project's CFD models show that when the tide is above the oyster castle surface, surface velocity actually increases. This explains part of why oyster castles do not prevent marsh platform loss, despite protecting sediments along the bed surface in the model's wake.

These simulations demonstrate how different oyster reefs interact with their flow environment, and inform questions regarding flow attenuation and long term reef growth and structural integrity. They reveal the mechanisms by which various natural and artificial oyster reefs attenuate flow, as well as how that flow attenuation influences sediment erosion. All models tested attenuate flow below crest height and increase flow above crest height, while also experiencing high bed shear stress towards the front of the model and lower bed shear stress towards the back. There is a distinct tradeoff between natural and constructed reefs, where oyster castles may better attenuate flow, but may have difficulty maintaining structural integrity under differential erosion trends.

However, there is still a knowledge gap regarding flow attenuation mechanisms of oyster reefs. For example, it is not known how wider reef sections may behave under these same flow conditions, and such a model would reveal trends and behaviors more accurate to field sites. Additionally, these models are highly idealized, simplified, and do not have the same density or oyster configuration as genuine reefs. Improving detail within the model would similarly help improve the accuracy of all predicted attenuation and shear trends. Finally, the chosen boundary conditions do not take wave action into consideration. Recreating this model with waves would provide insight into how oyster reef topography immediately affects wave height as it approaches a shoreline.

E. Appendix B

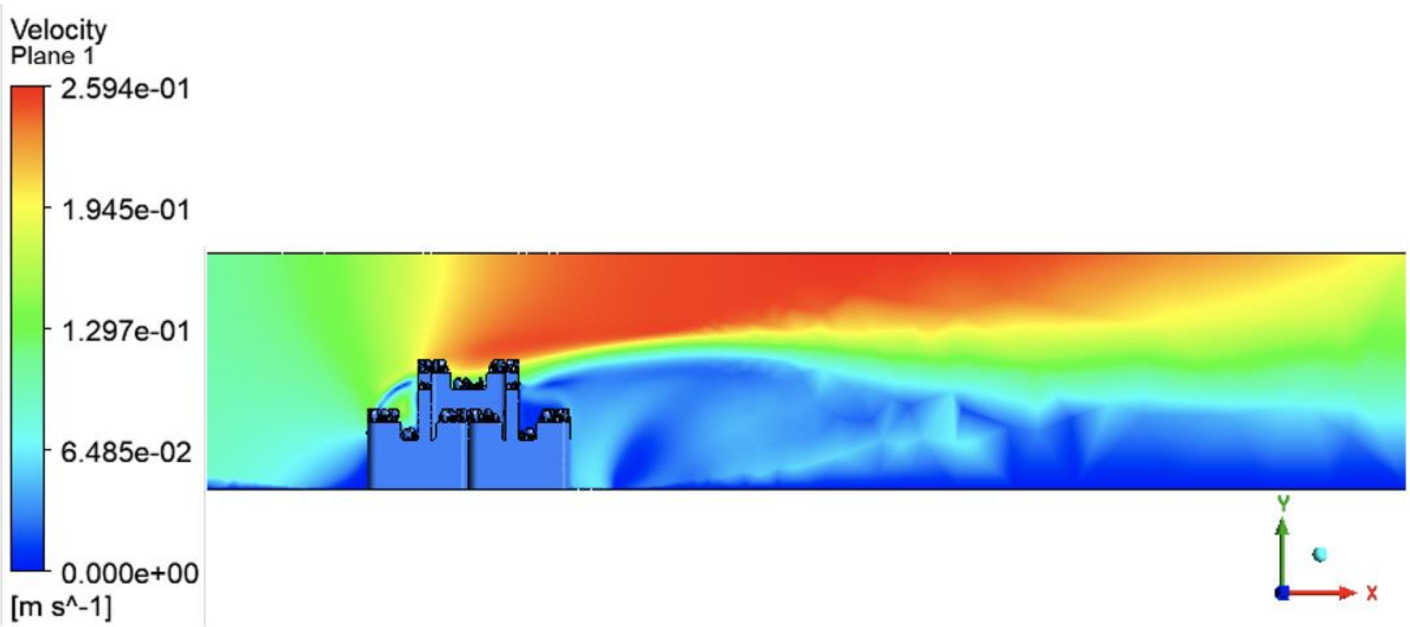

Locally scaled planar velocity of the juvenile reef

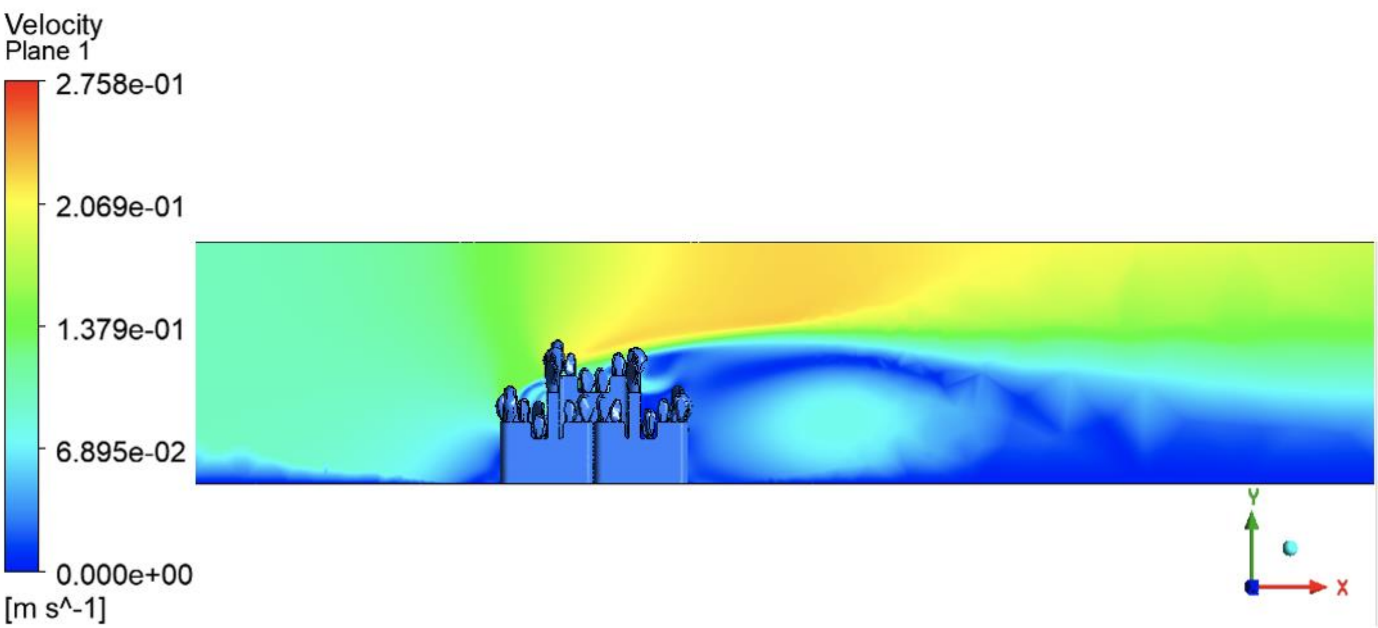

Locally scaled planar velocity of the adult reef

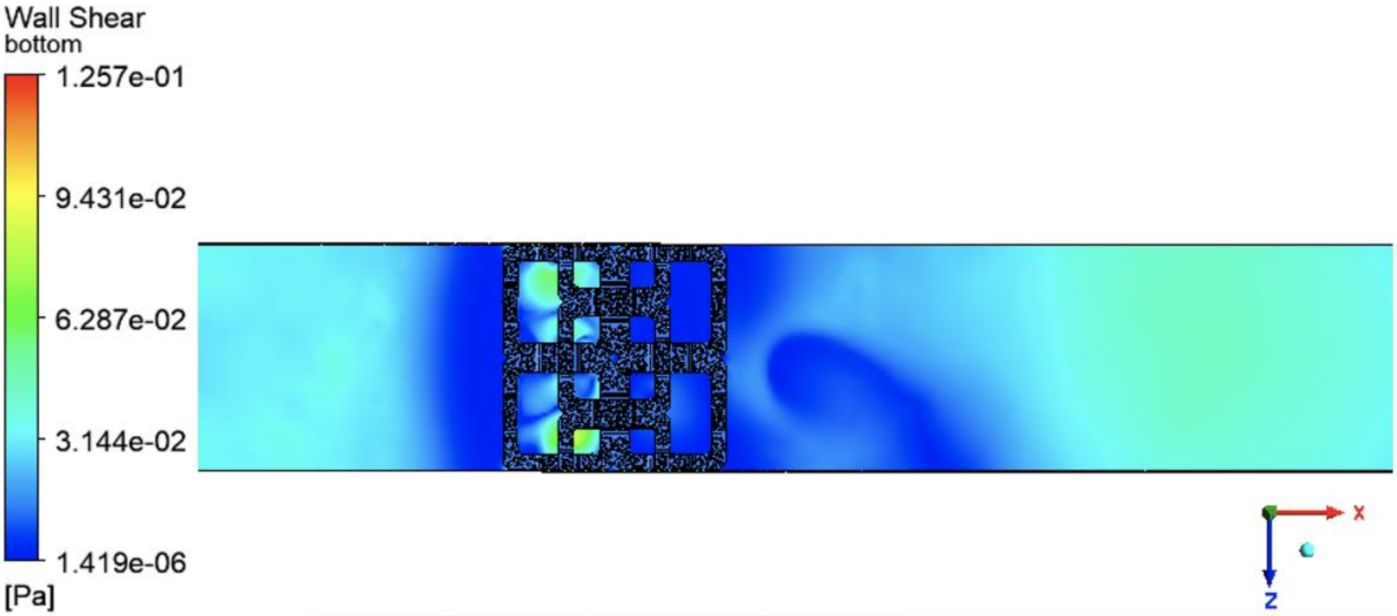

Locally scaled bed shear stress of the juvenile reef

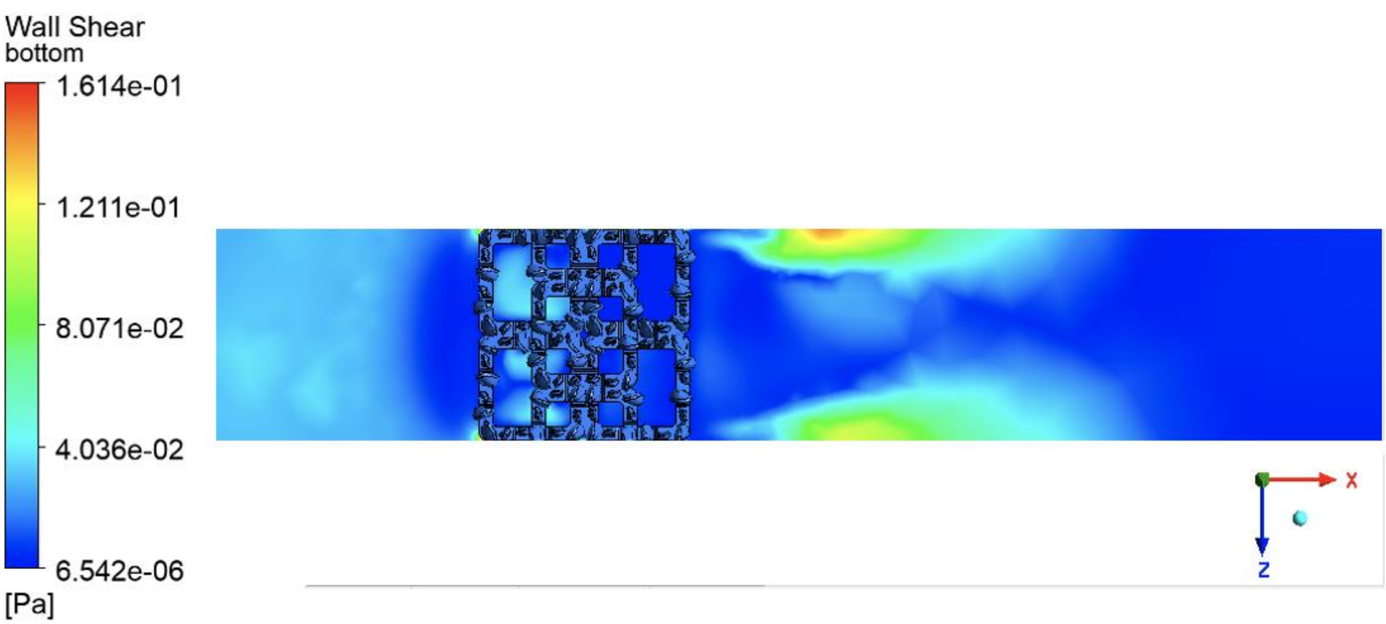

Locally scaled bed shear stress of the adult reef

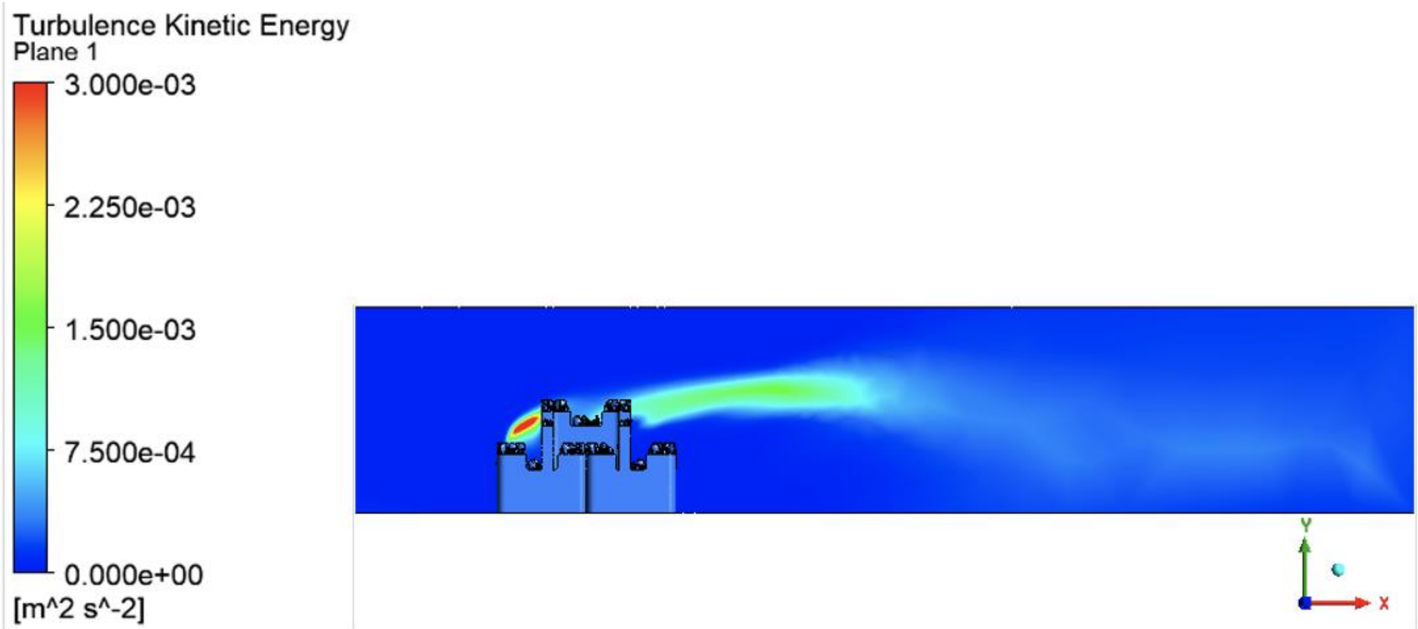

Locally scaled planar TKE of the juvenile reef

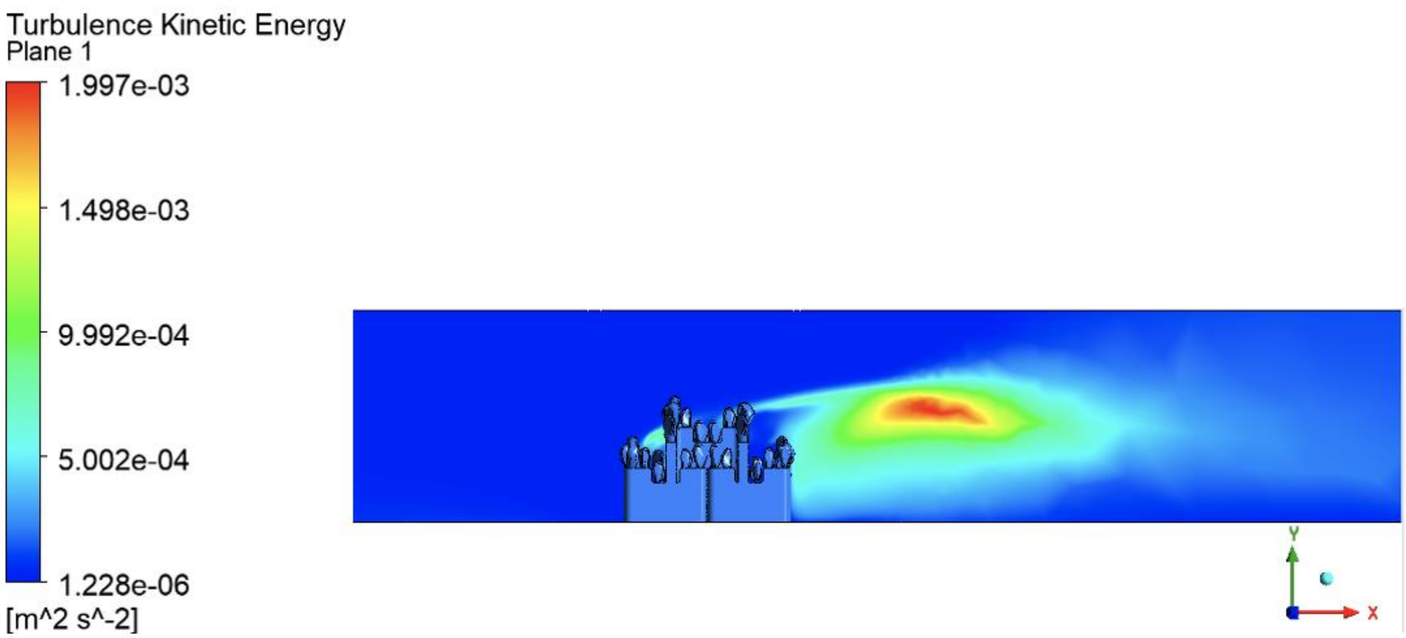

Locally scaled planar TKE of the adult reef

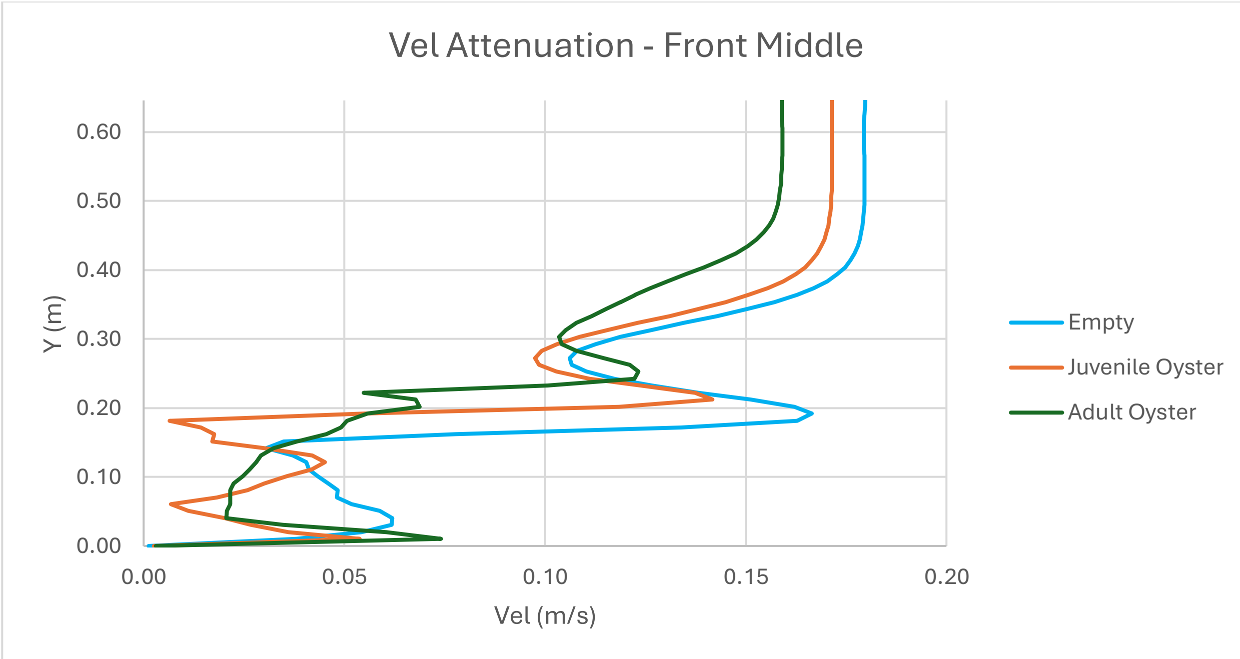

Vertical velocity profiles along the ‘Front Middle’ profile section

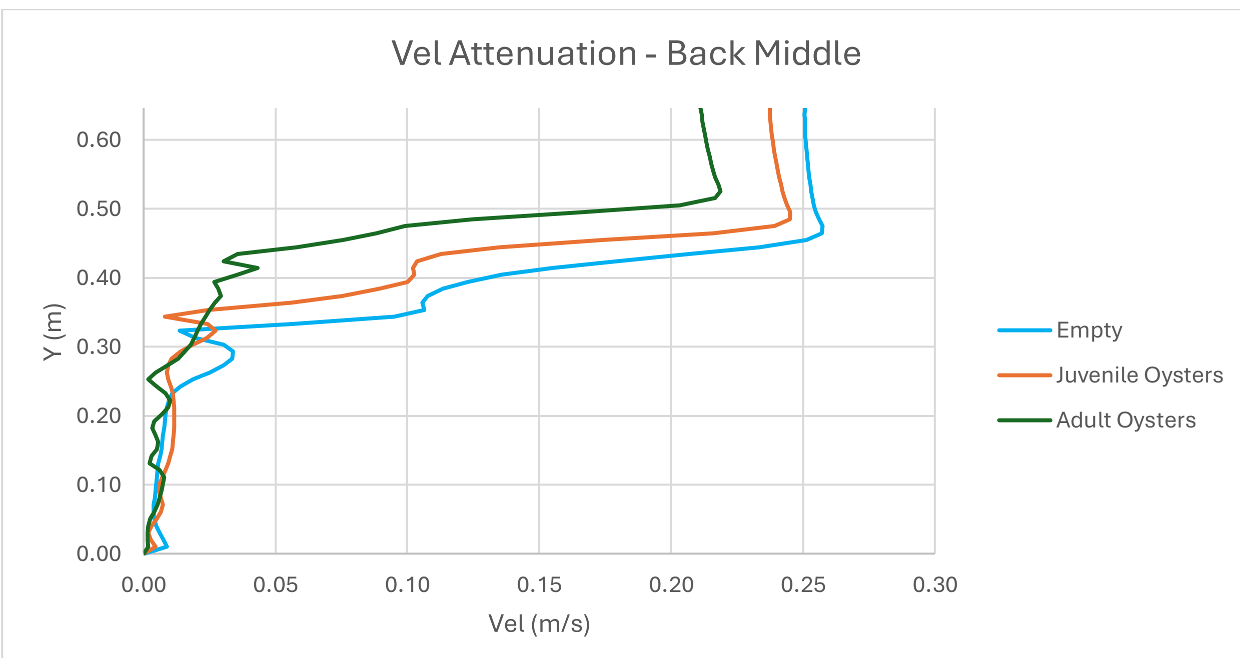

Vertical velocity profiles along the ‘Back Middle” profile section

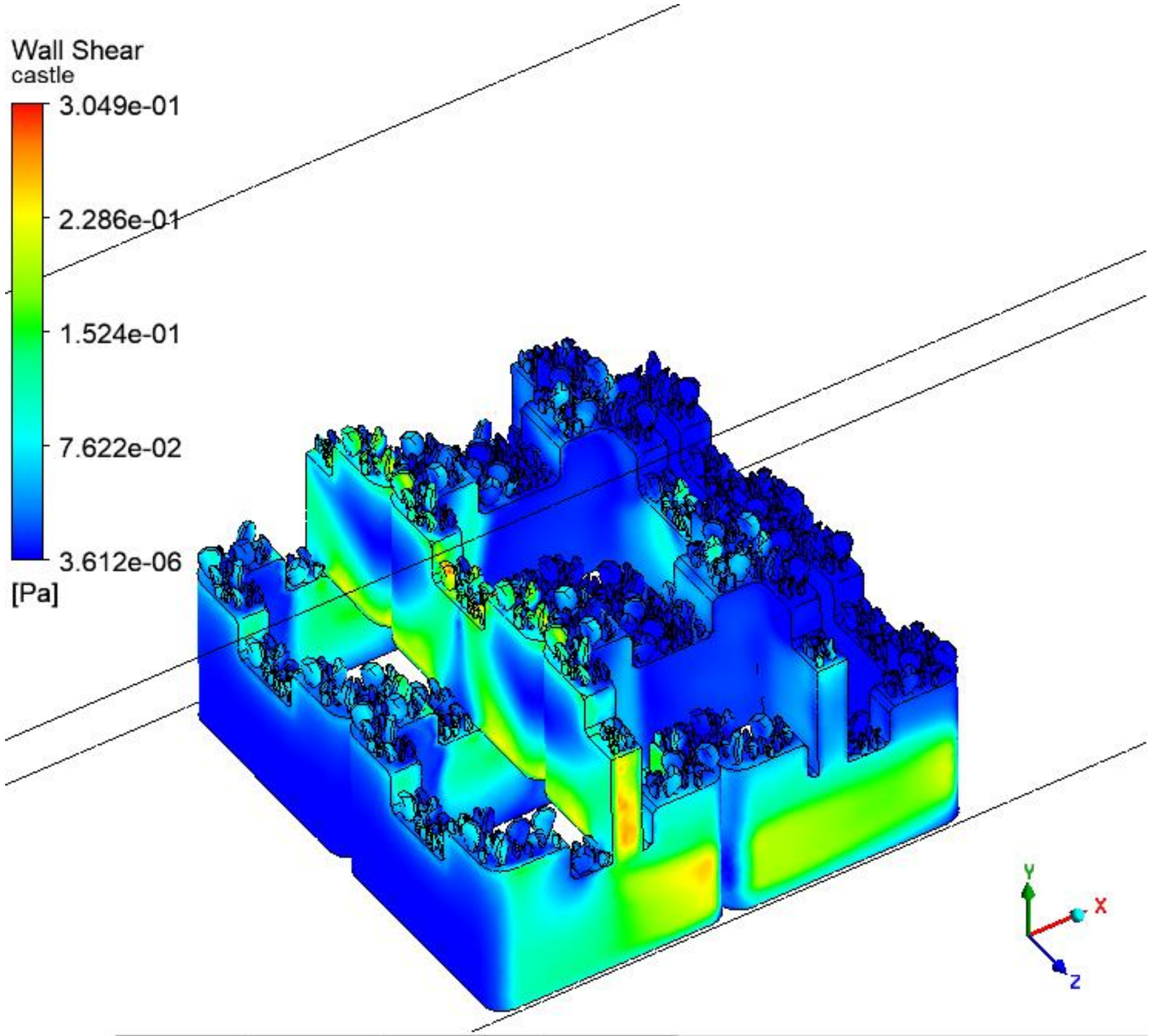

Locally scaled surface shear stresses along the juvenile reef surface

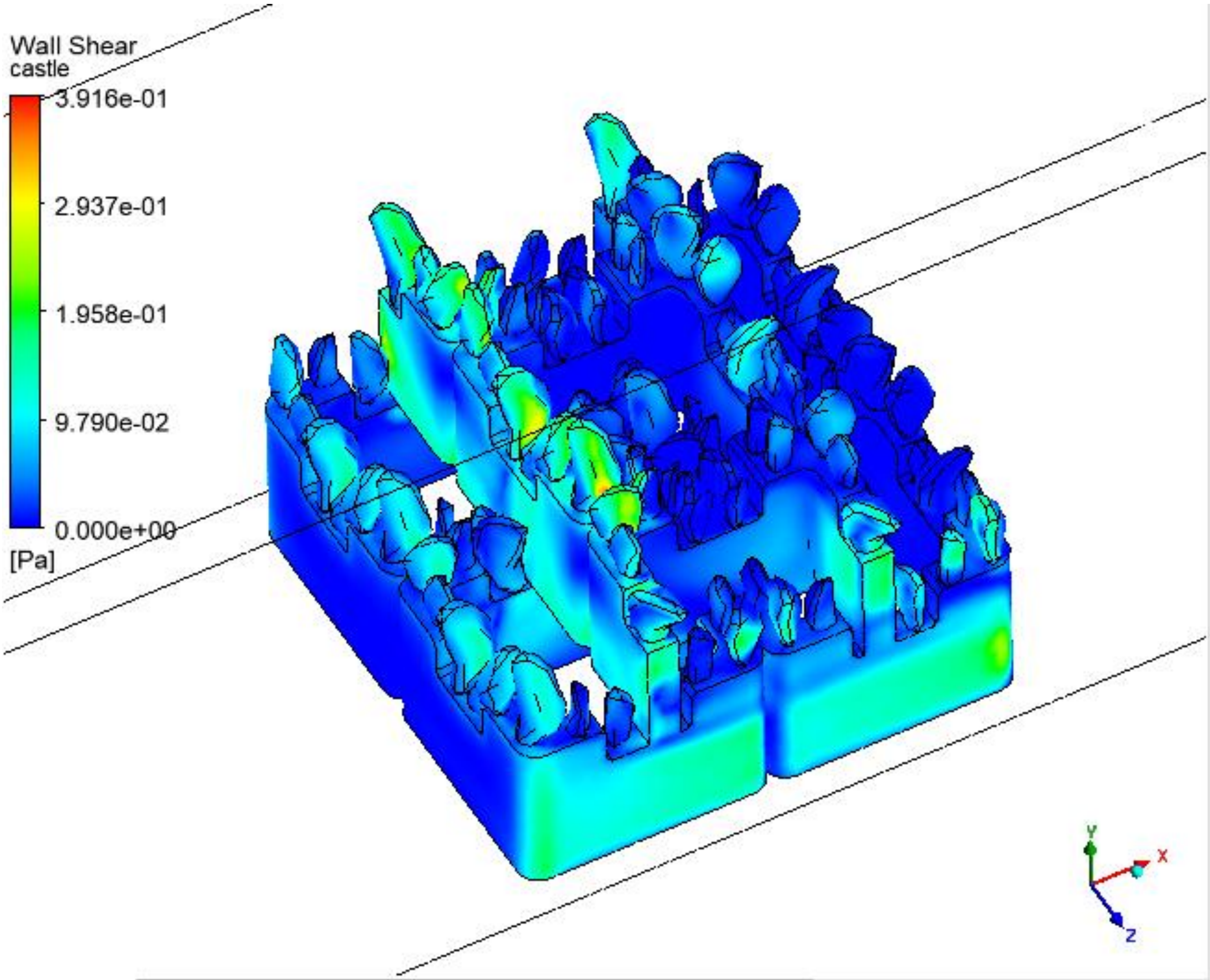

Locally scaled surface shear stresses along the adult reef surface

V. Literature Cited:

Andrews, J. et al. “Oyster Mortality Studies in Virginia: Epizootiology of a Disease Caused by Haplosporidium costale”. Journal of Insect Pathology: 4(3), page 327. 1962.

Bartol, Ian K. et al. "Growth and mortality of oysters (Crassostrea virginica) on constructed intertidal reefs: effects of tidal height and substrate level." Journal of Experimental Marine Biology and Ecology. Vol 237:2, pages 157-184. 1999

Bertness, M. et al. “Flood Tolerance and the Distribution of IVA-Frutescens Across New England Salt Marshes”. Oecologia: 91(2), pages 171-178. Aug 1992

Bieri, L. “Evaluating Coastal Protection Benefits of Restored Oyster Reef Designs”. University of Virginia. Nov, 2022.

Bishop, C. and Donelan, A. “Measuring Surface Waves with Pressure Transducers”. Coastal Engineering: 11(4), pages 309-328. Nov 1987.

Blum, L.K. et al. “Processes Influencing Marsh Elevation Change in Low- and High-Elevation Zones of a Temperate Salt Marsh” Estuaries and Coasts. Vol 44, pages 818–833. 2021

Burns, C. et al. “Historical Changes in the Vegetated Areas of Salt Marshes”. Estuaries and Coasts: 44(1), pages 162-177. Jan 2021.

Colden, A. and Lipcius R. “Lethal and sublethal effects of sediment burial on the eastern oyster Crassostrea virginica”. Marine Ecology Progress Series. Vol 527, pages 105-117. May 2015

Colden, A. et al. “Sediment Suspension and Deposition Across Restored Oyster Reefs of Varying Orientation to Flow: Implications for Restoration”. Estuaries and Coasts. Vol 39:5, pages 1435-1448. Sep 2016.

Crosby, S. et al. “Salt Marsh Persistence Is Threatened by Predicted Sea Level Rise”. Estuarine and Coastal Shelf Science: 181, pages 93-99. Nov 2016.

Day, J. et al. “Soil Accretionary Dynamics, Sea-Level Rise and the Survival of Wetlands in Venice Lagoon: A Field and Modeling Approach”. Estuarine Coast and Shelf Science: 49(5), pages 607-628. Nov 1999.

Deaton, C. et al. “Barrier Island Migration Dominates Ecogeomorphic Feedbacks and Drives Salt Marsh Loss Along the Virginia Atlantic Coast, USA”. Geology: 45(2), pages 123-126. Feb 2017.

DePiper, G. et al. “Valuing Ecosystem Services: Oysters, Denitrification, and Nutrient Trading Programs”. Marine Resource Economics: 32(1), pages 1-20. 2017.

Donatelli, C. et al. “Salt Marsh Loss Affects Tides and the Sediment Budget in Shallow Bays”. Journal of Geophysical Research - Earth Surface. Vol 123:10, pages 2647-2662. Oct 2018.

Eggleston, D. et al. "Soundscapes and larval settlement: larval bivalve responses to habitat-associated underwater sounds." The effects of noise on aquatic life II. Springer New York, 2016.

Ezer, Tal and Atkinson, Larry P. "Sea Level Rise in Virginia – Causes, Effects and Response," Virginia Journal of Science: Vol 66:3. 2015

Fagherazzi, S. and Furbish, D. "On the Shape and Widening of Salt Creek Marshes". Journal of geophysical Research – Oceans: 106(C1), 991-1003. Jan 2001

Fagherazzi, S. et al. "Salt Marsh Dynamics in a Period of Accelerated Sea Level Rise". Journal of Geophysical Research: Earth Surface. Vol 125:8. July, 2020

Gallegos, C. "Calculating optical water quality targets to restore and protect submersed aquatic vegetation: Overcoming problems in partitioning the diffuse attenuation coefficient for photosynthetically active radiation". Estuaries: 24, pages 381-397. Jun 2001

Gaurier, B. et al. "Experimental and Numerical Characterization of an Oyster Farm Impact on the Flow". European Journal of Mechanics B-Fluids: 30(5), pages 513-525. Sep 2011.

Gawde, R. et al. "A High Resolution Hydrodynamic-Biogeochemical-Oyster-Filtration Model Predicts That the Presence of Oysters (*Crassostrea virginica)*) Can Improve, or Reduce, Water Quality Depending Upon Oyster Abundance and Location". Ecological Modelling: 496. Oct 2024.

Godfrey, Paul J., and Melinda M. Godfrey. "The role of overwash and inlet dynamics in the formation of salt marshes on North Carolina barrier islands." Ecology of halophytes. Pages 407-427. 1974

Grabowksi, J. et al. "Economic Valuation of Ecosystem Services Provided by Oyster Reefs". Bioscience: 62(10), pages 900-909. Oct 2012.

Hansen, J. and Reidenbach, M. "Wave and Tidally Driven Flows in Eelgrass beds and Their Effect on Sediment Suspension". Marine Ecology Progress Series: 448, pages 271-287. 2012

Hansen, J. and Reidenbach, M. "Seasonal Growth and Senescence of a Zostera marina Seagrass Meadow Alters Wave-Dominated Flow and Sediment Suspension Within a Coastal Bay". Estuaries and Coasts: 36(6), pages 1099-1114. Nov 2013.

Hayden, Bruce P., and Nils R. Hayden. "Decadal and century-long changes in storminess at long-term ecological research sites." Climate variability and ecosystem response at long-term ecological research sites. Pages 262-285. 2003

Henderson, Jim E., and L. Jean O'Neil. "Economic values associated with construction of oyster reefs by the Corps of Engineers." Engineer Research and Development Center. 2003

Hogan, S. et al. "Utilizing airborne LiDAR data to quantify marsh edge morphology and the role of oyster reefs in mitigating marsh erosion". Marine Ecology Progress Series. Vol 669, pages 17-31. Jul 2021.

Hogan, S. and Reidenbach, M. "Quantifying Tradeoffs in Ecosystem Services Under Various Oyster Reef Restoration Designs". Estuaries and Coasts. Vol 45:3, pages 667-690. May 2022.

Hogan S, and Reidenbach MA. "Quantifying and mapping intertidal oyster reefs utilizing LiDAR-based remote sensing" Mar Ecol Prog Ser. Vol 630:, pages 83-99. Nov 2019.

Jackson, R. et al "Application of the AMBUR R package for spatio-temporal analysis of shoreline change: Jekyll Island, Georgia, USA". Computers and Geosciences. Vol 41, Pages 199-207. 2012

Kastler, J. and Wiberg, P. “Sedimentation and Boundary Changes of Virginia Salt Marshes”. Estuarine Coastal and Shelf Science: 43, pages 683-700. 1996.

Kelletat, D. “Coastal Erosion and Protection Measures at the German North Sea Coast”. Journal of Coastal Research: 8(3), pages 699-711. 1992

Kirwan, Matthew L., et al. "Sea level driven marsh expansion in a coupled model of marsh erosion and migration." Geophysical Research Letters. Vol 43:9, pages 4366-4373. 2016

Lawson, S. “Sediment suspension as a control on light availability in a coastal lagoon”. University of Virginia. Jan 2004.

Lauzon, R. et al. “Effects of Marsh Edge Erosion in Coupled Barrier Island-Marsh Systems and Geometric Constraints on Marsh Evolution”. Journal of Geophysical Research – Earth Surface: 123(6), pages 1218-1234. Jun 2018.

Leonardi, N. and Fagherazzi, S. “Effect of Local Variability in Erosional Resistance on Large-Scale Morphodynamic Response of Salt Marshes to Wind Waves and Extreme Events”. Geophysical Research Letters: 42(14), pages 5872-5879. Jul 2015

Leonardi, N. et al “Dynamic Interactions Between Coastal Storms and Salt Marshes – A Review”. Geomorphology: 301, pages 92-107. Jan 2018

Lillis, A. et al. "Soundscape manipulation enhances larval recruitment of a reef-building mollusk." PeerJ. Vol 3:e999. June 2015

Lowe, R. et al. “Oscillatory Flow Through Submerged Canopies: 1. Velocity Structure”. Journal of Geophysical Research – Oceans: 110(C10). Oct 2005.

Mackenzie, C. "Causes Underlying The Historical Decline in Eastern Oyster (Crassostrea Virginica Gmelin, 1791) Landings". Journal of Shellfish Research: 26(4), pages 927-938. Dec 2007.

Mani, J. “Beach Accretion and Erosion with S-Type Rubble Mound Sea Wall”. Journal of Coastal Research: 23(4), pages 921-929. Jul 2007.

Marani, M. et al. “The importance of being coupled: Stable states and catastrophic shifts in tidal biomorphodynamics”. Journal of Geophysical Research – Earth Surface. Vol 115. Oct 2010.

Mariotti, G., and J. Carr. "Dual role of salt marsh retreat: Long-term loss and short-term resilience." Water Resources Research. Vol 50:4, pages 2963-2974. 2014

Matias, A. et al. “Classification of washover dynamics in barrier islands”. Geomorphology. Vol 97:3-4, pages 655-674. May 2008.

Mazzocco, V. et al. “Economic Value of Salt Marshes Under Uncertainty of Sea Level Rise: A Case Study of the Narragansett Bay”. Coastal Management: 50(4), pages 306-324. Jul 2022.

McLoughlin, S. “Erosional Processes Along Salt Marsh Edges at The Eastern Shore of Virginia”. University of Virginia. Dec, 2010.

McLoughlin, Sean M., et al. "Rates and forcing of marsh edge erosion in a shallow coastal bay." Estuaries and Coasts. Vol 38, Pages 620-638. 2015

Morris, R. et al. “Large-scale variation in wave attenuation of oyster reef living shorelines and the influence of inundation duration”. Ecological Applications. Vol 31:6. Sep, 2021.

Morris, R. et al. “The application of oyster reefs in shoreline protection: Are we over-engineering for an ecosystem engineer?”. Journal of Applied Ecology. Vol 56:7, Pages 1703-1711. July 2019.

The Nature Conservancy. “Oyster Restoration in Virginia”. https://www.nature.org/en-us/about-us/where-we-work/united-states/virginia/stories-in-virginia/oyster-restoration-in-va/. Aug 2023.

Pannozzo, N. et al. “Salt Marsh Resilience to Sea Level Rise and Increased Storm Intensity”. Geomorphology: 389. Sep 2021.

Pannozzo, N. et al. “Storm Sediment Contribution to SaltbMarsh Accretion and Expnasion”. Geomorphology: 430. Jun 2023.

Perricone, V. et al. “Nature-Based and Bioinspired Solutions for Coastal Protection: an Overview Among Key Ecosystems and a Promising Pathway for New Functional and Sustainable Designs”. ICES Journal of Marine Science: 80(5), pages 1218-1239. Jun 2023.

Peteet, N. et al. “Sediment starvation destroys New York City marshes' resistance to sea level rise”. Preceeding of the National Academy of Sciences of the United States of America. Vol 115:41, pages 10281-10286. Oct 2018.

Priestas, Anthony M., et al. "Coupled wave energy and erosion dynamics along a salt marsh boundary, Hog Island Bay, Virginia, USA." Journal of Marine Science and Engineering Vol 3:3, Pages 1041-1065. 2015

Reed, D.J. “Sea-level rise and coastal marsh sustainability: Geological and ecological factors in the Mississippi delta plain” Geomorphology. Vol 48:1-3, pages 233–243. 2002

Reeves, I. et al. “Impacts of Seagrass Dynamics on the Coupled Long-Term Evolution of Barrier-Marsh-Bay Systems”. Journal of Geophysical Research-Biosciences: 125(2). Feb 2020.

Reidenbach, M. et al. “Hydrodynamics of Intertidal Oyster Reefs: The Influence of Boundary Layer Flow Processes on Sediment and Oxygen Exchange”. Limnology and Oceanography: 3(1), pages 225-239. Dec 2013

Rothschild, B. et al. “Decline of the Chesapeake Bay oyster population: a century of habitat destruction and overfishing”. Marine Ecology Progress Series. Vol 111, pages 29-39

Salatin, R. et al. “Assessing Wave Attenuation With Rising Sea Levels for Sustainable Oyster Reef-Based Living Shorelines”. Frontiers In Built Environment: 8. Jun 2022.

Shi, B. et al. “Determination of Critical Shear Stresses for Erosion and Deposition Based on In Situ Measurements of Currents and Waves over an Intertidal Mudflat”. Journal of Coastal Research: 31(6), pages 1344-1356. Nov 2015.

Smith, R. et al. “Long Term Data Reveal Greater Intertidal Oyster Biomass in Predicted Suitable Habitat”. Marine Ecology Progress Series: 683, pages 221-226. Feb 2022.

Stanley, r. et al. “A model for understanding the effects of flow conditions on oyster reef development and impacts to wave attenuation”. Ecological Modeling: 489, pages . Mar 2024.

Stocking, J. et al. “Structure and dynamics of turbulent boundary layer flow over healthy and algae-covered corals”. Coral Reefs: 35, pages 1047-1059. April 2016.

Stocking, J. et al. “Hydrodynamic interactions with coral topography and its impact on larval settlement”. Coral Reefs: 35, pages 505-519. Feb 2021.

Stoorvogel, M. et al. “Salt Marshes for Nature-Based Flood Defense: Sediment Type, Drainage, and Vegetation Drive the Development of Strong Sediment Beds”. Ecological Engineering: 207. Oct 2024.

Stricklin, A. G. et al. “Do Small, Patchy, Constructed Intertidal Oyster Reefs Reduce Salt Marsh Erosion As Well As Natural Reefs?” Gulf and Caribbean Research. Vol 22:1, Pages 21-27. 2010

Styles, R. “Flow and Turbulence Over an Oyster Reef”. Journal of Coastal Research: 31(4), pages 978-985. Jul 2015.

Theuerkauf, S. et al. "Settlement, growth, and survival of eastern oysters on alternative reef substrates." Journal of Shellfish Research. Vol 34:2, Pages 241-250. 2015

Tedford, K. and Castorani, M. “Meta-Analysis Reveals Controls on Oyster Predation”. Frontiers In Marine Science: 9. Dec 2022.

Tonelli, M. et al. "Modeling wave impact on salt marsh boundaries." Journal of geophysical research: Oceans. Vol 115. 2010

Townend, I. et al. “A Review of Salt Marsh Dynamics”. Water And Environmental Journal. Vol 25:4, pages 477-488. Dec 2011.

Vona, L. et al. “Hydrodynamics of Artificial and Oyster-populated Breakwaters: A Laboratory Study with Scaled-Down Oyster Castles Under Unidirectional Flow”. Journal of Environmental Management: 365. Aug 2024.

Whitman, E. and Reidenbach, M. “Benthic flow environments affect recruitment of *Crassostrea virginica* larvae to an intertidal oyster reef”. Marine Ecological Progress Series. Vol 463, pages 177-191. 2012.

Wiberg, P. et al. “Wave Attenuation by Oyster Reefs in Shallow Coastal Bays”. Estuaries and Coasts: 42(2), pages 331-347. Mar 2019.